

UC Berkeley

SEMM Reports Series

Title

Cyclic Testing of Four Full-Scale Steel Beam-Column Connections with "Dogbones"

Permalink

<https://escholarship.org/uc/item/93p1153t>

Authors

Popov, Egor

Blondet, J.

Stepanov, Lev

Publication Date

1997-02-01

**REPORT NO.
UCB/SEMM-97/04**

**STRUCTURAL ENGINEERING
MECHANICS AND MATERIALS**

**CYCLIC TESTING OF
FOUR FULL-SCALE STEEL
BEAM-COLUMN CONNECTIONS
WITH "DOGBONES"**

BY

**EGOR P. POPOV
MARCIAL BLONDET
and
LEV STEPANOV**

Report to DASSE Design, Inc.

FEBRUARY 1997

**DEPARTMENT OF CIVIL AND
ENVIRONMENTAL ENGINEERING
UNIVERSITY OF CALIFORNIA
BERKELEY, CALIFORNIA**

INTRODUCTION

This report summarizes the results of an experimental program involving cyclic testing of four full scale beam-column connection specimens. The specimens were designed by DASSE Design Inc for McCandless Tower #2 (Santa Clara, California). The tests were carried out in the Structural Testing Laboratory of the Department of Civil and Environmental Engineering of the University of California at Berkeley under Service to Industry Project No. ES-2081. The Principal Investigator was Professor Egor P. Popov.

The test specimens simulated beam-column assemblies with connections described as “cover plated flange with dogbone”. Two beam-column assemblages were studied. The first assemblage consisted of a W33x130 beam and a W36x280 column. The second assemblage was made of heavier sections, namely a W36x194 beam and a W33x387 column. All sections were made of grade 50 steel. The beams were weakened through circular cuts (“dogbones”) on both beam flanges, made at strategic locations. These cuts were designed to predetermine the location and capacity of the plastic hinge, such that the highest stresses occurred in the reduced section, away from the welded beam-column connections. Results of recent tests of full scale steel beam-column connections [1, 2] indicate that circular cut dogbones are effective in improving the performance of moment resisting connections.

Three specimens, two with the smaller sections and one with the heavier sections, were initially fabricated and scheduled for testing. The two specimens with small sections behaved adequately under the cyclic loading program. The heavier specimen, however, failed suddenly with abrupt fracture of the welds between the column and bottom continuity plates. This specimen was visually inspected before the test, and it was observed that its continuity plates were significantly distorted and that the column was slightly crooked and warped. In spite of the obvious fabrication imperfections, it was decided to test the specimen, under the assumption that these could be taken as representative of field conditions. Inspection of the damaged specimen after the test seemed to indicate that the cause of the fracture was mainly related to the quality of the welds. As a result of this unexpected failure, another specimen of the same type was fabricated and tested with more attention given to weld inspection. This fourth specimen sustained successfully the testing program.

TEST SPECIMENS

All test specimens were fabricated by The Herrick Corporation. The following table describes the sections used:

Test Assembly	Specimens	Beam	Column
1	1, 2	W33x130	W36x280
2	3, 4	W36x194	W33x387

All sections were made of ASTM A572 Gr.50 steel. Material properties according to mill certificates and coupon tests (performed by Schwein/Cristensen Laboratories) are presented in Appendix A. Figure 1 shows the dimensions and geometry of the specimens. The connection details are presented in Figure 2.

TEST SETUP, INSTRUMENTATION & DATA ACQUISITION

The specimens were tested in the Structural Testing Laboratory of UC Berkeley. The test setup was designed to accommodate specimens in a horizontal position, as shown in Figure 3. The photograph in Figures 4 shows view of a test in progress.

The support system consisted of three reinforced concrete reaction blocks pre-stressed to the floor with high strength rods. The ends of the column were also pre-stressed to the reaction blocks. The bottom column end support restrained displacement in two directions and thus simulated a hinged connection (Figure 5); the top end support simulated a roller support (Figure 6). Steel support seats, relatively flexible in bending, were made of W-sections and placed between the column and the reaction blocks to allow for the rotation of the column end sections.

The load was applied to the cantilever beam end by a hydraulic actuator, through a clevis bolted to the beam end plate (Figure 7). The actuator had a displacement range of ± 6 inches and a capacity of ± 350 kips when controlled via a 3,000 psi servovalve, and a capacity of ± 500 kips with a manually operated pump. No axial load was applied to the column. To prevent out of plane motion of the beam, a horizontal bracing system was provided near the beam end.

Many sensors were used to monitor the response of the specimens during the tests in order to understand its behavior. Figures 8 and 9 show the location of measuring instruments on specimens. Table 1 gives a brief description of the instruments and their actual usage for all specimens.

Linear potentiometers were installed to measure the global behavior of the specimen: beam end deflection, joint rotation, and panel zone shear deformation. These sensors were calibrated to have an accuracy better than ± 0.01 inch. Note that, since the displacement history was used to command the actuator, the actual beam end displacement was somewhat smaller. Displacement transducers were therefore provided to measure both the actuator and beam end displacements (channels 78 and 79 in Figure 8, respectively; channel 1 was used for actuator feedback). Additional sensors were placed to detect possible movement of the supports (channels 73 to 76; no significant movement was observed during any test).

Strain gages and rosettes were glued at critical locations to investigate the local response. These gages had a range of at least 3% strain, and were thus functional well within the plastic range. They were calibrated to obtain strain readings within $\pm 0.01\%$. The applied load was read with a 500 kip load cell (channel 2) attached to the actuator. Load readings were accurate to ± 0.5 kip.

All the instruments were connected to a computer-based data acquisition and control system shown in Figure 10a. This system consisted of a Neff 470 box with a capacity of 240 input channels and 16 output channels, connected to a 50 MHz 486 PC running under the QNX operating system. A Keithley DAS 1601 card installed inside the computer was used to send the displacement command signal to a Moog controller connected to the actuator servovalve. The Autonet software was used to develop a computer program to generate and apply the required actuator displacement history (for servo-controlled tests) and to read the instrumental measurements. Readings were stored in binary format (Autonet LDF) during testing, and at the end of each test, data was backed up and exported as an ASCII text file through the Department's Ethernet network to another PC for processing.

Extremely valuable visual (and sometimes aural) information was generated by videotaping (Figure 10b) and taking numerous photographs during each test. White-wash coating (hydrated lime) was used for revealing the qualitative patterns of strain distribution in the specimen during the test.

LOADING HISTORY

The testing program was based on the ATC-24 document "Guidelines for Cyclic Seismic Testing of Steel Structures" [3]. The specimens were tested under displacement control, following a loading history consisting of stepwise increasing deformation cycles. Each loading step was defined by the peak deformation (actuator displacement) and by the number of cycles, as shown in Figure 11.

DATA PROCESSING

The specimen behavior was characterized by the following parameters: applied load, beam end displacement, plastic rotation, column deformation, panel zone shear deformation, and beam deflection. A test specimen layout, corresponding measurements, and chosen positive direction of applied load, measured displacements, and rotations are shown in Figure 12.

Total displacement of the beam end (δ_{total}) is caused by the deformations of beam itself, column and panel zone. As a result of the column and panel zone deformations, the panel zone rotates on a certain angle (θ_c) and changes its initial configuration. The panel zone position and configuration for a deformed specimen are shown in Figure 13. Four displacement measurements ($\delta_1, \delta_2, \delta_3$, and δ_4) were used to compute the connection rotation (θ_c) and panel zone shear deformation (γ). The total displacement of the beam end (δ_{total}) can be separated into three components: displacement due to deformation of the beam itself (δ_b), displacement caused by rigid connection rotation (δ_c), and the contribution from the panel zone shear (δ_s) as shown in Figure 14. These values were determined as follows:

- Beam end displacement: δ_{total}
- Total rotation: $\theta_{total} = \frac{\delta_{total}}{L}$
where L is the "clear length" of the beam. For the DASSE specimens this value was calculated with respect to the center of the plastic hinge ($L = L_b - L_{cc}$).
- Connection rotation: $\theta_c = \frac{\delta_1 - \delta_2}{d_{12}}$
- Panel zone shear deformation: $\gamma = \frac{\sqrt{a^2 + b^2}}{2ab}(\delta_3 - \delta_4)$

where a and b are the dimensions of the rectangular panel zone area used for measuring the panel zone shear deformation.

- Beam deflection: $\delta_b = \delta_{total} - \theta_c \cdot \left(L_b + \frac{d_c}{2} \right) + \gamma \frac{d_c}{2}$
- Total plastic rotation: $(\theta_{total})_{pl} = \theta_{total} - \frac{M}{K_\theta}$

where $M = Q(L_{act} - L_{cp})$ is the moment at the bottom cover plate edge and K_θ is the elastic stiffness determined from the $M - \theta_{total}$ curve. The unloading path of one of the elastic cycle

below the reverse point was used to estimate stiffness, to avoid the influence of initial imperfections, clearances, hysteresis, etc. The range from $0.8M_{peak}$ to $0.2M_{peak}$ was fit in a least-squares sense to determine the slope of the elastic curve.

A set of MATLAB (v4.0) programs was created to process data and to plot results in accordance with the procedure described above.

TEST RESULTS

SPECIMEN 1

Specimen 1 was tested on August 20, 1996. The specimen sustained all loading steps up to and including the 5.5" actuator displacement cycles without fracture. The imposed loading history is shown in Figure 15.

First spalling of the white-wash due to yielding was noticed during 0.75" cycles on the top beam flanges near the cover plate. During 1" and 2" cycles white-wash flakes covered the beam flanges on more than three quarters of the cut zone and extended into the beam web near the cut center line. The white-wash flakes distribution indicated conclusively that plastic hinge developing began in the weakened zone of the beam. During 3" actuator displacement cycles the plastic hinge was formed and local buckling of the bottom beam flange was noticed near the cut center. The beam web also started buckling. Beam buckling during 3" and following cycles was accompanied by degradation of the maximum load. At the maximum displacement (-5.5") the strength deterioration reached 57%. Beam buckling (measured after the test) can be briefly outlined as follows: top flange ~2.5" , bottom flange ~3.25"; and the out-of-plane buckling of the beam web had a wave shape with peak distortions +1.5" and -5.5" . There were no visible fractures observed.

Plots of applied load versus beam end displacement response and moment at column face versus plastic rotation are presented in Figures 16 and 17, respectively. Plastic rotation was calculated with respect to the center of the plastic hinge. A graph showing the energy dissipated by the specimen versus cumulative actuator displacement is presented in Figure 18. Panel zone shear deformation (average) is shown in Figure 19. Beam deflection (total beam end displacement minus column and panel zone contributions) is shown in Figure 20. Plots of local strains in selected points are presented in Figures 21 - 28. Photographs in Figures 29 - 34 illustrate the observed behavior of the beam during the test.

Key parameters characterizing the specimen performance presented in Table 2.

SPECIMEN 2

Specimen 2 was tested on September 16, 1996. The overall behavior of Specimen 2 was very similar to that of Specimen 1. The specimen sustained all loading steps up to and including two 5.5" actuator displacement cycles without fracture. Test was continued and the specimen failed during the 3rd 5.5" cycle. The imposed loading history is shown in Figure 35.

First spalling of the white-wash due to yielding was noticed during 0.5" cycles on the top beam flange near the cover plate. During 2" cycles white-wash flakes covered the beam flanges on more than half of the cut zone and extended into the beam web between the ends of cover plates and the cut center line. The white-wash flakes distribution indicated conclusively that plastic hinge developing began in the weakened zone of the beam. During 3" actuator displacement cycles the plastic hinge was formed and local buckling of the beam flanges (bottom flange - first) was noticed near the cut center. The beam web also started buckling. Beam buckling during 3" and following cycles was accompanied by degradation of the maximum load. At the maximum displacement (-5.5") the strength deterioration reached 54%. Beam buckling (measured after the test) can be briefly outlined as follows: top flange ~3" , bottom flange ~3.5"; and the out-of-plane buckling of the beam web had a wave shape with peak distortions from the initial beam web plane equal +1.5" and -4" .

Cracks were noticed on the bottom beam flange during the third 5.5" cycle. Cracks development was accompanied by rapid deterioration of the load and at the end of the cycle the major crack cut a half of the bottom beam flange. At that point the test was stopped.

Plots of applied load versus beam end displacement response and moment at column face versus plastic rotation are presented in Figures 36 and 37, respectively. Plastic rotation was calculated with respect to the center of the plastic hinge. A graph showing the energy dissipated by the specimen versus cumulative actuator displacement is presented in Figure 38. Panel zone shear deformation (average) is shown in Figure 39. Beam deflection (total beam end displacement minus column and panel zone contributions) is shown in Figure 40. Plots of local strains in selected points are presented in Figures 41 - 60. Photographs in Figures 61 - 66 show behavior of the specimen during the test.

Key parameters characterizing the specimen performance are presented in Table 2.

SPECIMEN 3

Specimen 3 was tested on August 27, 1996. The specimen failed suddenly during the second 3" cycle. Imposed loading history is shown in Figure 67. It should be noted that, prior the testing noticeable distortions (about 0.5") of both column stiffeners (continuity plates) were observed which seemed to indicate the presence of unanticipated residual stresses.

First spalling of the white-wash due to yielding was noticed during 1" cycles on the column web. They occurred in the beam side corners of the panel zone. During 2" cycles white-wash flakes appeared on the beam web and beam flanges near the cut center. The white-wash flakes distribution indicated conclusively that plastic hinge developing began in the weakened zone of the beam.

The specimen failed suddenly during the second 3" cycle. Welds between bottom continuity plates and column fractured and the cracks cut the column web at about 9" each way from the continuity plate. It should be noted that only two fractured welds had back-up bars left in place. Six others welds of this type were rejected by UT (as it was reported) and repaired.

Plots of applied load versus beam end displacement response and moment at column face versus plastic rotation are presented in Figures 68 and 69, respectively. Plastic rotation was calculated with respect to the center line of the circular cuts. A graph showing the energy dissipated by the specimen versus cumulative actuator displacement is presented in Figure 70. Panel zone shear deformation (average) is shown in Figure 71. Beam deflection (total beam end displacement minus column and panel zone contributions) is shown in Figure 72. Plots of local strains in selected points are presented in Figures 73 - 80. Photographs in Figures 81 - 83 show behavior of the specimen during the test. Fracture details are shown in Figures 84 - 88.

Key parameters characterizing the specimen behavior presented in Table 2.

On August 28 the test was continued to determine the ability of the connection to withstand applied load after fracture. During this post-fracture test the actuator displacement cycles were exercised only in one direction (negative sense) to prevent further propagation of cracks. Crack propagation was observed when the load reached +170 kips. The imposed displacement history and corresponding load response are shown in Figures 89 and 90, respectively. The following peak values were measured during this test:

- Max Actuator Displacement -5.48 inches
- Maximum Load -379 kips

Additional metallurgical analysis of the failed weld joint were performed by Schwein/Cristensen Laboratories, Inc. According to their study [5] both welded joints were cracked prior to the test at UC Berkeley. This was because "the preheat temperature was not properly maintained and/or the 150°F minimum code requirement is inadequate for this thickness of material and the highly constrained joint condition."

SPECIMEN 4

Specimen 4 was tested on August 27, 1996. The specimen dimensions, geometry, and materials were the same as for Specimen 3 (W36x194 beam and W33x387 column of A572-Gr50 steel). Because of the sudden failure of Specimen 3, weld inspection was emphasized during the

fabrication of this specimen. It should be noted that the beam bottom flange had an initial distortion in the dogbone region measuring about 1/4".

The specimen sustained all loading steps up to and including the 5.5" actuator displacement cycles without fracture. The imposed loading history is shown in Figure 91.

First spalling of the white-wash due to yielding was noticed during 1" cycles in the beam side corners the column panel zone. Flaking was less than what was observed for Specimen 3. During 2" cycles white-wash flakes appeared on the beam web and beam flanges near the cut center. The white-wash flakes distribution indicated conclusively that plastic hinge developing began in the weakened zone of the beam. During 3" cycles the plastic hinge was formed and local buckling of the beam bottom flange and beam web was noticed near the cut center line. Buckling of the beam top flange was moderate and was accompanied only by small force degradation and the maximum strength deterioration was less than 15%. There were no visible fractures observed except a few small local cracks in the most deformed zones of the beam bottom flange (the maximum length of the cracks did not exceed 1/4").

Plots of applied load versus beam end displacement response and moment at column face versus plastic rotation are presented in Figures 92 and 93, respectively. Plastic rotation was calculated with respect to the center line of the circular cuts. A graph showing the energy dissipated by the specimen versus cumulative actuator displacement is presented in Figure 94. Panel zone shear deformation (average) is shown in Figure 95. Beam deflection (total beam end displacement minus column and panel zone contributions) is shown in Figure 96. Plots of local strains in selected points are presented in Figures 97 - 120. Photographs in Figures 121 - 128 show behavior of the specimen during the test.

Key parameters characterizing the specimen behavior presented in Table 2.

REFERENCES

1. Popov E., Blondet M., Stepanov L., *Application of "Dog Bones" for Improvement of Seismic Behavior of Steel Connections* (Report No. UCB/EERC-96/05), Earthquake Engineering Research Center, University of California at Berkeley, June 1996.
2. Engelhardt M., Winnerberger T., Zekany A., Potyraj T., *The Dogbone Connection: Part II*, *Modern Steel Construction*, 46 - 55, August 1996.
3. Krawinkler, H., *Guidelines for Cyclic Seismic Testing of Components of Steel Structures*, (Report No. ATC-24), Applied Technology Council, Redwood City, California, 1992.
4. Schwein/Christense Laboratories, Inc., "Continuity Plate Weld Failure - DASSE SMRF Test Connection #3 - McCandless Tower #2 Project", SCL Project 96290A, Report to DASSE Design, Inc., September 1996.

TABLE 1: CHANNEL - INSTRUMENT LIST

Box 17 (I/O Connector 1)

channel	cont. #	label	device	description	miscellaneous
1	1	KTEMPA	tempo	temposonic	
2	2	KLC	i.cell	load cell	
3	3	KEMP3		spare	
4	4	KEMP4		spare	
5	5	KEMP5		spare	
6	6	KEMP6		spare	
7	7	KEMP7		spare	
8	8	KEMP8		spare	
9	9	KEMP9		spare	
10	10	KEMP10		spare	
11	11	KEMP11		spare	
12	12	KEMP12		spare	
13	13	KEMP13		spare	
14	14	KEMP14		spare	
15	15	KEMP15		spare	
16	16	KP1B17	trafo	power supply	

Box 18 (I/O Connector 10)

channel	cont. #	label	device	description	miscellaneous
17	1	KSG17	sg 120	top flange 1 (edge)	All specimens
18	2	KSG18	sg 120	top flange 2 (axis)	All specimens
19	3	KSG19	sg 120	top flange 3 (edge)	All specimens
20	4	KSG20	rg 120	top "db" hor (edge)	All specimens
21	5	KSG21	rg 120	top "db" dia (edge)	Sp. 4 only
22	6	KSG22	rg 120	top "db" ver (edge)	Sp. 2 & 4 only
23	7	KSG23	rg 120	top "db" hor (axis)	All specimens
24	8	KSG24	rg 120	top "db" dia (axis)	Sp. 4 only
25	9	KSG25	rg 120	top "db" ver (axis)	Sp. 2 & 4 only
26	10	KSG26	sg 120	top "db" hor (edge)	All specimens
27	11	KSG27	sg 120	top stiffener	Sp. 2 & 4 only
28	12	KSG28	rg 120	PZ top corner hor	Sp. 2 & 4 only
29	13	KSG29	rg 120	PZ top corner dia	Sp. 2 & 4 only
30	14	KSG30	rg 120	PZ top corner ver	Sp. 2 & 4 only
31	15	KEMP31		spare	
32	16	KP1B18	trafo	power supply	

Box 19 (I/O Connector 11)

channel	cont. #	label	device	description	miscellaneous
33	1	KSG33	sg 120	bot flange 1 (edge)	All specimens
34	2	KSG34	sg 120	bot flange 2 (axis)	All specimens
35	3	KSG35	sg 120	bot flange 3 (edge)	All specimens
36	4	KSG36	sg 120	bot "db" hor (edge)	All specimens
37	5	KSG37	sg 120	bot "db" dia (edge)	Sp. 4 only
38	6	KSG38	sg 120	bot "db" ver (edge)	Sp. 2 & 4 only
39	7	KSG39	rg 120	bot "db" hor (axis)	All specimens
40	8	KSG40	rg 120	bot "db" dia (axis)	Sp. 4 only
41	9	KSG41	rg 120	bot "db" ver (axis)	Sp. 2 & 4 only
42	10	KSG42	rg 120	bot "db" hor (edge)	All specimens
43	11	KSG43	rg 120	bot stiffener	Sp. 2 & 4 only
44	12	KSG44	rg 120	PZ bot corner hor	Sp. 2 & 4 only
45	13	KSG45	rg 120	PZ bot corner dia	Sp. 2 & 4 only
46	14	KSG46	rg 120	PZ bot corner ver	Sp. 2 & 4 only
47	15	KEMP47		spare	
48	16	KP1B19	trafo	power supply	

Box 29 (I/O Connector 13)

channel	cont. #	label	device	description	miscellaneous
65	1	KEM129		spare	
66	2	KEM130		spare	
67-131	3	KPCNRT	spot 4"	cnct. rotation top	
68-132	4	KPCNRB	spot 4"	cnct. rotation bot	
69-133	5	KPWBST	spot 2"	web shear NE to SW	
70-134	6	KPWBSB	spot 2"	web shear SE to NW	
71	7	KEM135		spare	
72	8	KEM136		spare	
73-137	9	KPNSTT	spot 2"	north seat top	
74	10	KEM138		spare	
75-139	11	KPNSTA	spot 2"	north seat axial	
76-140	12	KPSSTT	spot 2"	south seat top	
77	13	KEM141		spare	
78-142	14	KWPTA	wpot 15"	control act displ	
79-143	15	KWPTD	wpot 15"	control tip dipl.	
80	16	KP2B29	trafo	power supply	

- sg 120: 120 Ω strain gage
- rg 120: 120 Ω rosette strain gage
- wpot 15": wire pot with 15" stroke
- spot 2": stick pot with 2" stroke
- spot 4": stick pot with 4" stroke

TABLE 2: SUMMARY OF TEST RESULTS

	#1	#2	#3	#4
Yield Load, [kips]	133	147	229	253
Beam End Displacement @Yield, [inch]	0.80	0.89	0.83	0.96
Max Measured Actuator Displacement, [inch] *	+5.48 -5.44	+5.47 -5.48	+3.00 -3.00	+5.51 -5.51
Max Beam End Displacement, [inch] *	+4.68 -4.92	+4.80 -4.95	+2.47 -2.51	+4.72 -4.95
Beam End Displacement @Failure, [inch]	N/A	N/A	1.65	N/A
Maximum Load, [kips] *	+201 -199	+200 -199	+359 -375	+372 -382
Load @Max Displacement, [kips] *	+97 -86	+102 -92	+350 -368	+320 -336
Load @Failure, [kips]	N/A	N/A	356	N/A
Plastic Rotation Range, [rad] *	+0.044 -0.048	+0.047 -0.049	+0.013 -0.013	+0.039 -0.041
Beam End Displacement @ 3% Plastic Rotation	3.66	3.66	N/A	4.12
Dissipated Energy, [kip-inch]	14, 250	15, 600	3, 200	27, 900

* Values are given for positive (+) and negative (-) excursions of loading cycles

FIGURE 1: TEST SPECIMEN

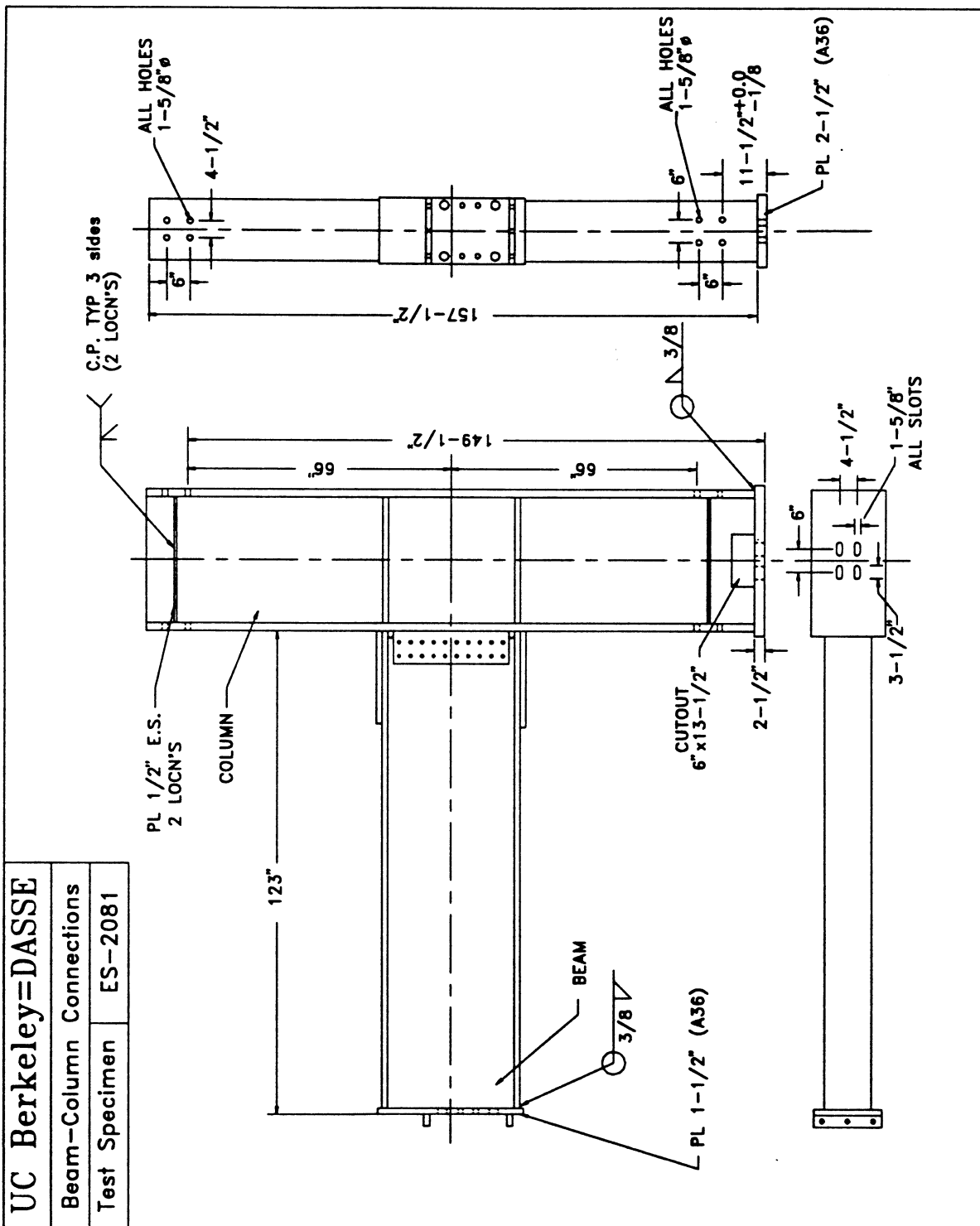


FIGURE 2: CONNECTION DETAILS

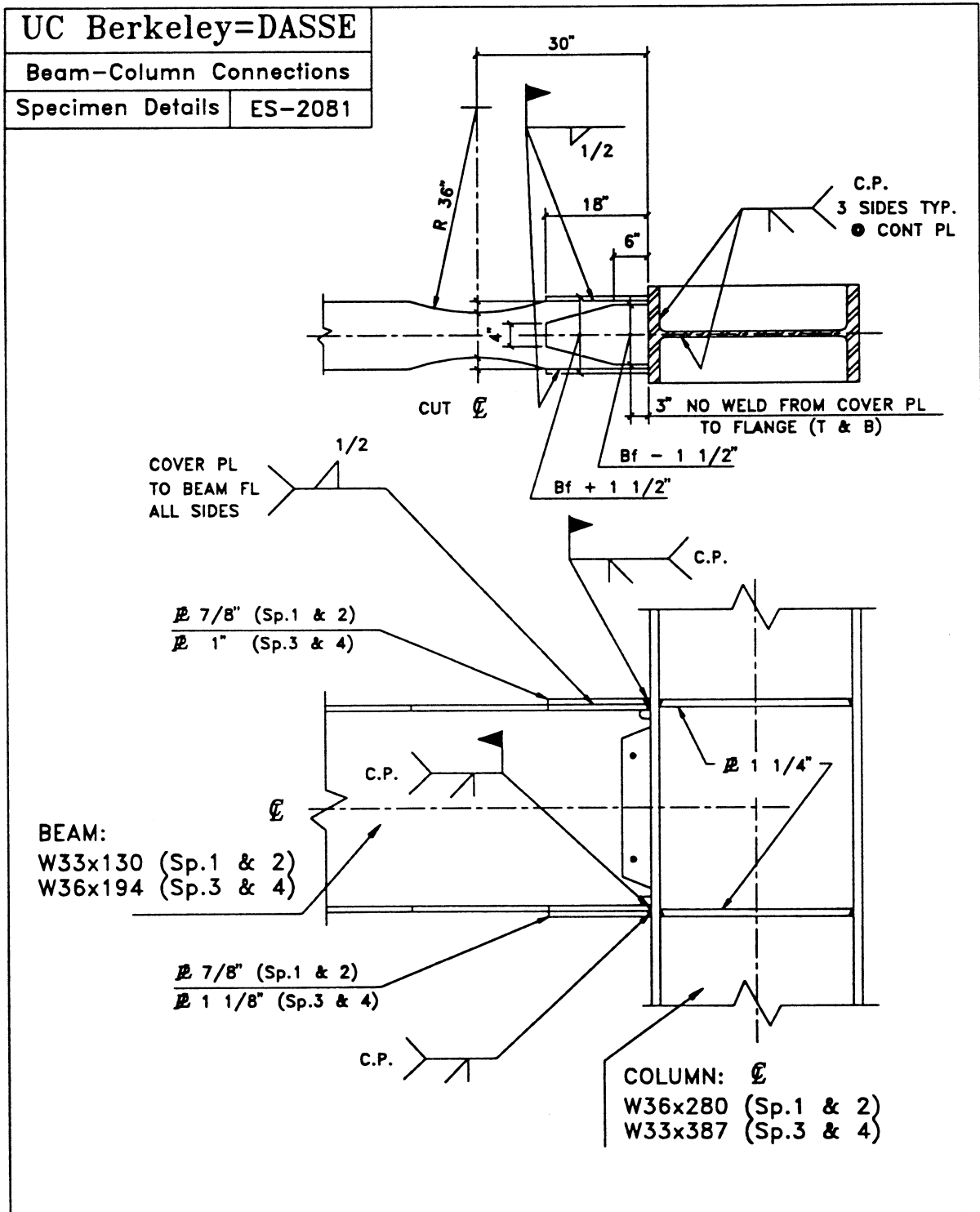


FIGURE 3: TEST SETUP

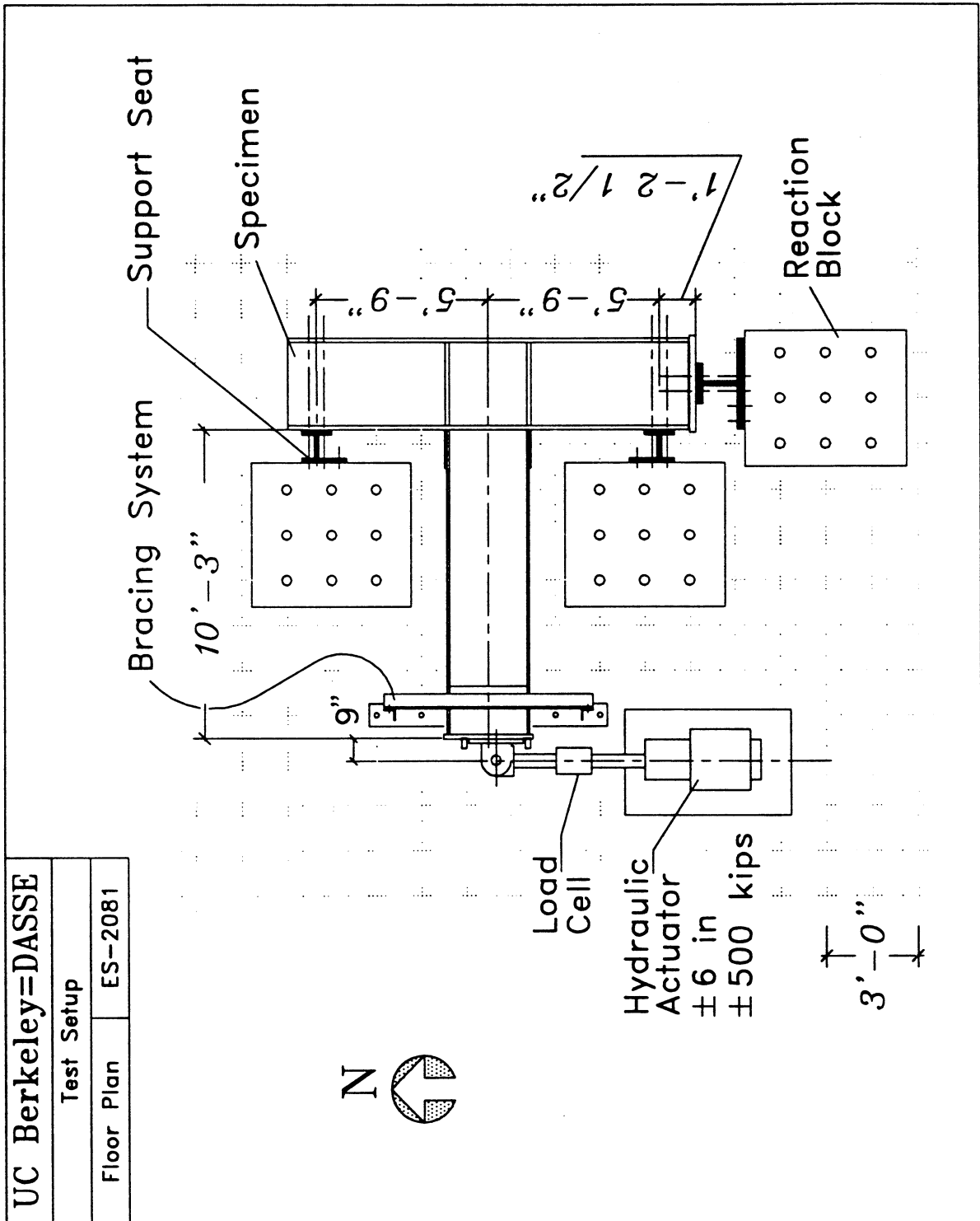


FIGURE 4: PHOTOGRAPH SHOWING A SPECIMEN TESTING

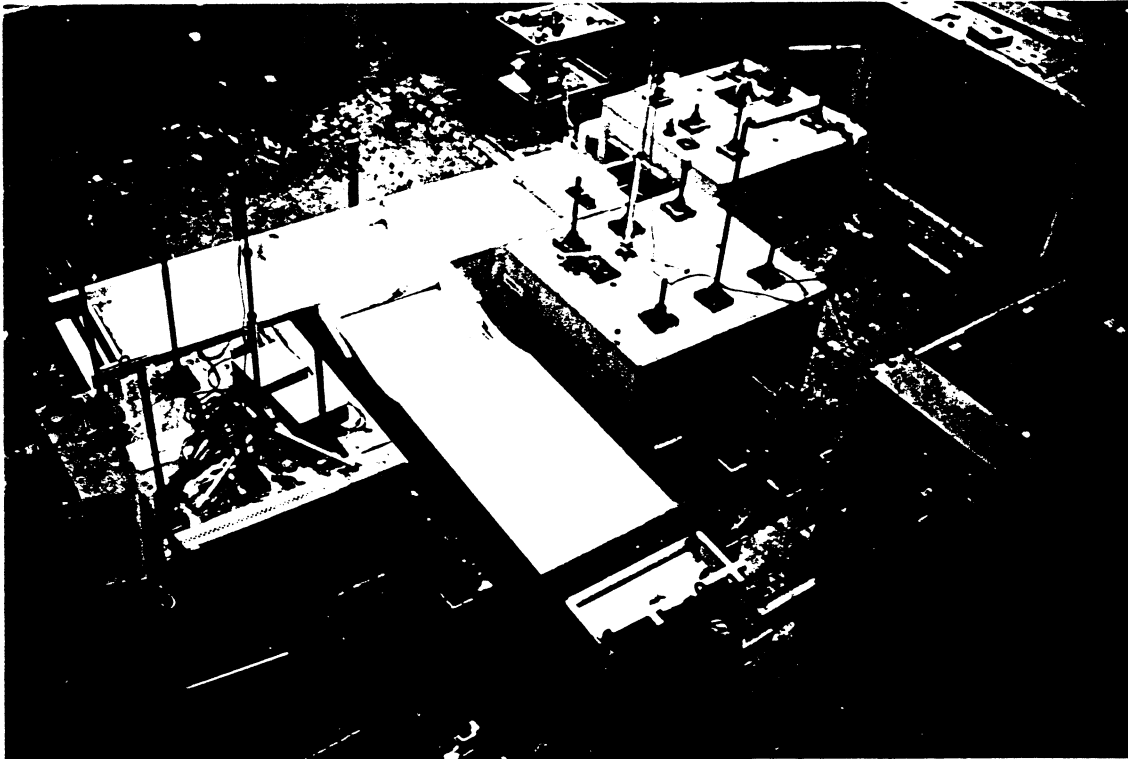


FIGURE 5: COLUMN BOTTOM END SUPPORT

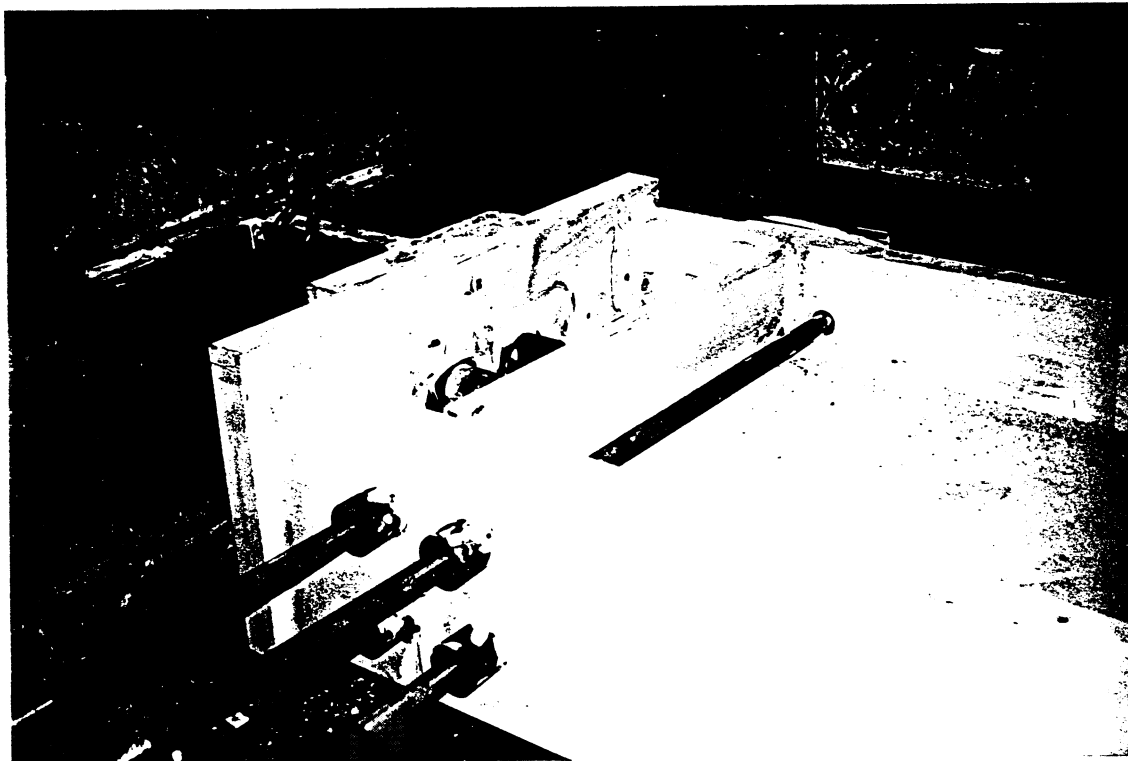


FIGURE 6: COLUMN TOP END SUPPORT

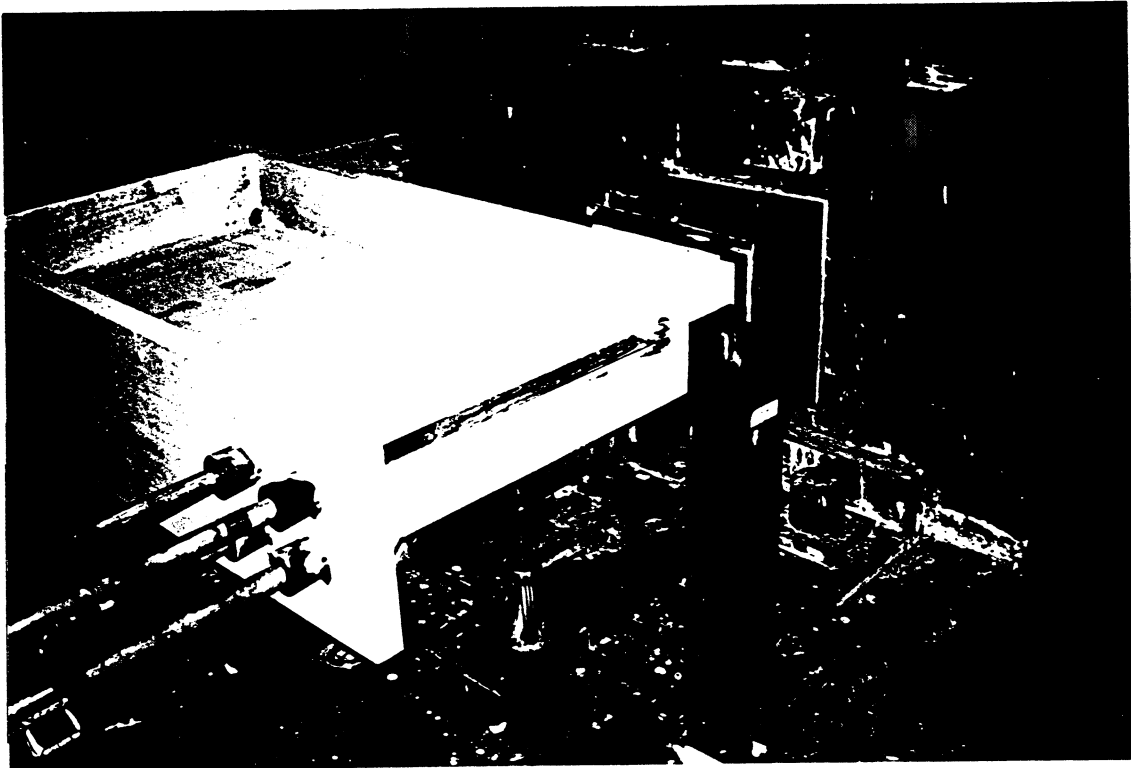


FIGURE 7: CLEVIS CONNECTING THE ACTUATOR TO THE BEAM END

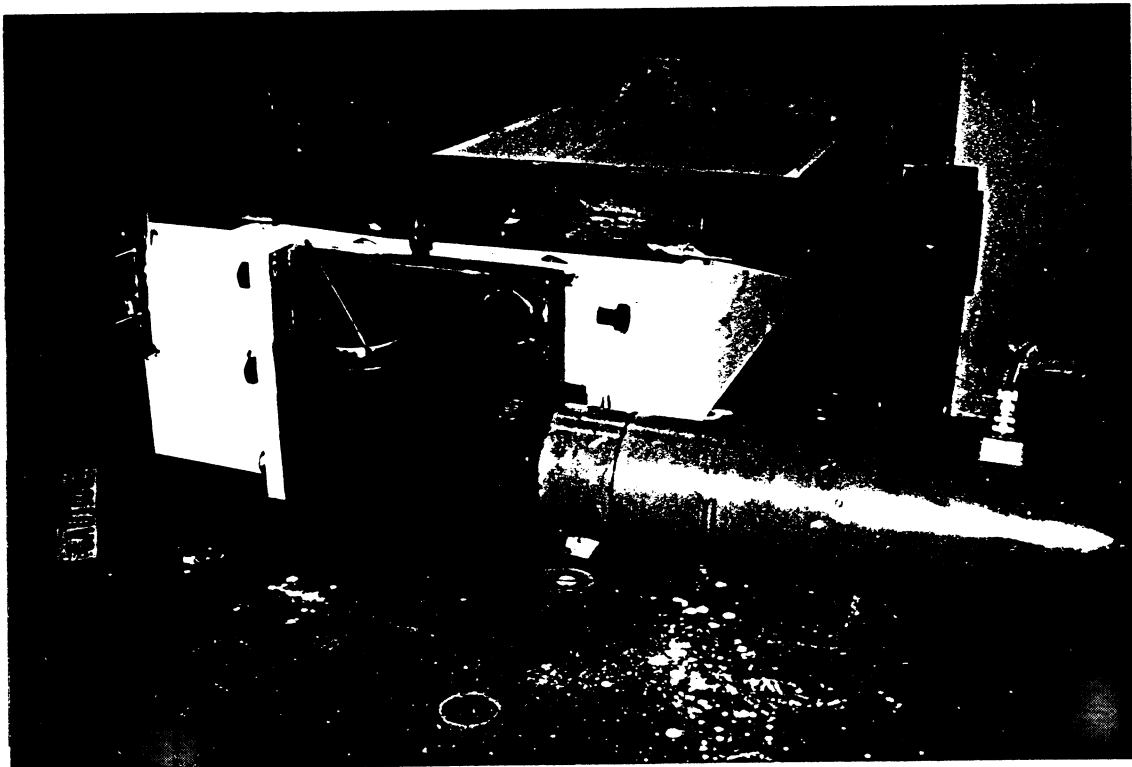


FIGURE 8: SPECIMEN INSTRUMENTATION -- POTENTIOMETERS

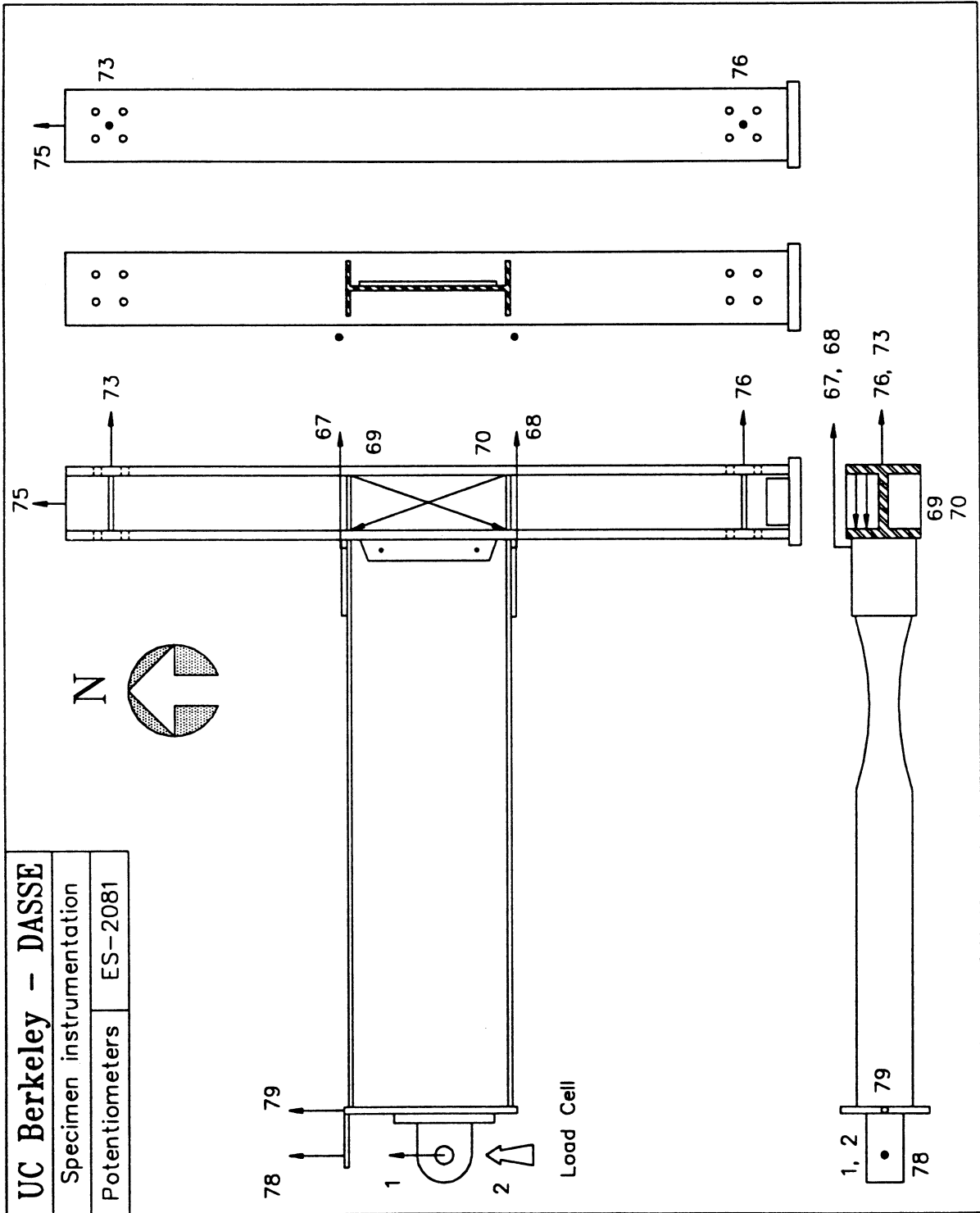


FIGURE 9: SPECIMEN INSTRUMENTATION -- STRAIN GAGES

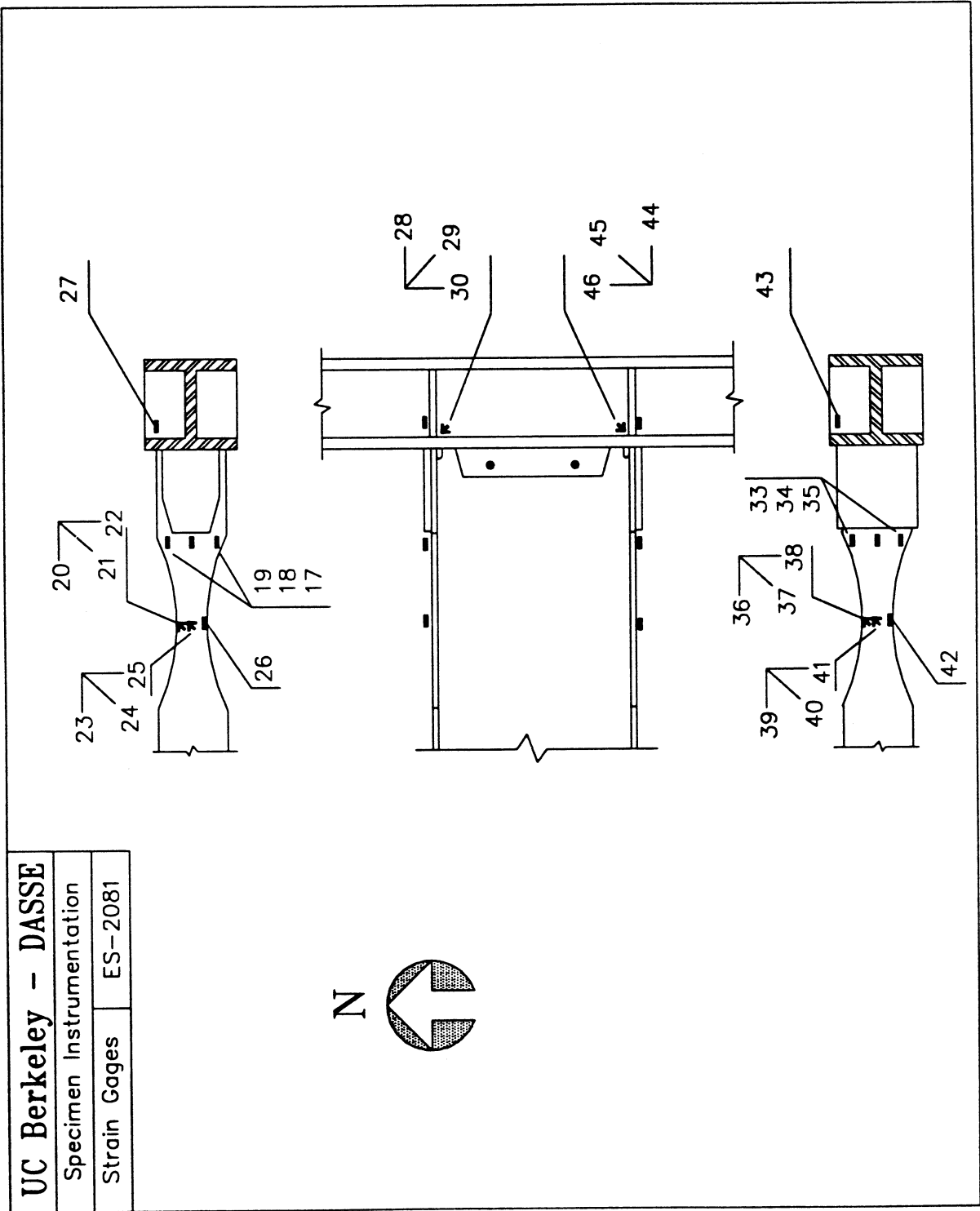


FIGURE 10A: DATA ACQUISITION AND CONTROL SYSTEM

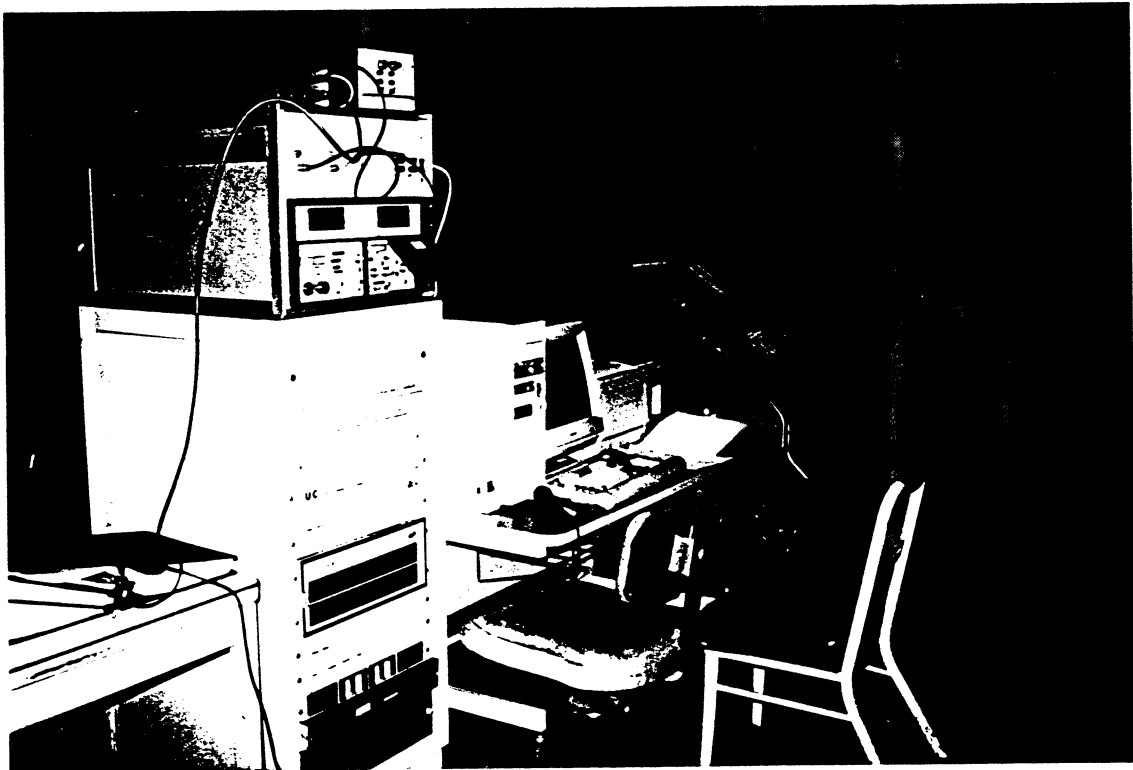
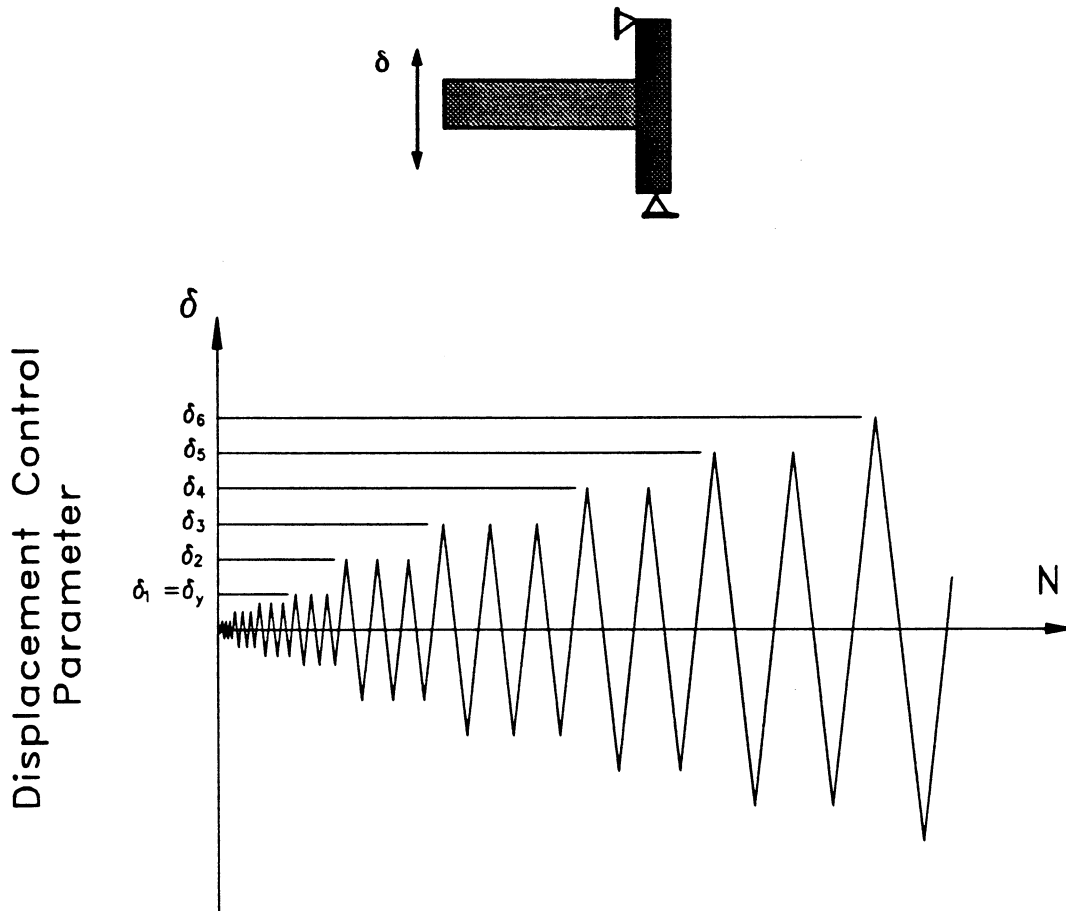


FIGURE 10B: VIDEOMONITORING OF SPECIMEN BEHAVIOR DURING THE TEST



FIGURE 11: TEST PROGRAM



Load Step	Peak Displacement [inch]	Displacement Rate [in/sec]	Number of Cycles	Comments
1	0.10	0.05	2	Equipment Test
2	0.25	0.01	3	
3	0.50	0.01	3	
4	0.75	0.01	3	
5	1.00	0.01	3	Reference point
6	2.00	0.01	3	
7	3.00	0.01	3	
8	4.00	0.01	2	
9	5.00	0.02	2	
10	5.50	0.02	n	

FIGURE 12: TEST SPECIMEN -- REFERENCE DIMENSIONS AND MEASUREMENTS

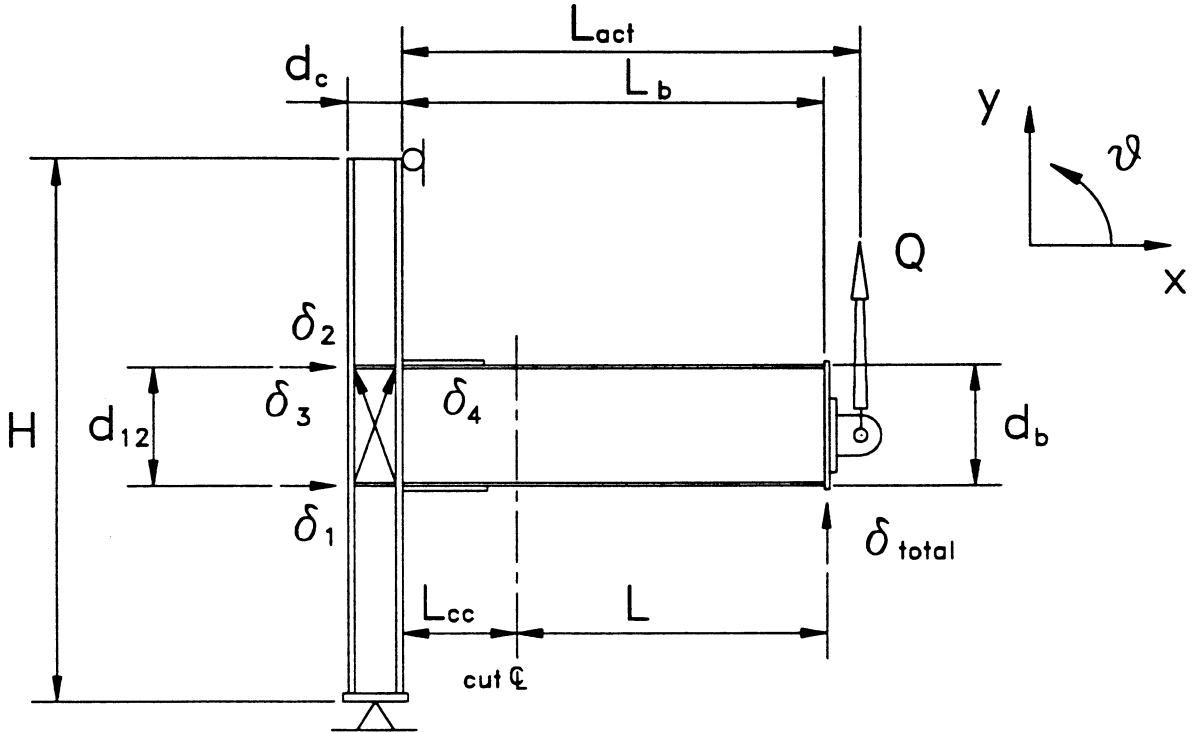


FIGURE 13: PANEL ZONE DEFORMATION

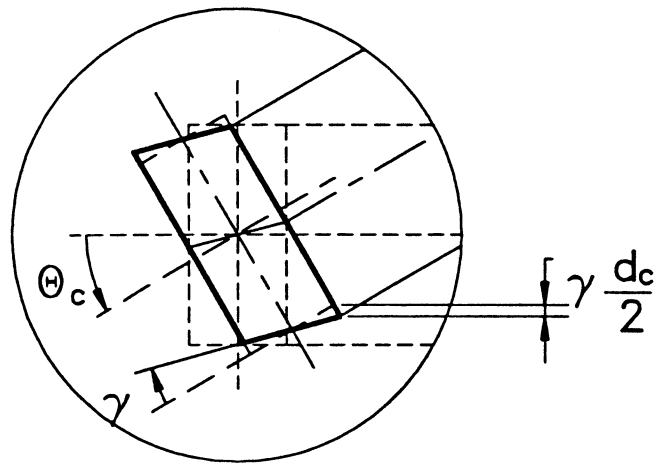


FIGURE 14: CONTRIBUTIONS IN TOTAL BEAM END DISPLACEMENT

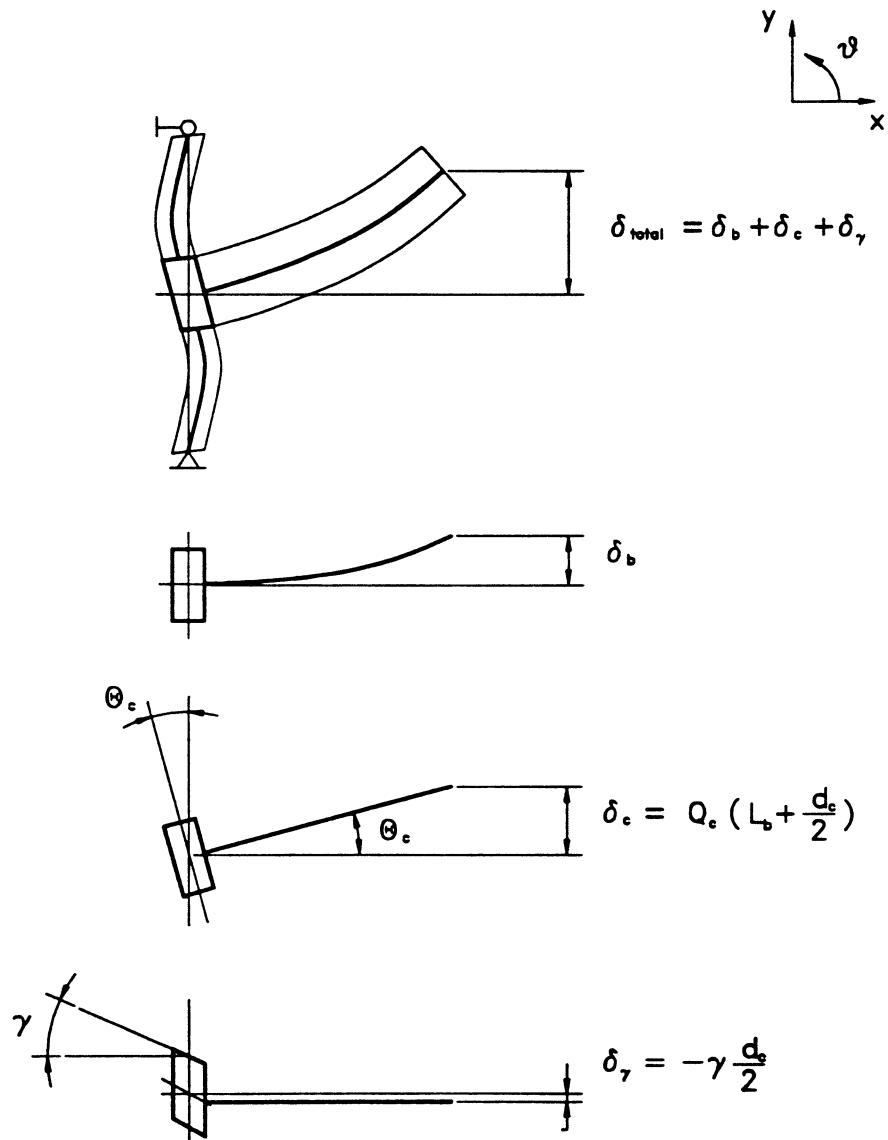


FIGURE 15: IMPOSED LOADING HISTORY -- ACTUATOR DISPLACEMENT

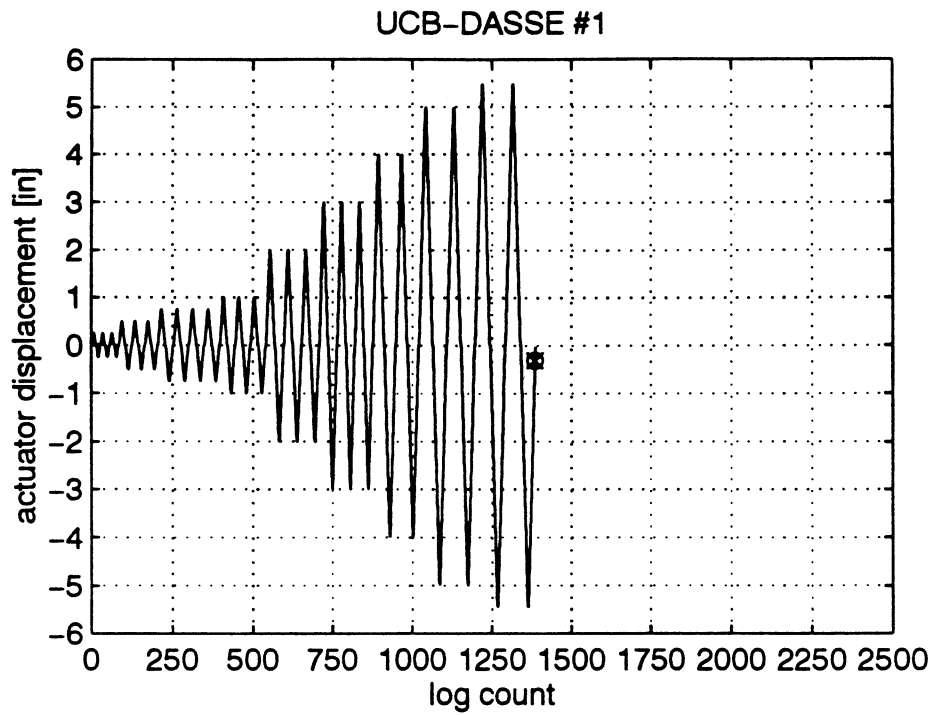


FIGURE 16: APPLIED LOAD / BEAM END DISPLACEMENT RESPONSE

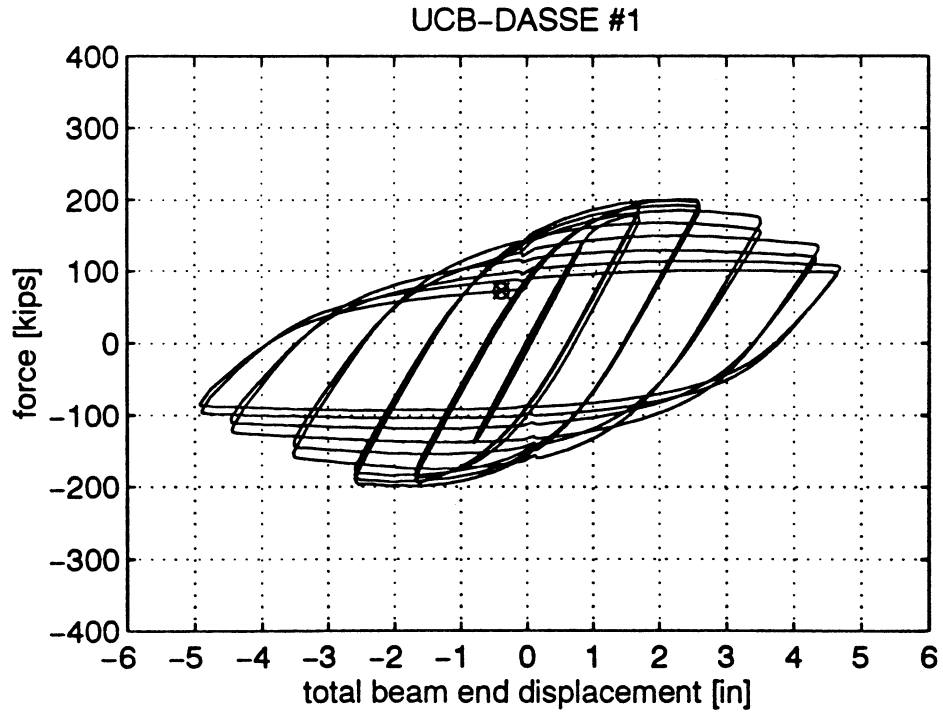


FIGURE 17: PLASTIC ROTATION VERSUS MOMENT @ COVER PLATE EDGE

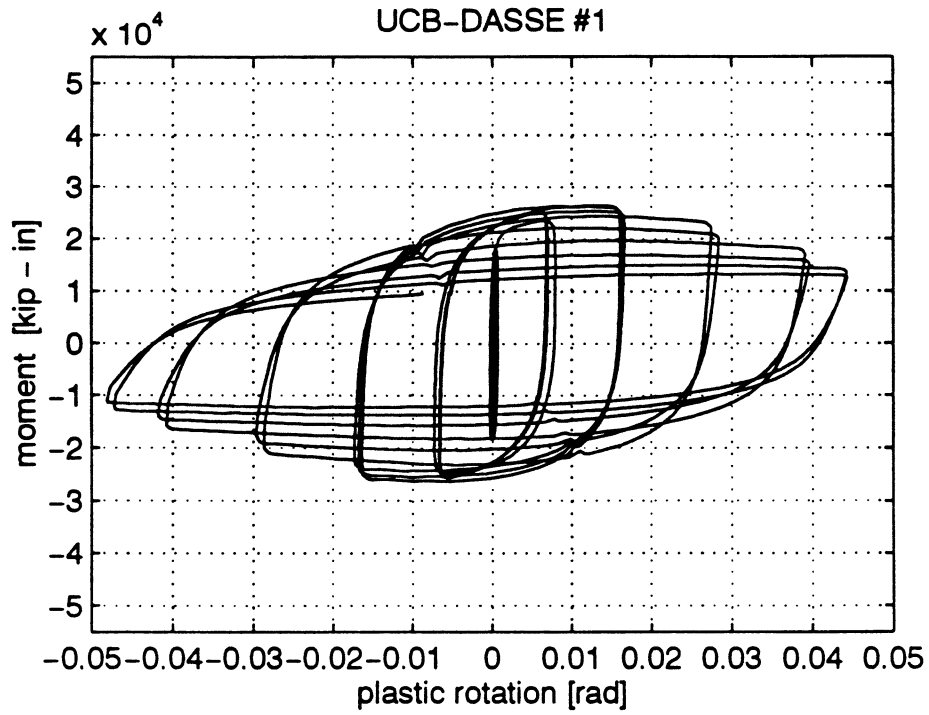


FIGURE 18: DISSIPATED ENERGY

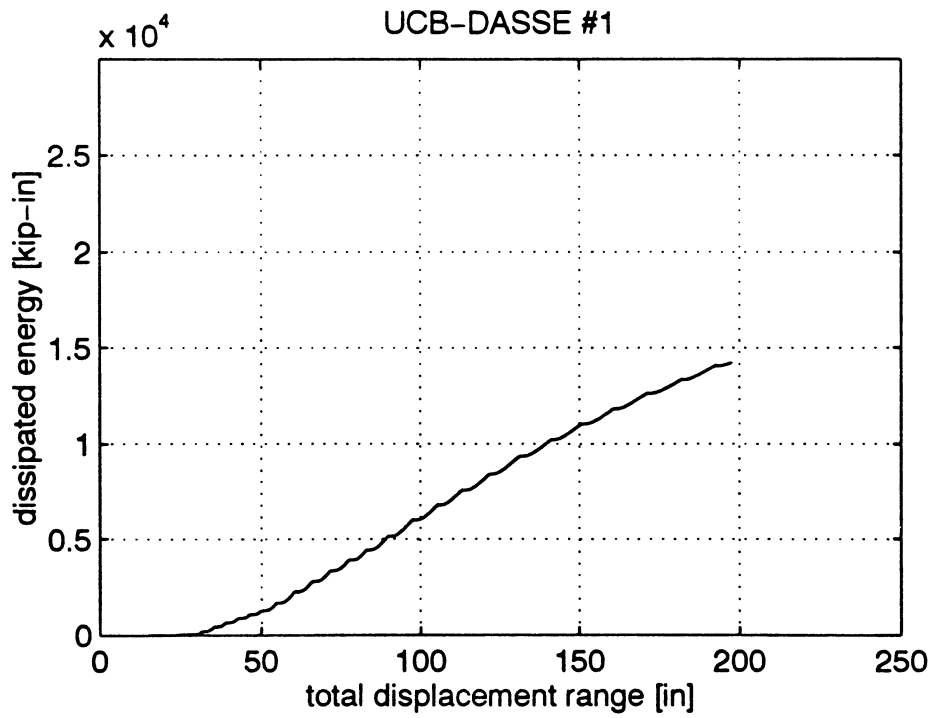


FIGURE 19: PANEL ZONE SHEAR DEFORMATION

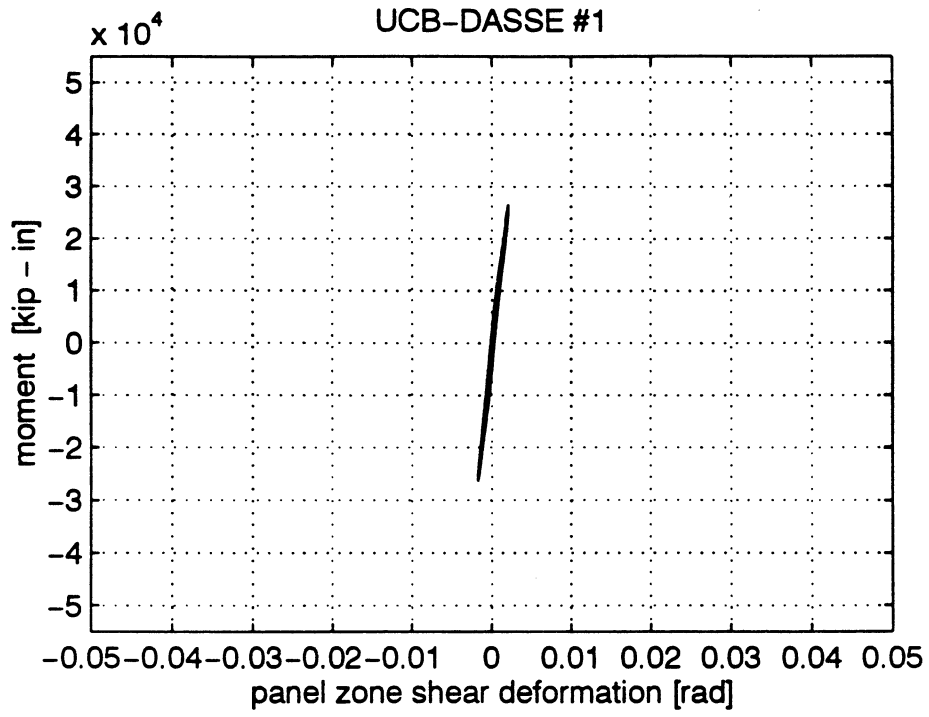


FIGURE 20: BEAM CONTRIBUTION TO TOTAL DISPLACEMENT

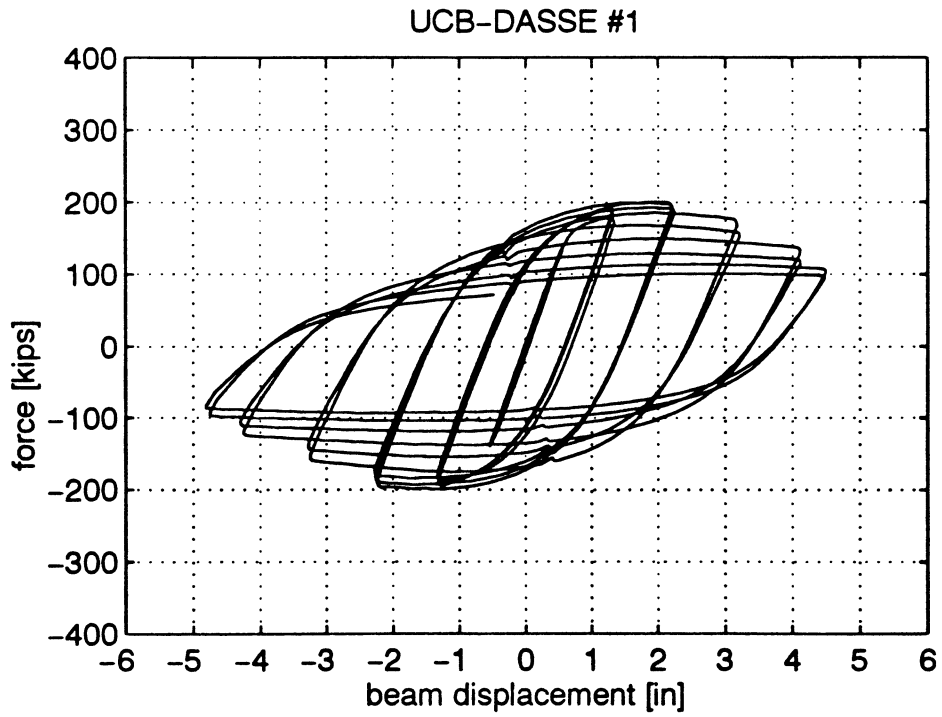


FIGURE 21: LOCAL RESPONSE -- TOP BEAM FLANGE EDGE (@ COVER PLATE)

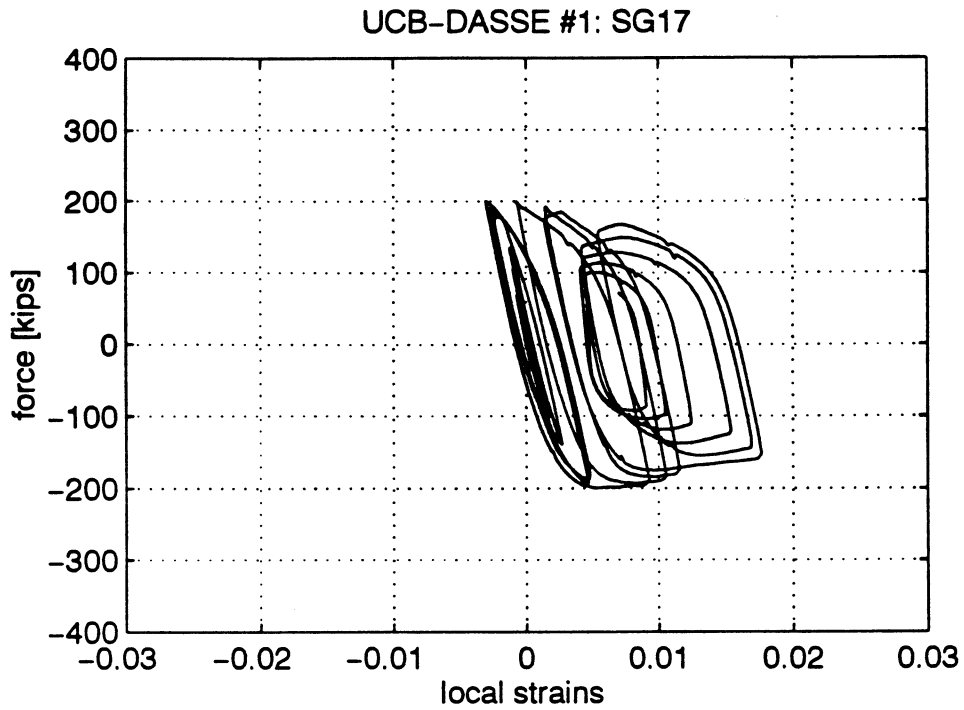


FIGURE 22: LOCAL RESPONSE -- TOP BEAM FLANGE AXIS (@ COVER PLATE)

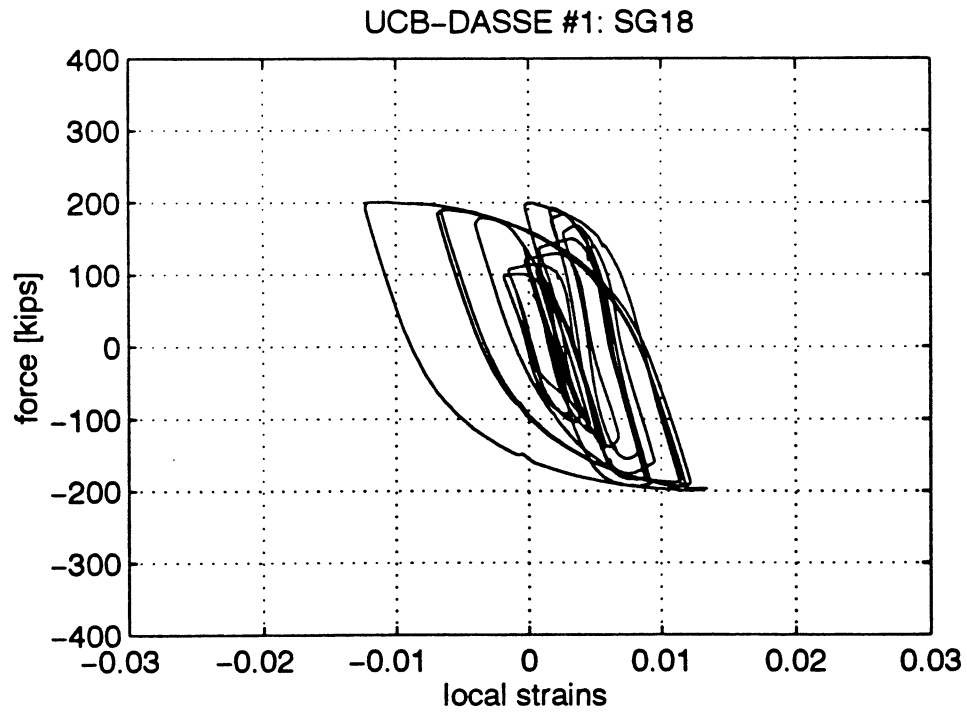


FIGURE 23: LOCAL RESPONSE -- BOTTOM BEAM FLANGE EDGE (@ COVER PLATE)

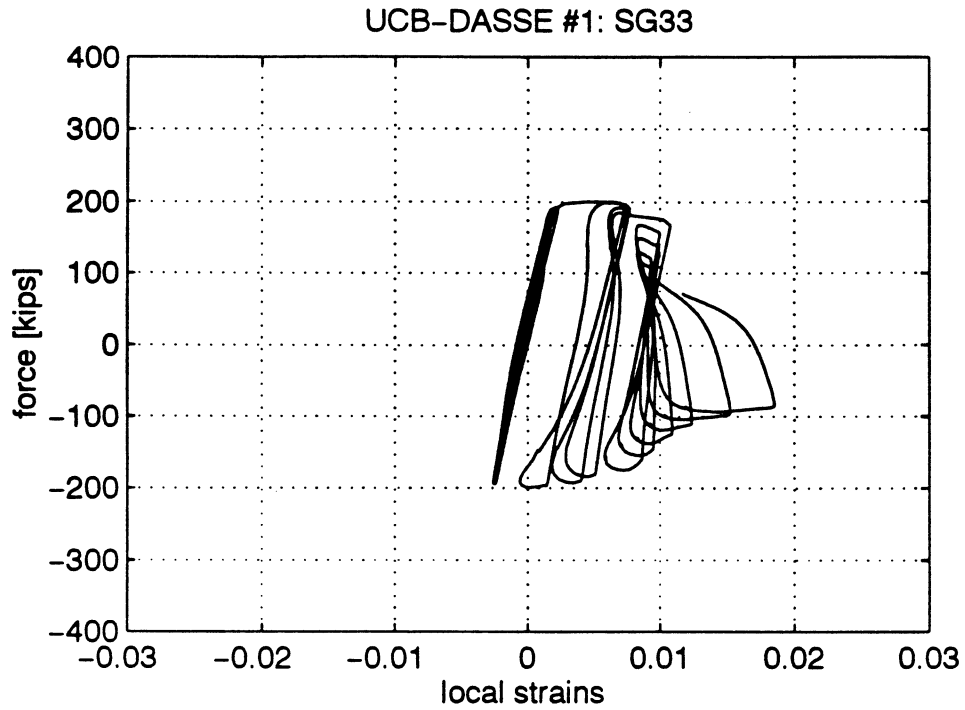


FIGURE 24: LOCAL RESPONSE -- BOTTOM BEAM FLANGE AXIS (@ COVER PLATE)

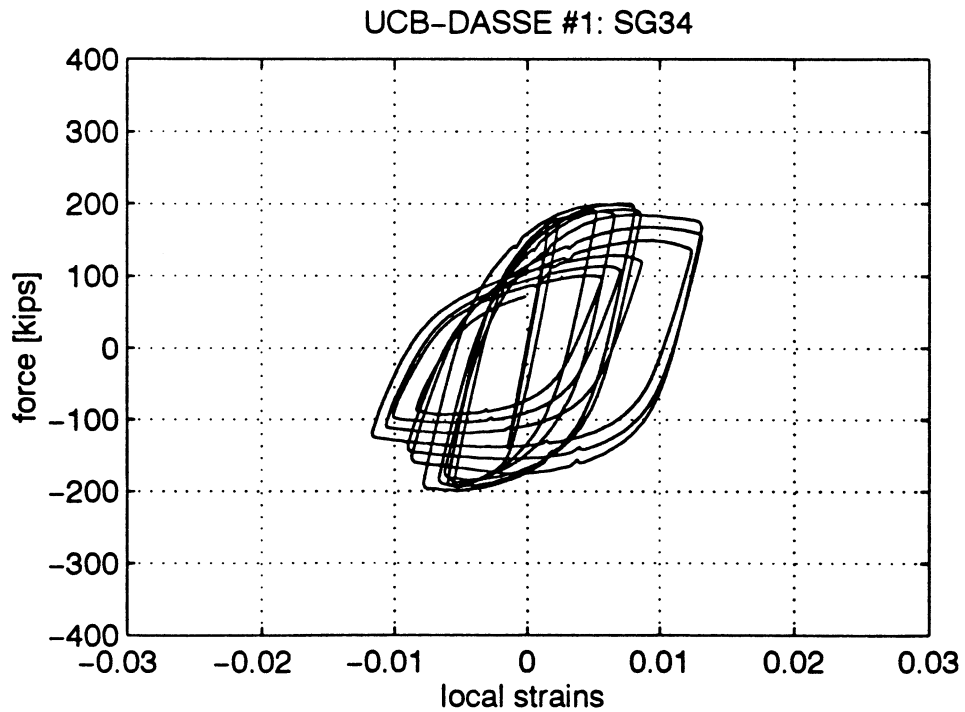


FIGURE 25: LOCAL RESPONSE -- TOP FLANGE EDGE (@ "DOG BONE")

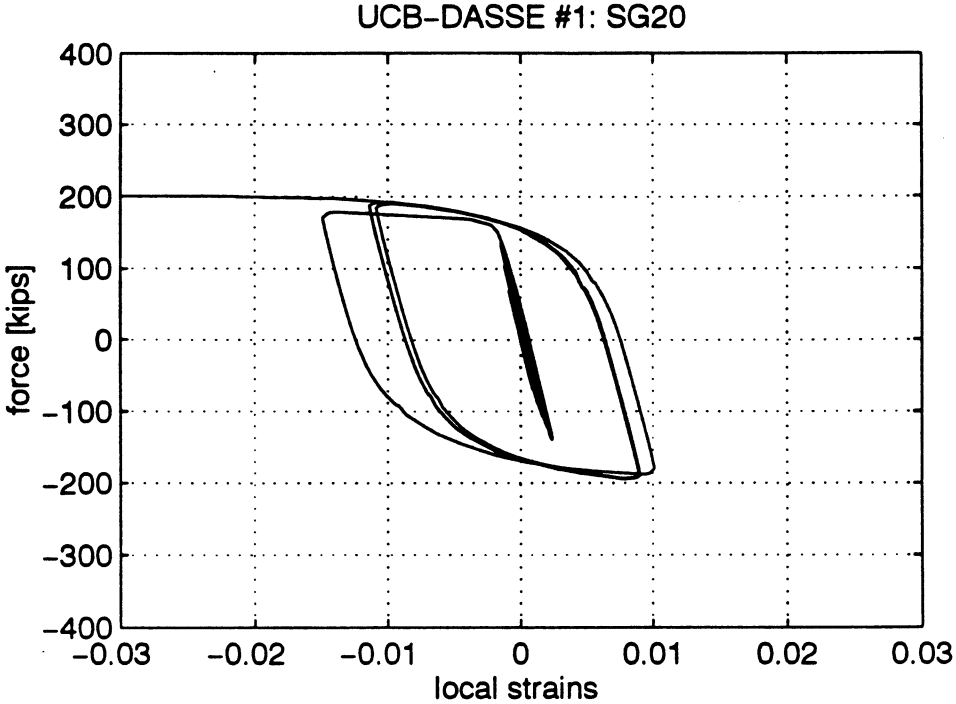


FIGURE 26: LOCAL RESPONSE -- TOP FLANGE AXIS (@ "DOG BONE")

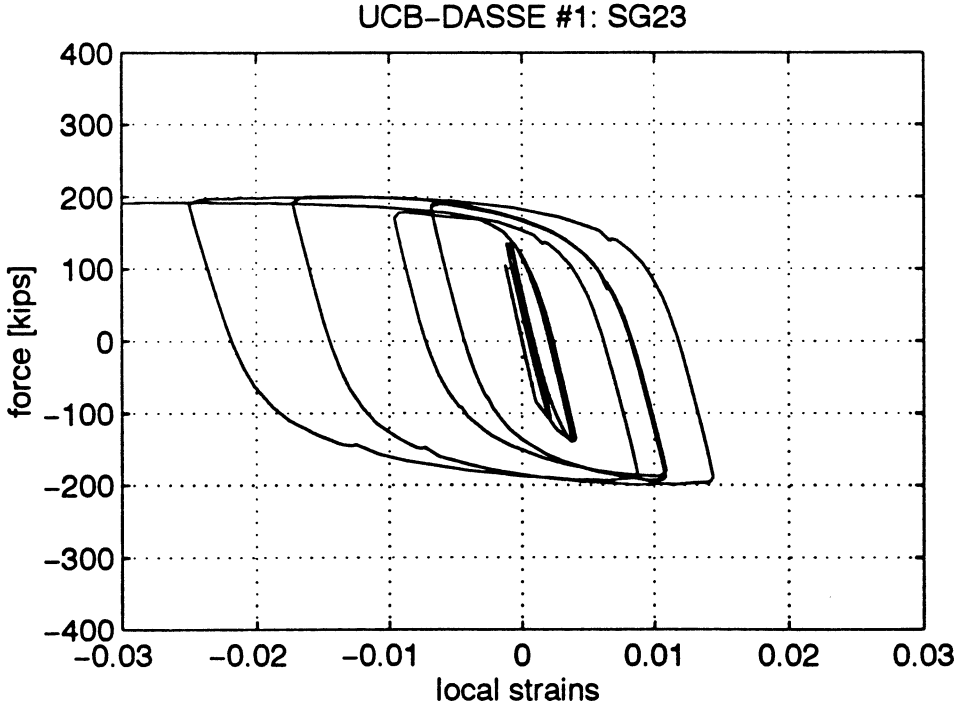


FIGURE 27: LOCAL RESPONSE -- BOTTOM FLANGE EDGE (@ "DOG BONE")

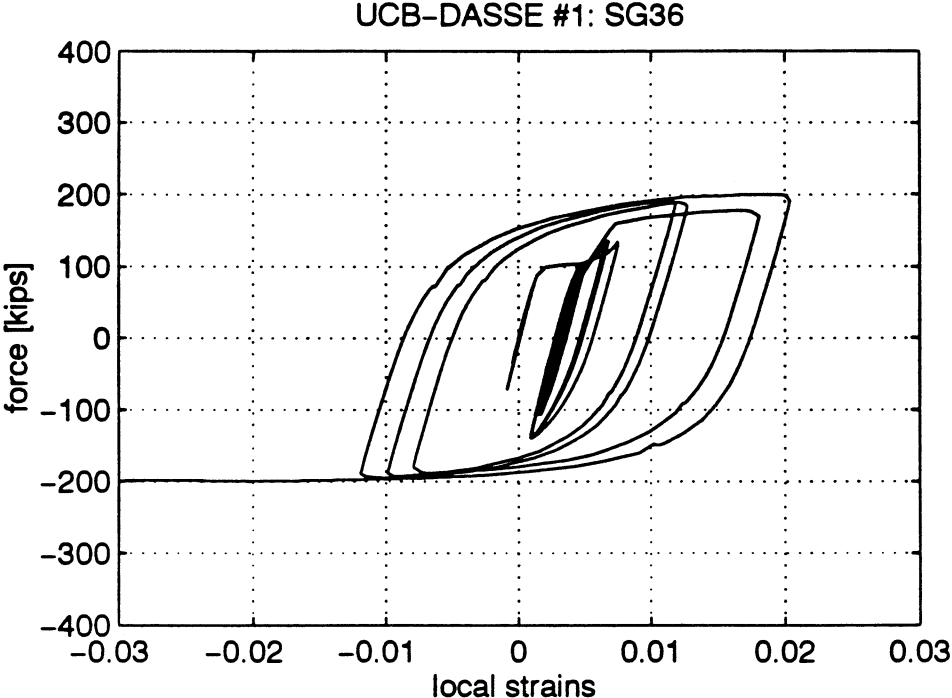


FIGURE 28: LOCAL RESPONSE -- BOTTOM FLANGE AXIS (@ "DOG BONE")

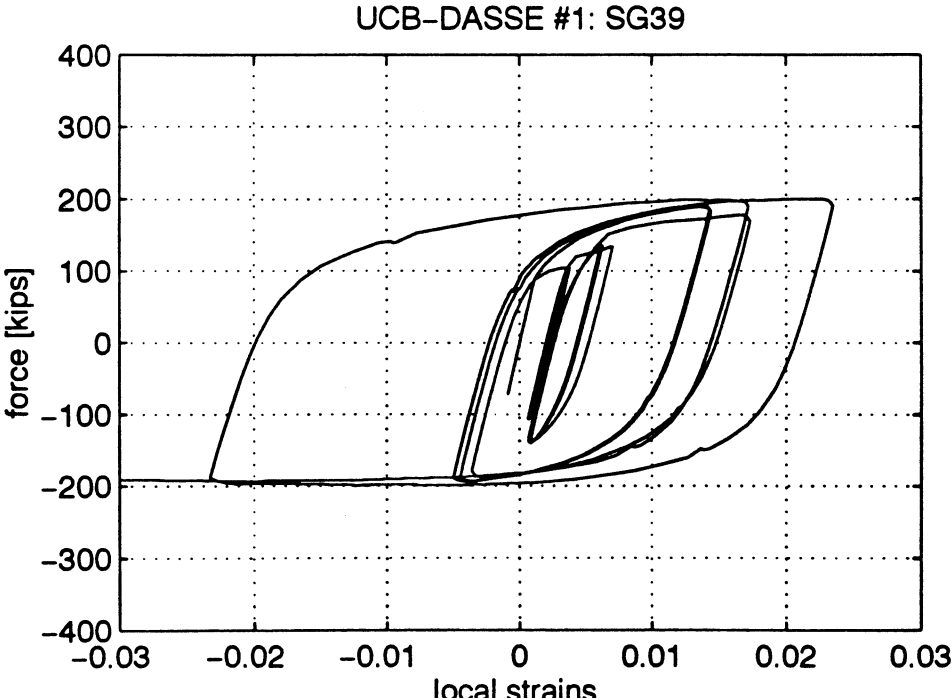


FIGURE 29: SPECIMEN 1 -- FIRST WHITE-WASH FLAKES ON BEAM TOP FLANGE
(@ 0.75" actuator displacement)

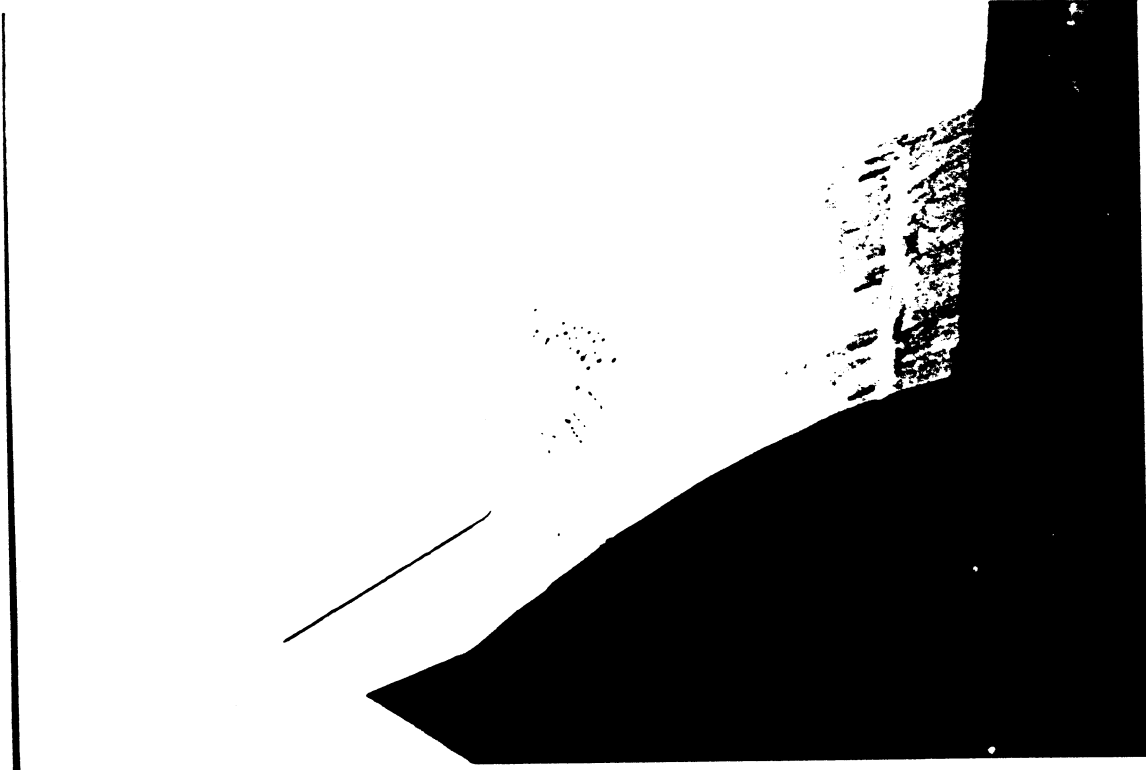


FIGURE 30: SPECIMEN 1 -- BEAM TOP FLANGE
(@ 1" actuator displacement)

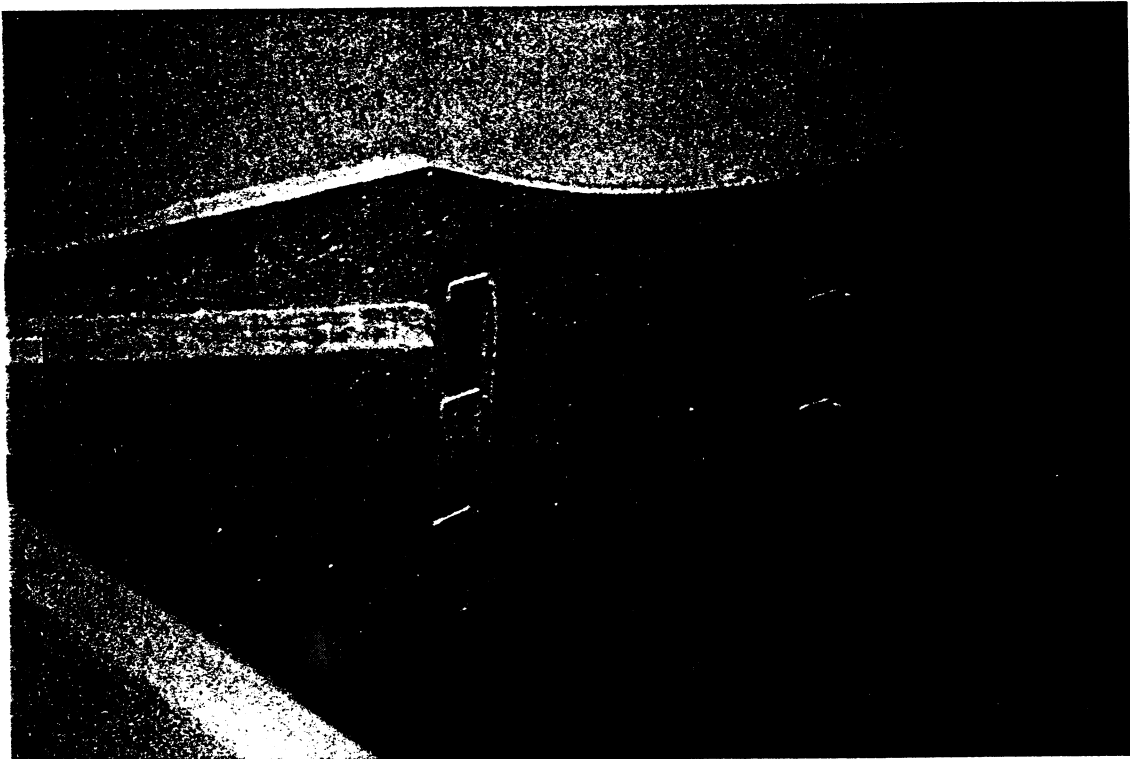


FIGURE 31: SPECIMEN 1 -- BEAM TOP FLANGE
(@+2" actuator displacement)

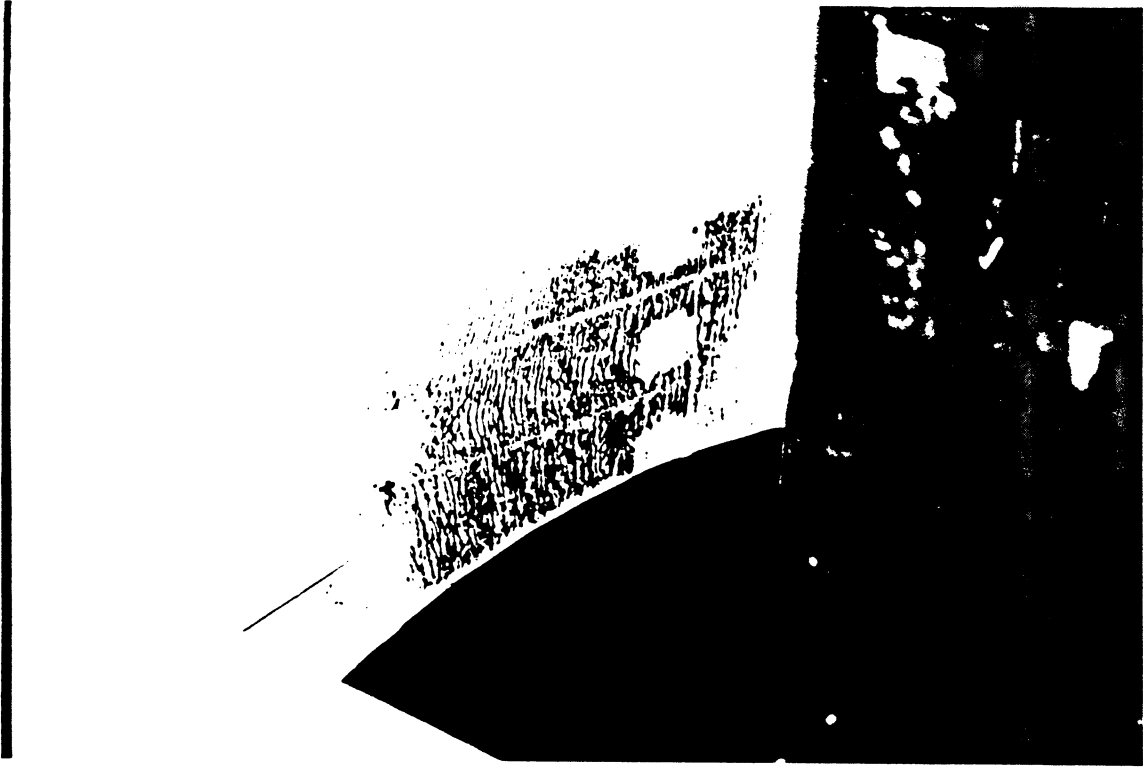


FIGURE 32: SPECIMEN 1 -- BEAM AFTER 2" CYCLES



FIGURE 33: SPECIMEN1 -- BEAM AFTER 4" CYCLES

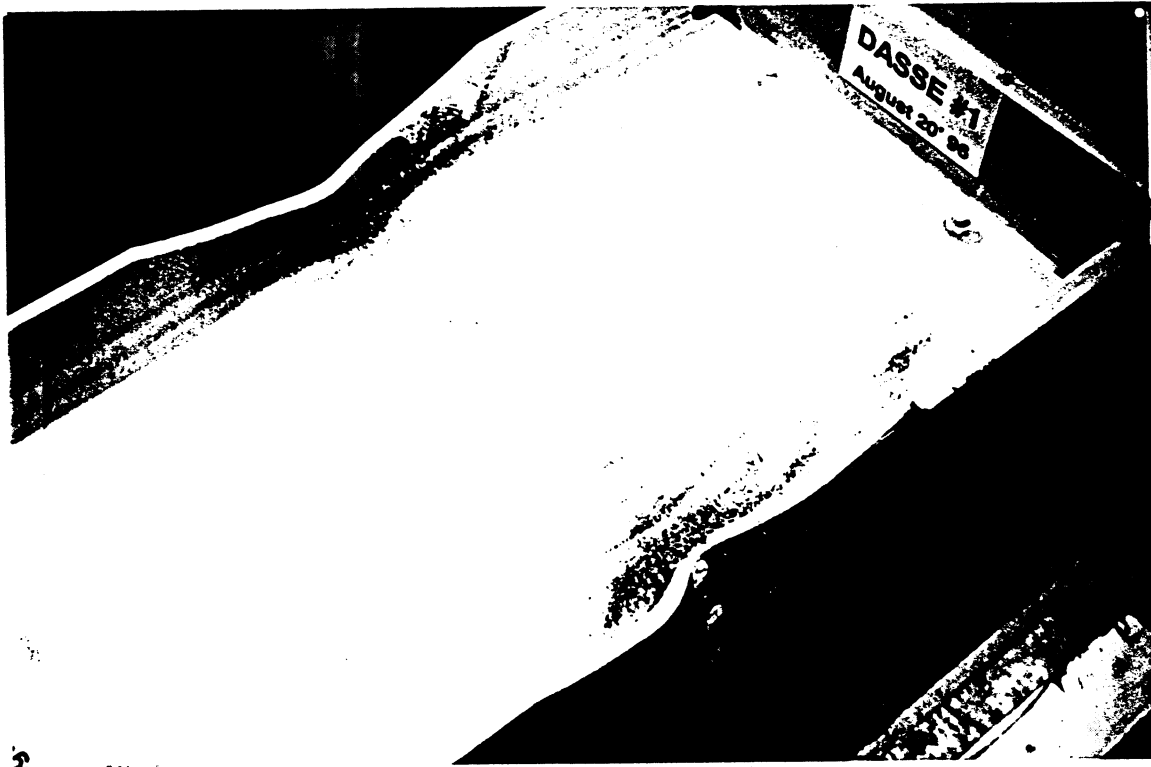


FIGURE 34: SPECIMEN1 -- BEAM AFTER THE TEST



FIGURE 31: SPECIMEN 1 -- BEAM TOP FLANGE
(@+2" actuator displacement)

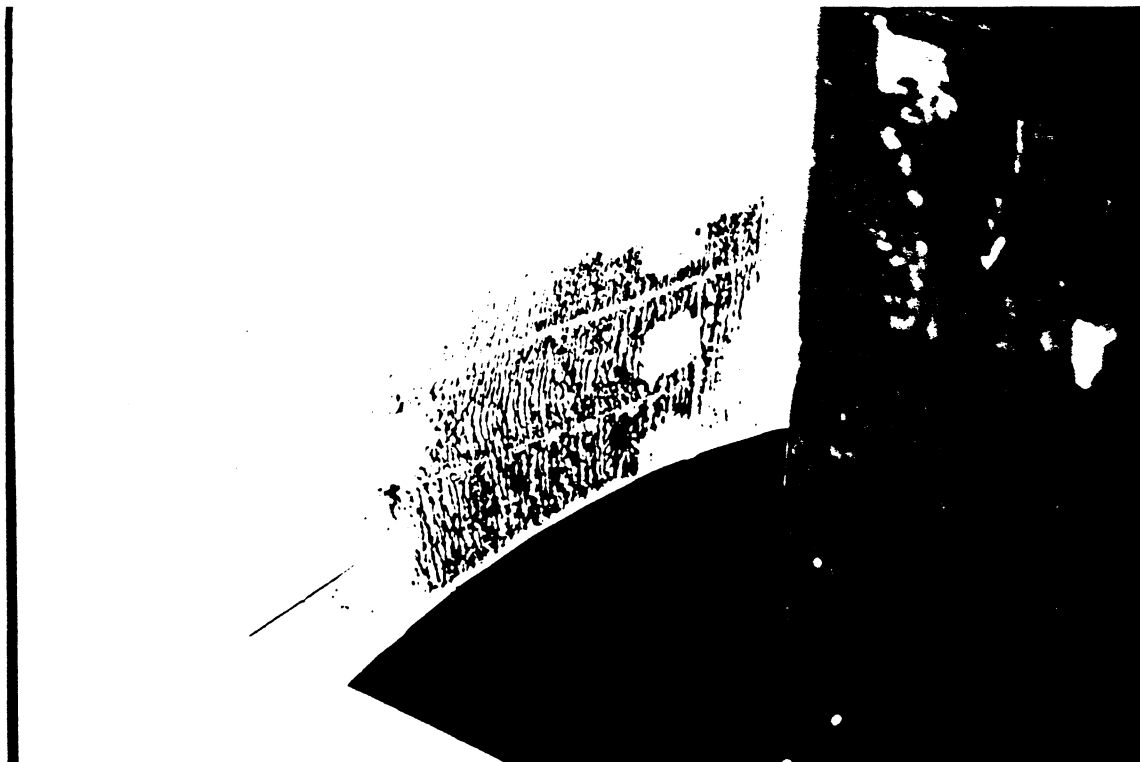


FIGURE 32: SPECIMEN 1 -- BEAM AFTER 2" CYCLES



FIGURE 29: SPECIMEN 1 -- FIRST WHITE-WASH FLAKES ON BEAM TOP FLANGE
(@ 0.75" actuator displacement)

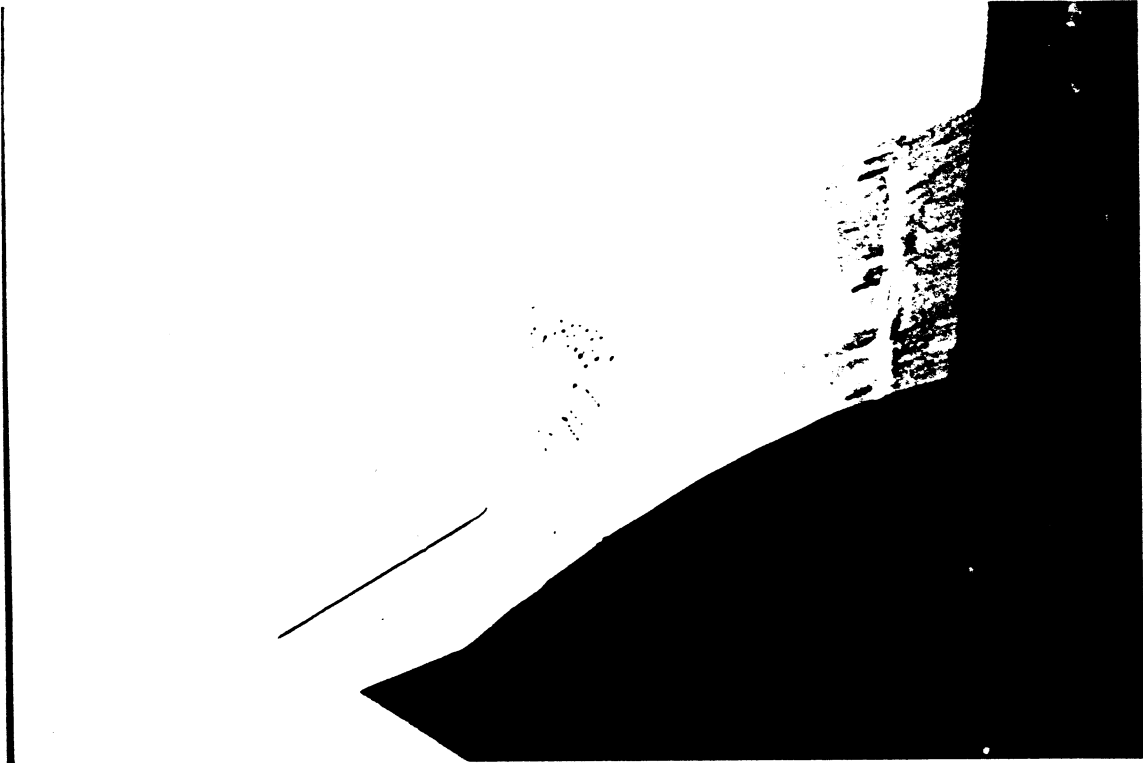


FIGURE 30: SPECIMEN 1 -- BEAM TOP FLANGE
(@ 1" actuator displacement)

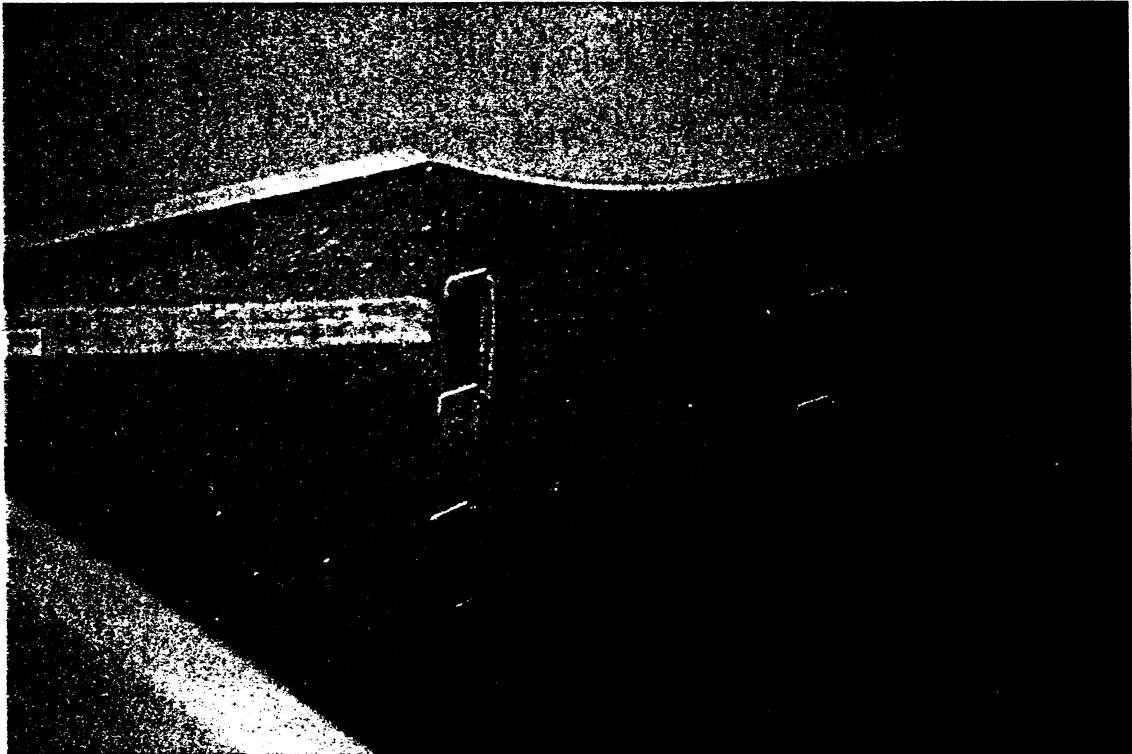


FIGURE 35: IMPOSED LOADING HISTORY -- ACTUATOR DISPLACEMENT
UCB-DASSE #2

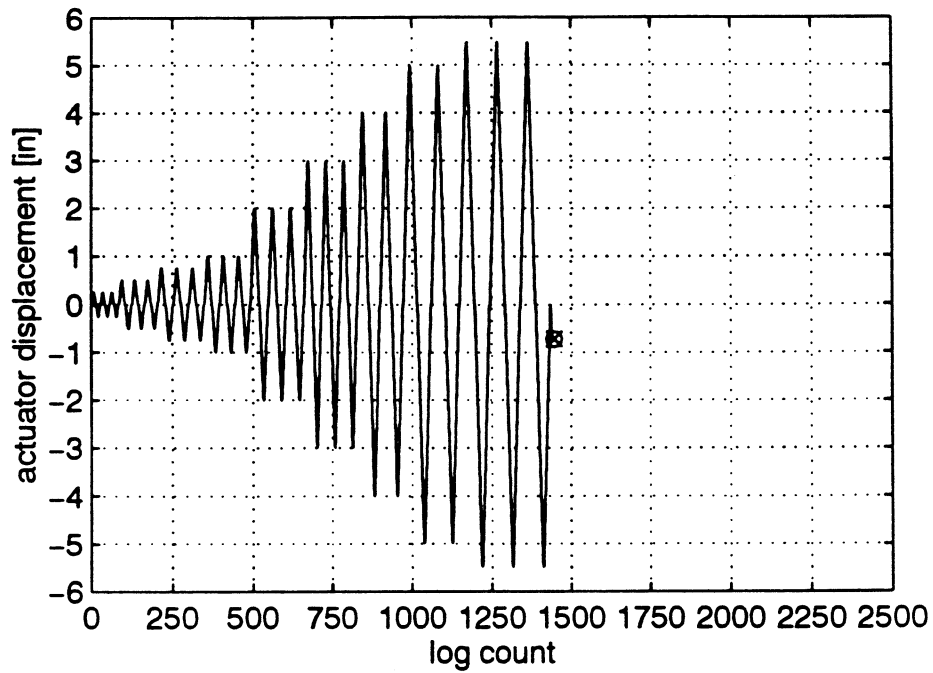


FIGURE 36: APPLIED LOAD / BEAM END DISPLACEMENT RESPONSE
UCB-DASSE #2

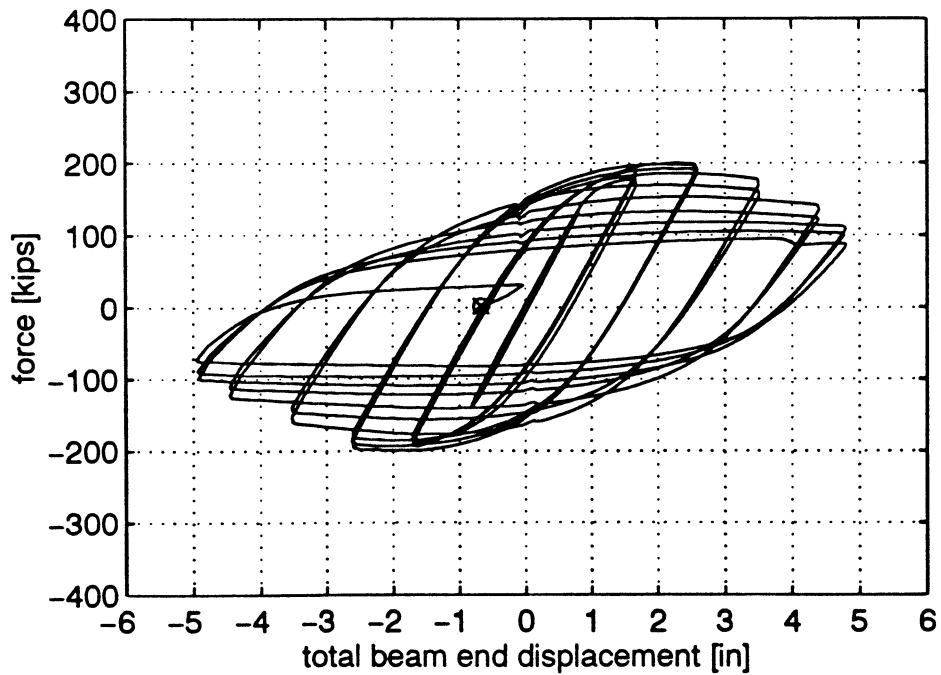


FIGURE 37: PLASTIC ROTATION VERSUS MOMENT @ COVER PLATE EDGE

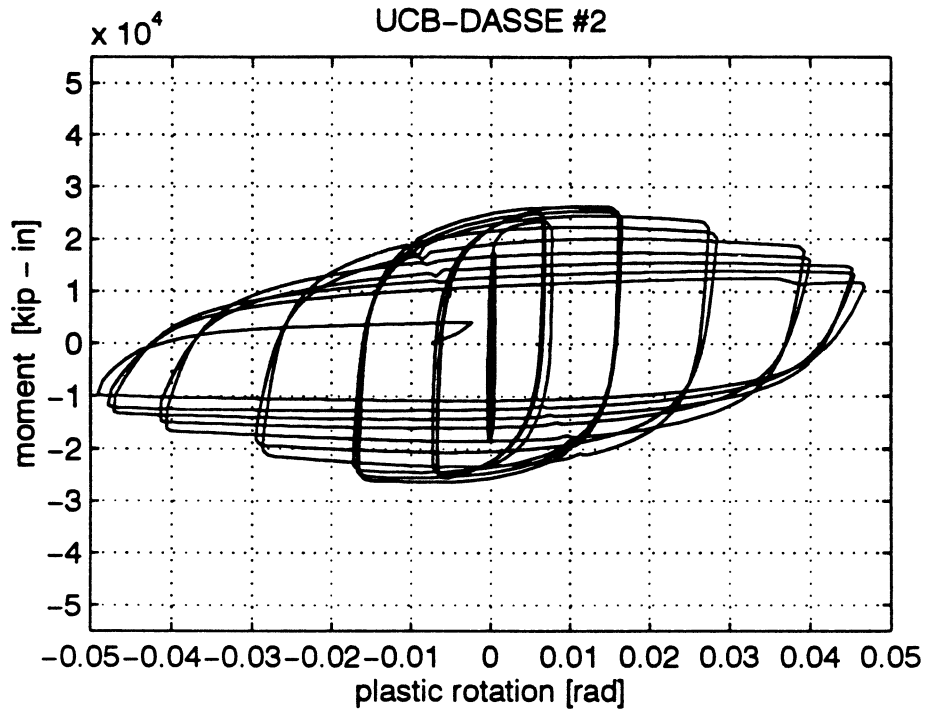


FIGURE 38: DISSIPATED ENERGY

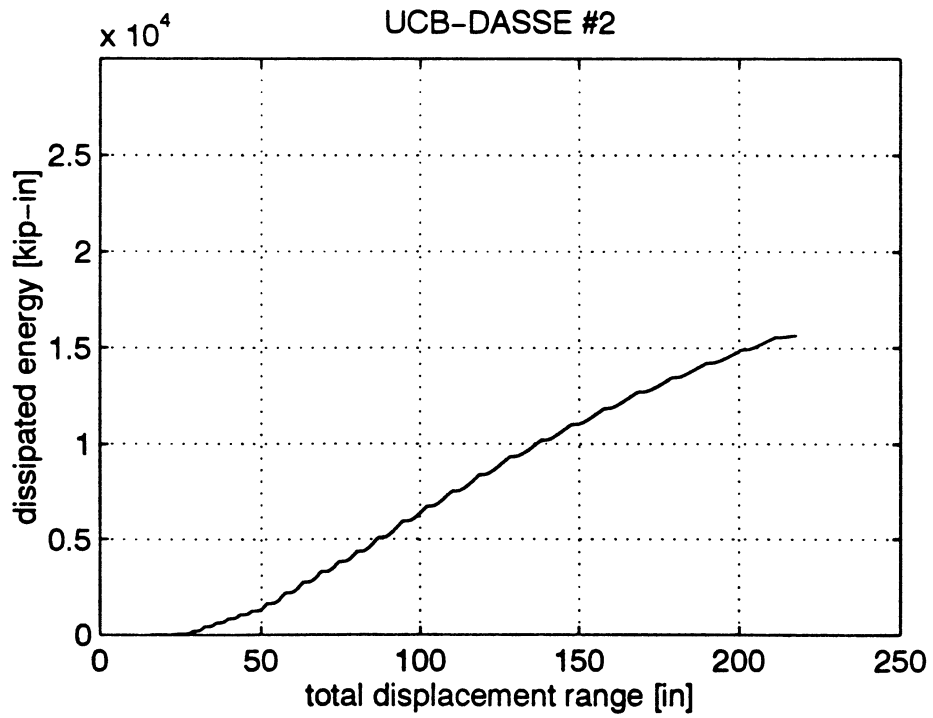


FIGURE 41: LOCAL RESPONSE -- TOP BEAM FLANGE EDGE (@ COVER PLATE)

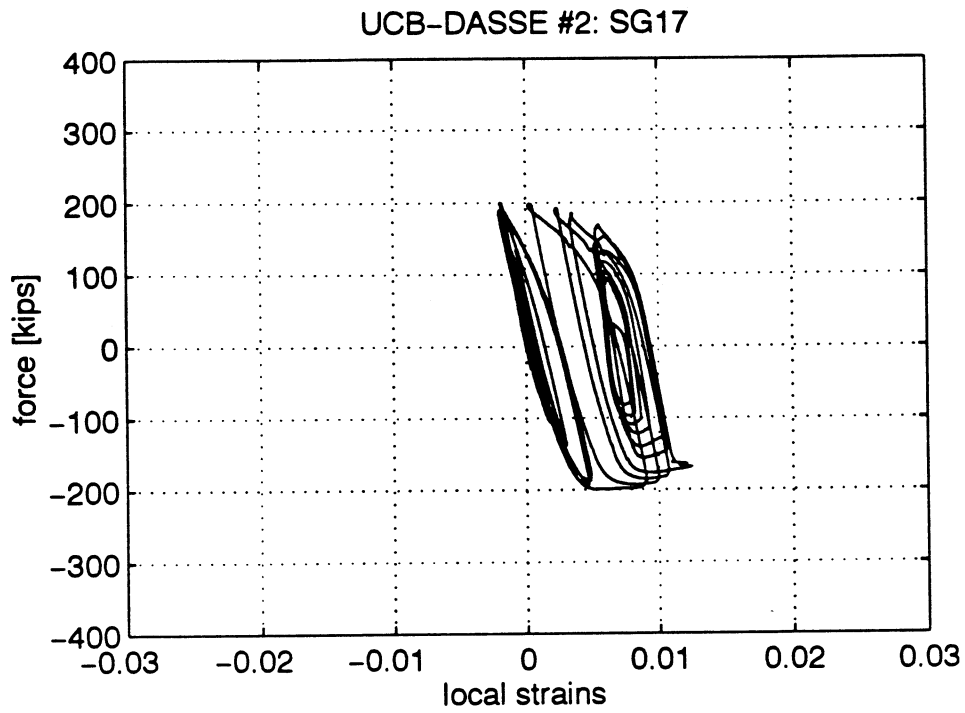


FIGURE 42: LOCAL RESPONSE -- TOP BEAM FLANGE AXIS (@ COVER PLATE)

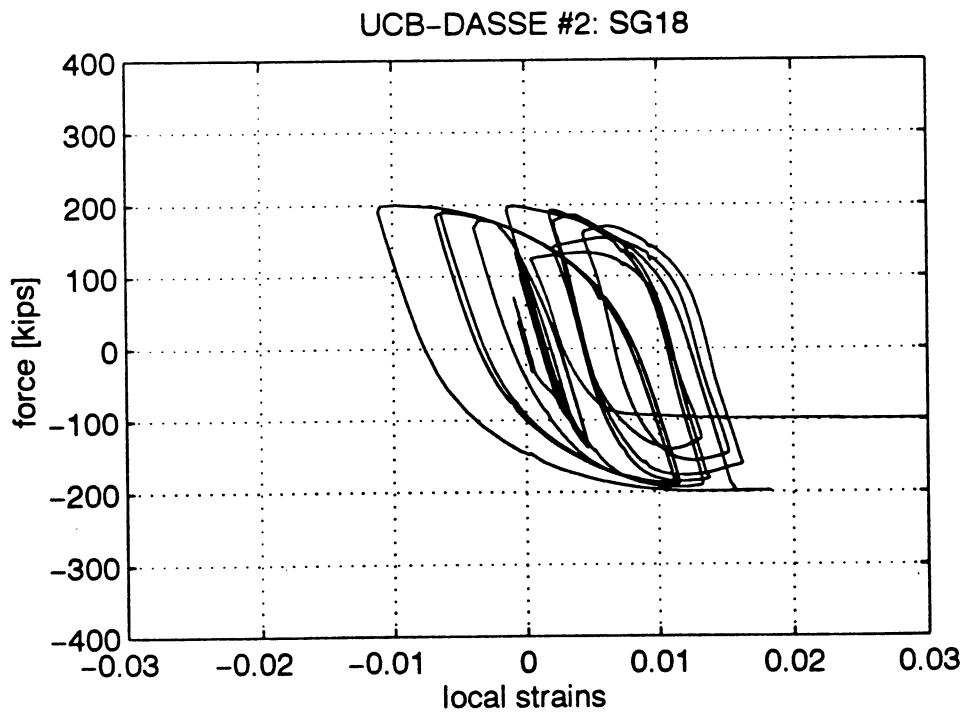


FIGURE 39: PANEL ZONE SHEAR DEFORMATION

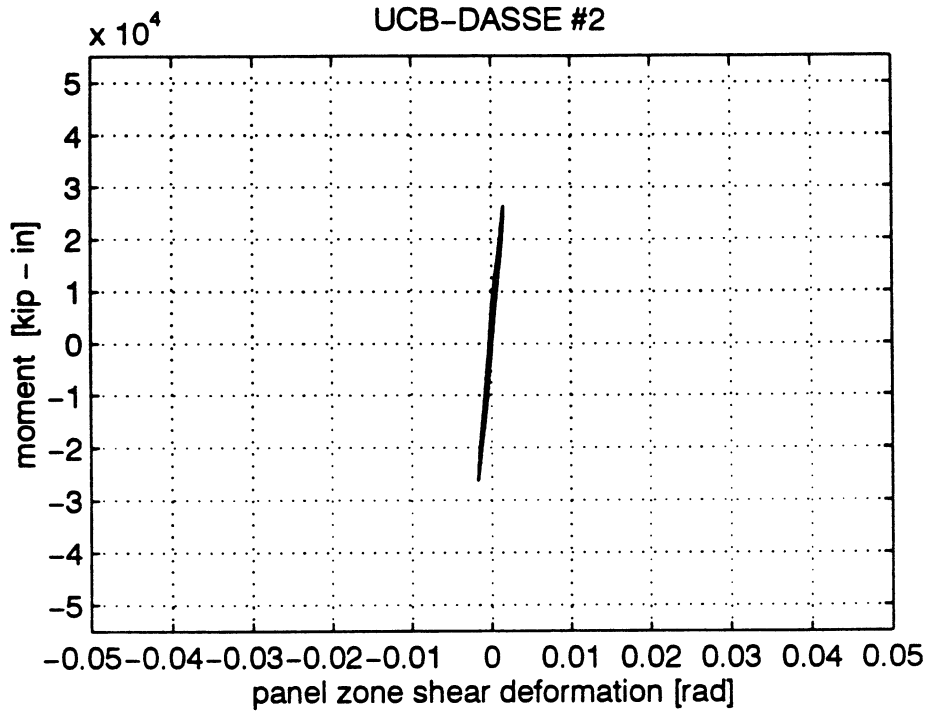


FIGURE 40: BEAM CONTRIBUTION TO TOTAL DISPLACEMENT

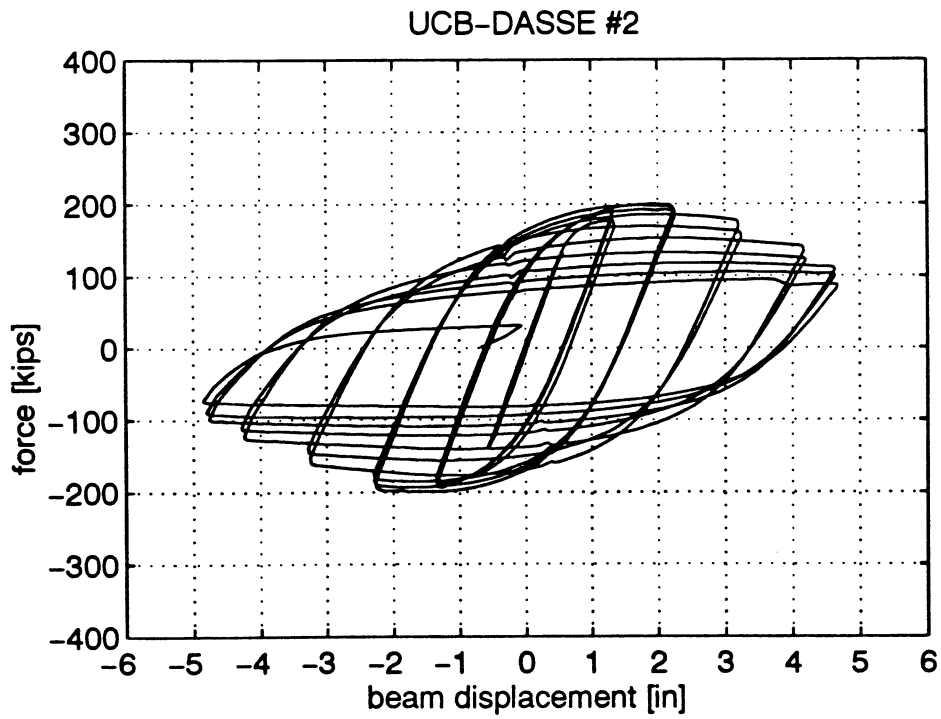


FIGURE 43: LOCAL RESPONSE -- BOTTOM BEAM FLANGE EDGE (@ COVER PLATE)

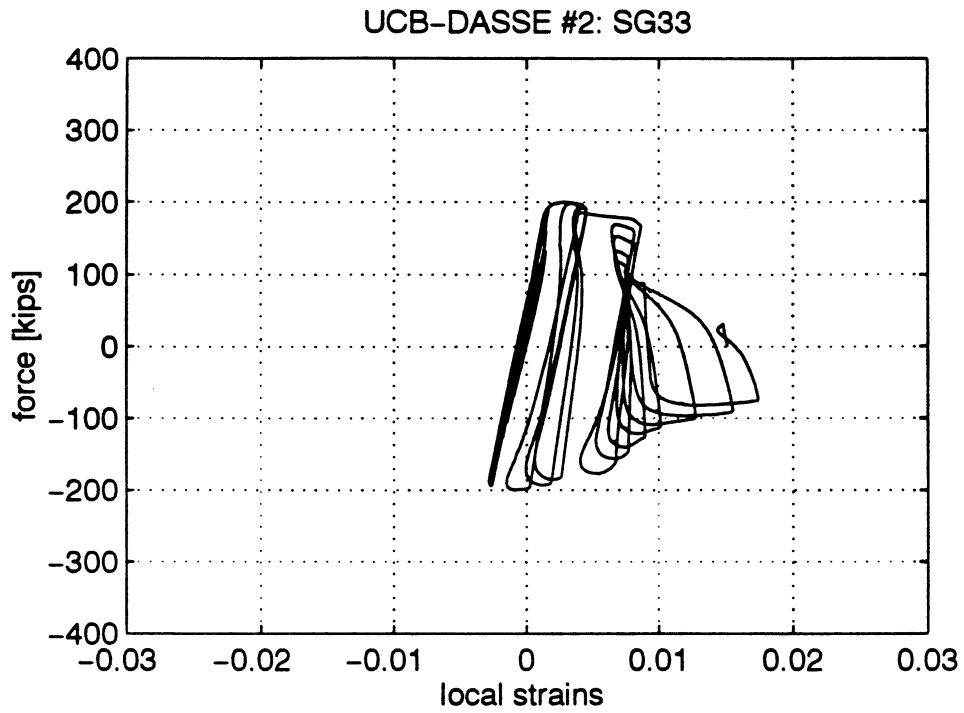


FIGURE 44: LOCAL RESPONSE -- BOTTOM BEAM FLANGE AXIS (@ COVER PLATE)

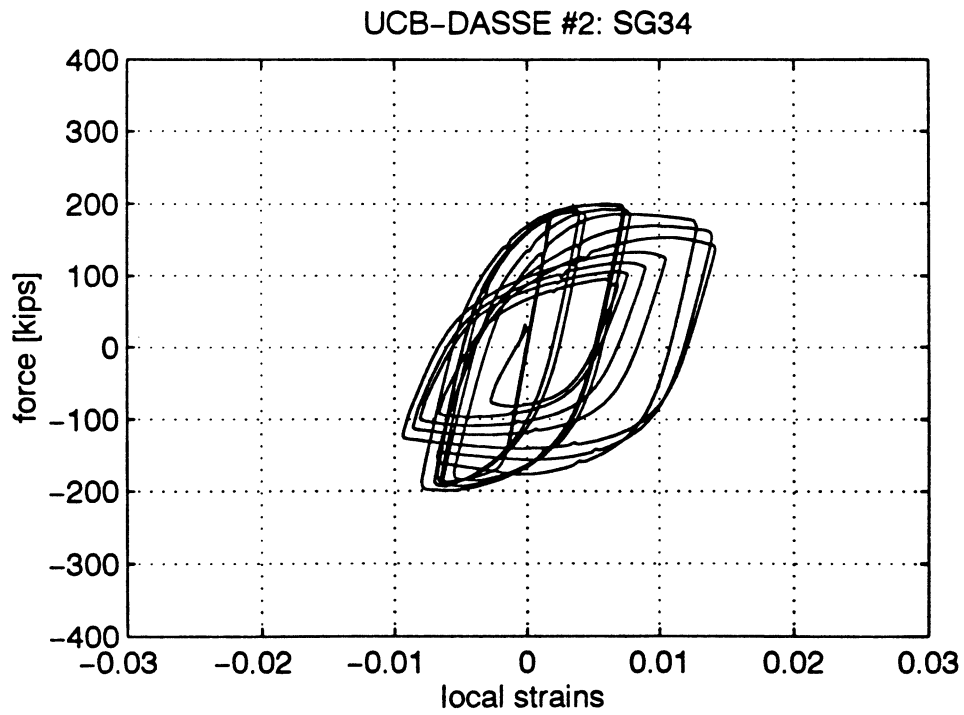


FIGURE 45: LOCAL RESPONSE -- TOP FLANGE EDGE HOR (@ "DOG BONE")

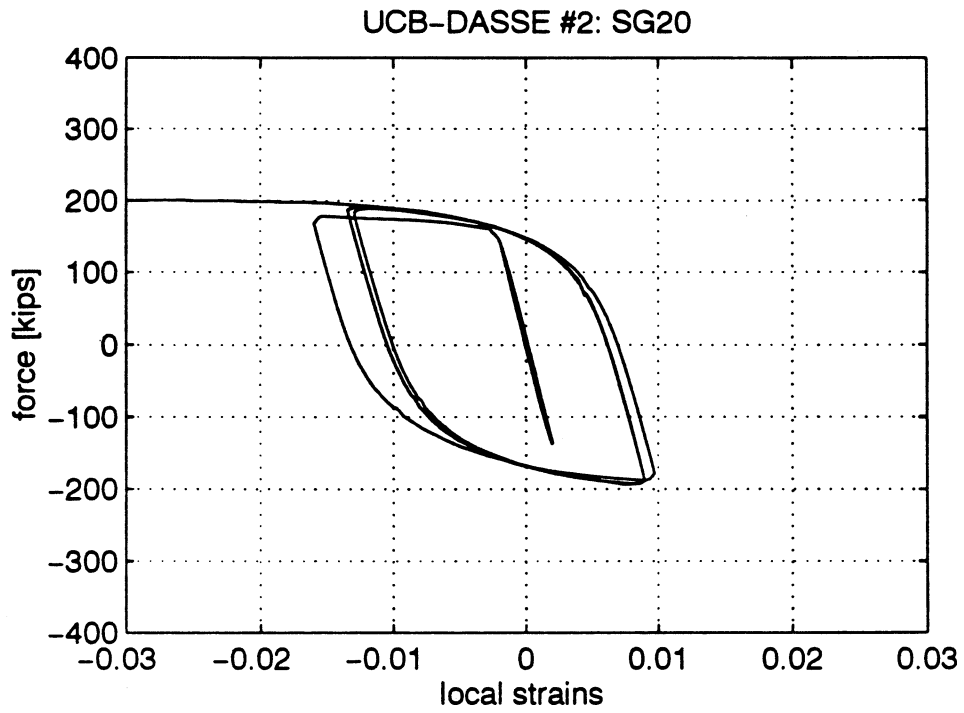


FIGURE 46: LOCAL RESPONSE -- TOP FLANGE EDGE VER (@ "DOG BONE")

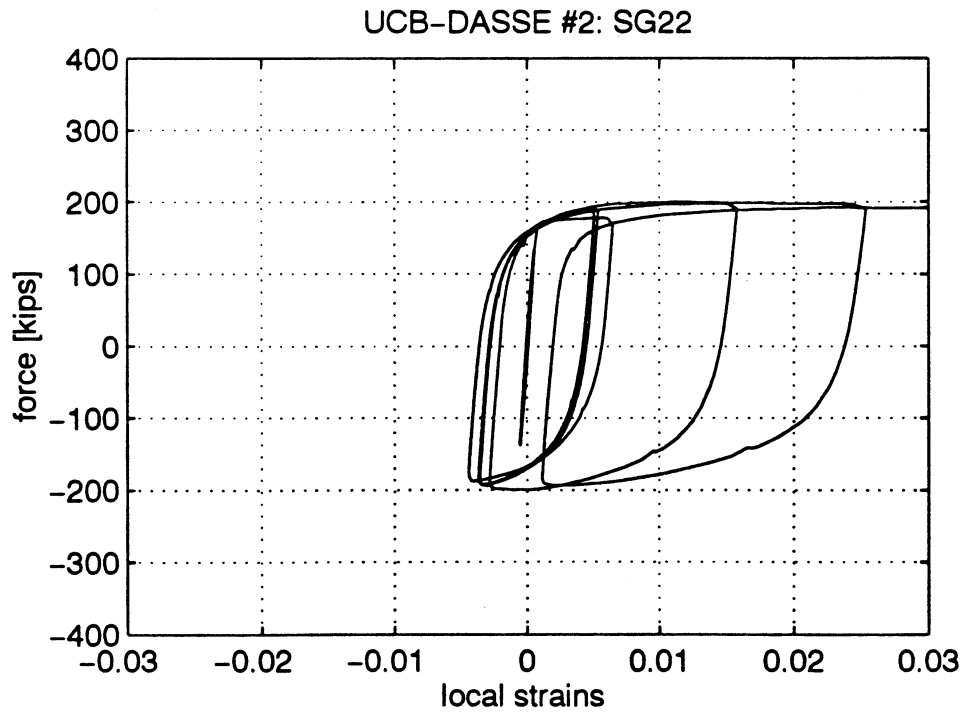


FIGURE 47: LOCAL RESPONSE -- TOP FLANGE AXIS HOR (@ "DOG BONE")
UCB-DASSE #2: SG23

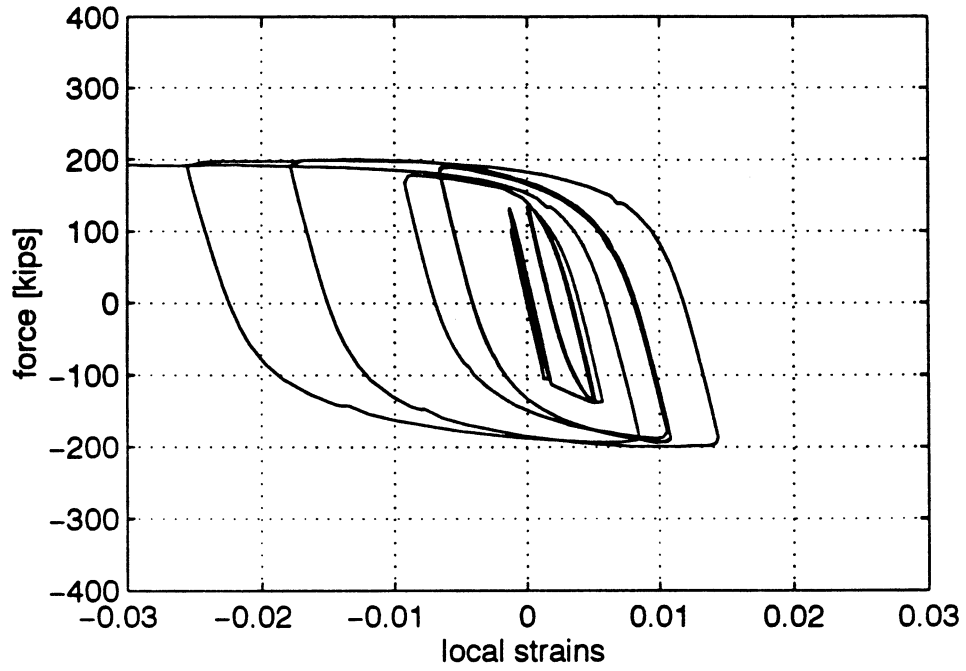


FIGURE 48: LOCAL RESPONSE -- TOP FLANGE AXIS VER (@ "DOG BONE")
UCB-DASSE #2: SG25

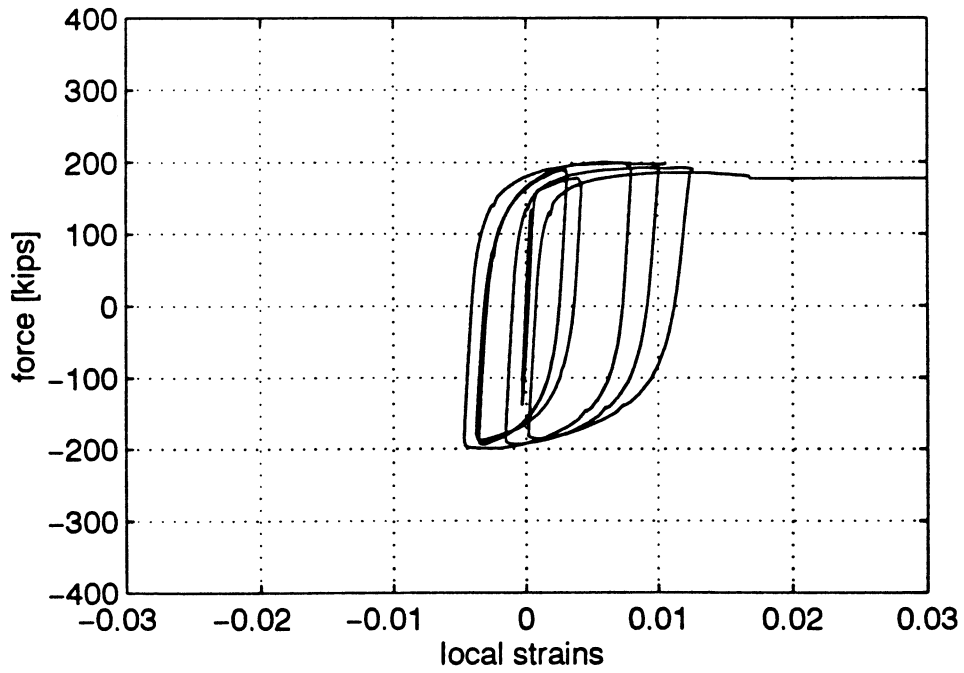


FIGURE 49: LOCAL RESPONSE -- BOTTOM FLANGE EDGE HOR (@ "DOG BONE")

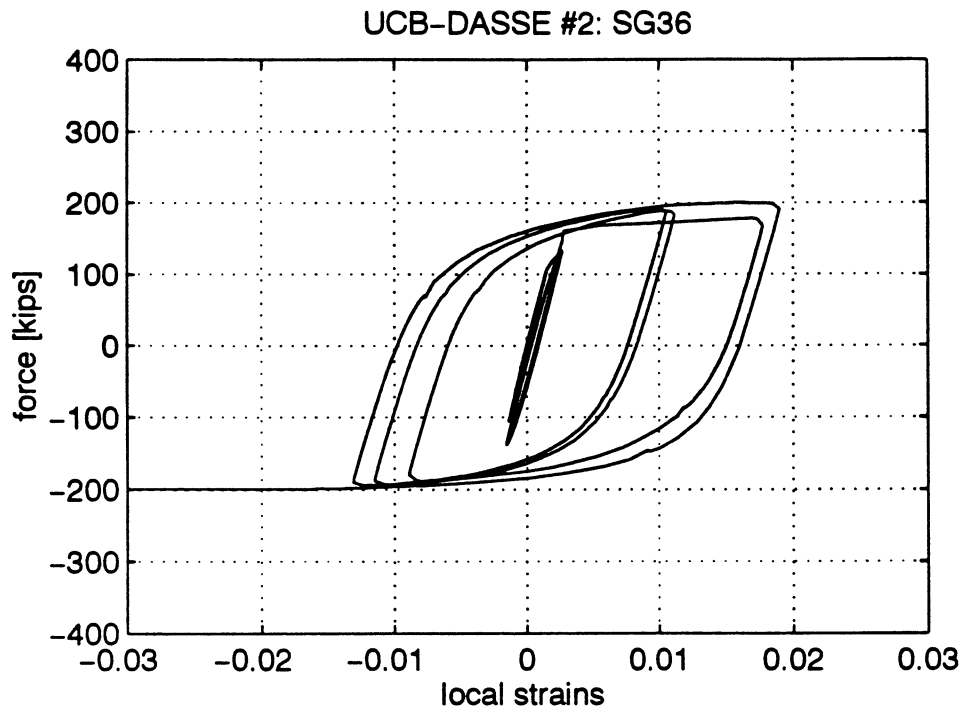


FIGURE 50: LOCAL RESPONSE -- BOTTOM FLANGE EDGE VER (@ "DOG BONE")

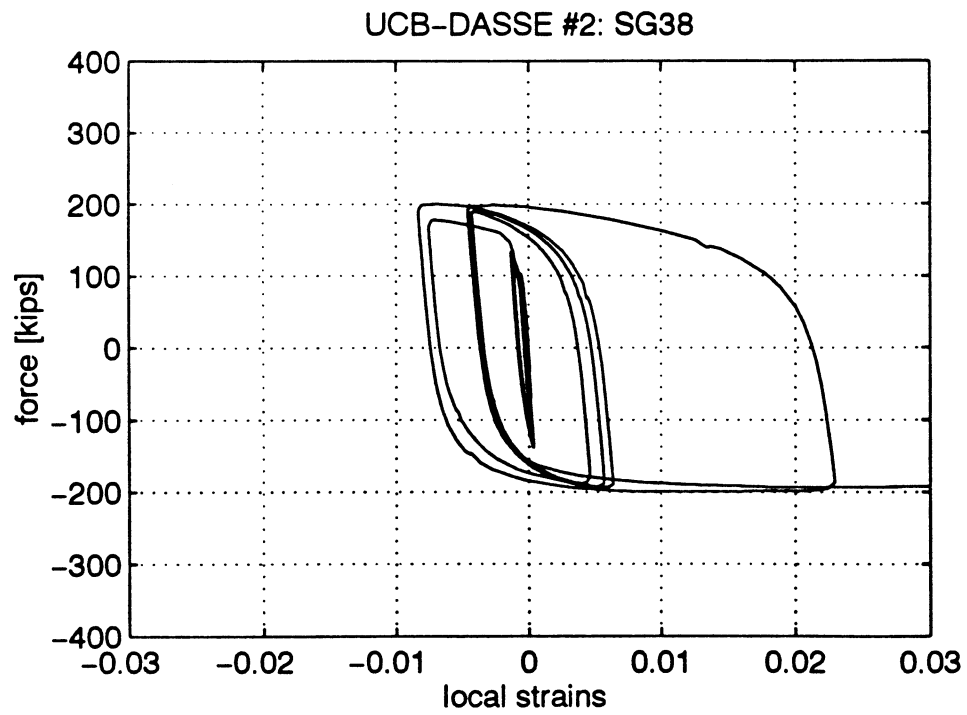


FIGURE 51: LOCAL RESPONSE -- BOTTOM FLANGE AXIS HOR (@ "DOG BONE")

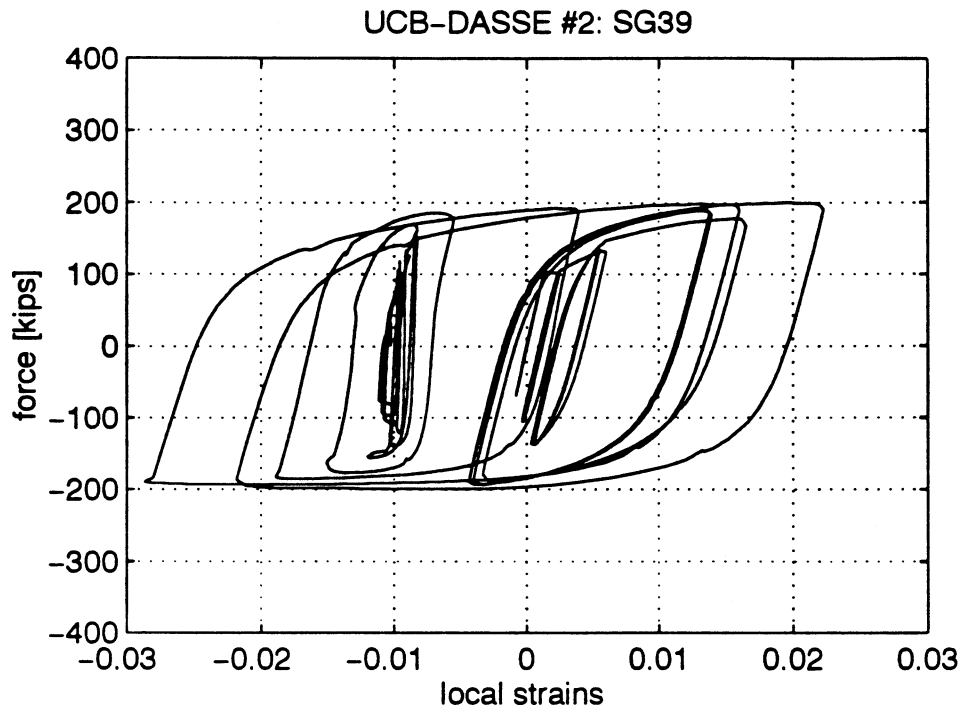


FIGURE 52: LOCAL RESPONSE -- BOTTOM FLANGE AXIS VER (@ "DOG BONE")

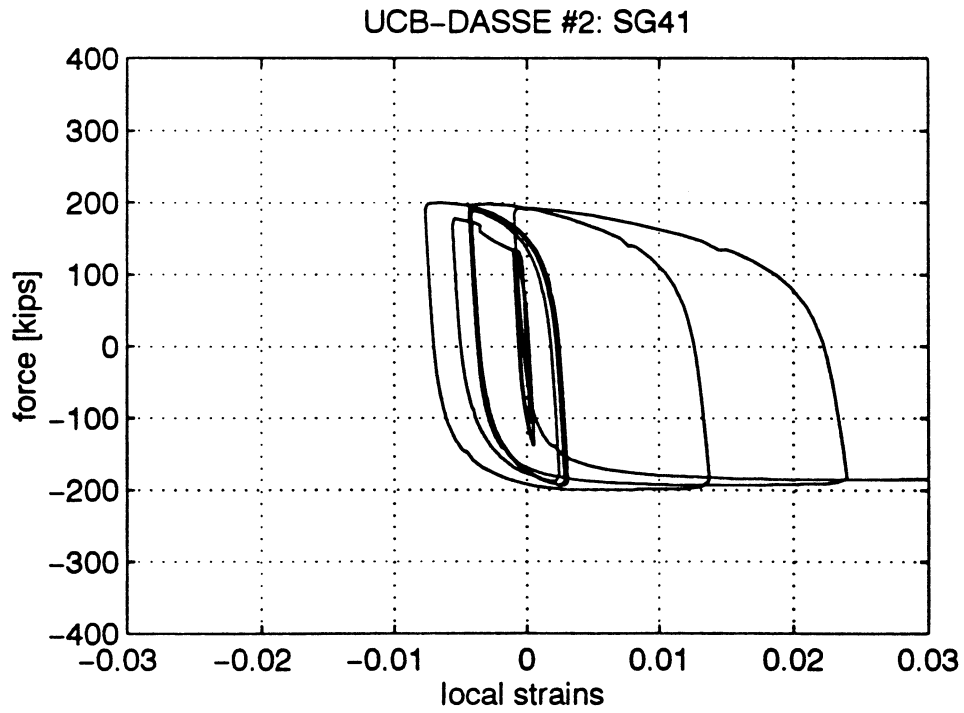


FIGURE 53: LOCAL RESPONSE -- TOP STIFFENER

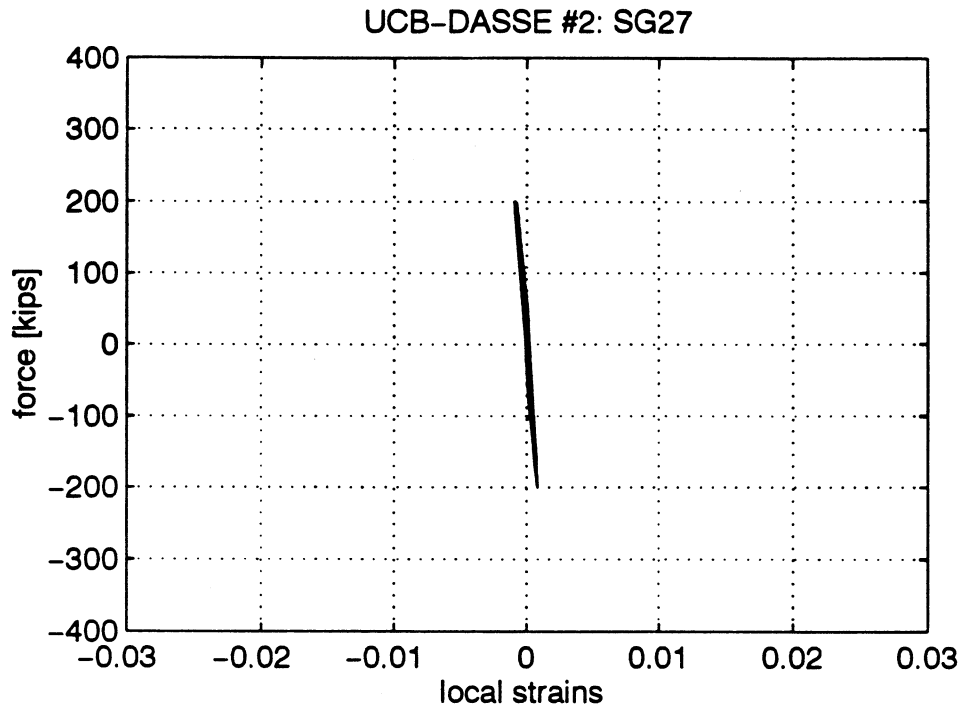


FIGURE 54: LOCAL RESPONSE -- BOTTOM STIFFENER

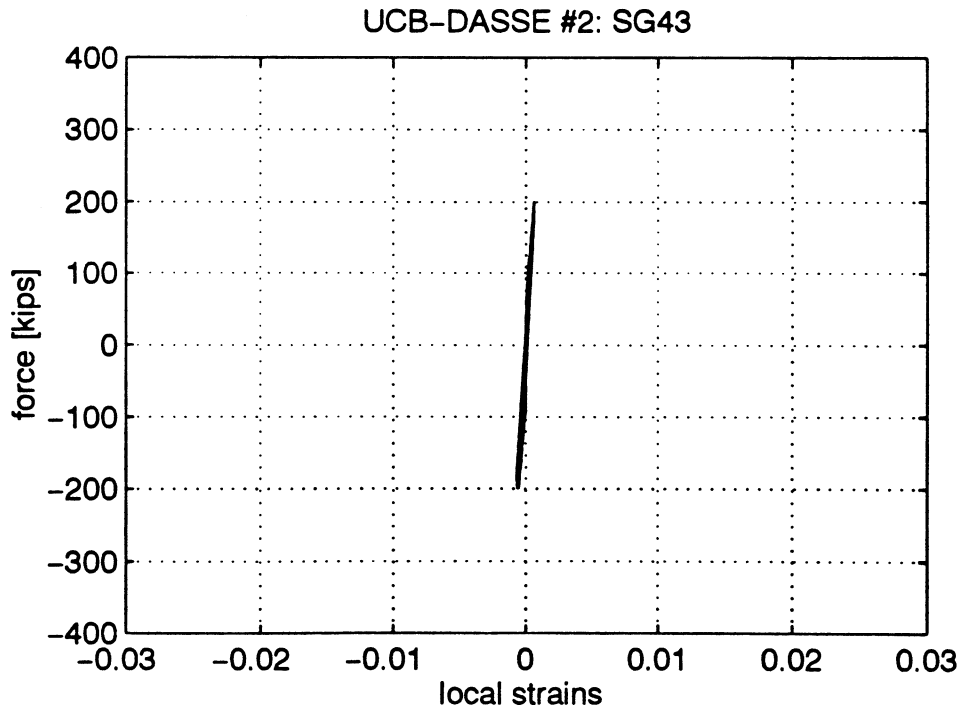


FIGURE 55: LOCAL RESPONSE -- PANEL ZONE (TOP CORNER HOR)

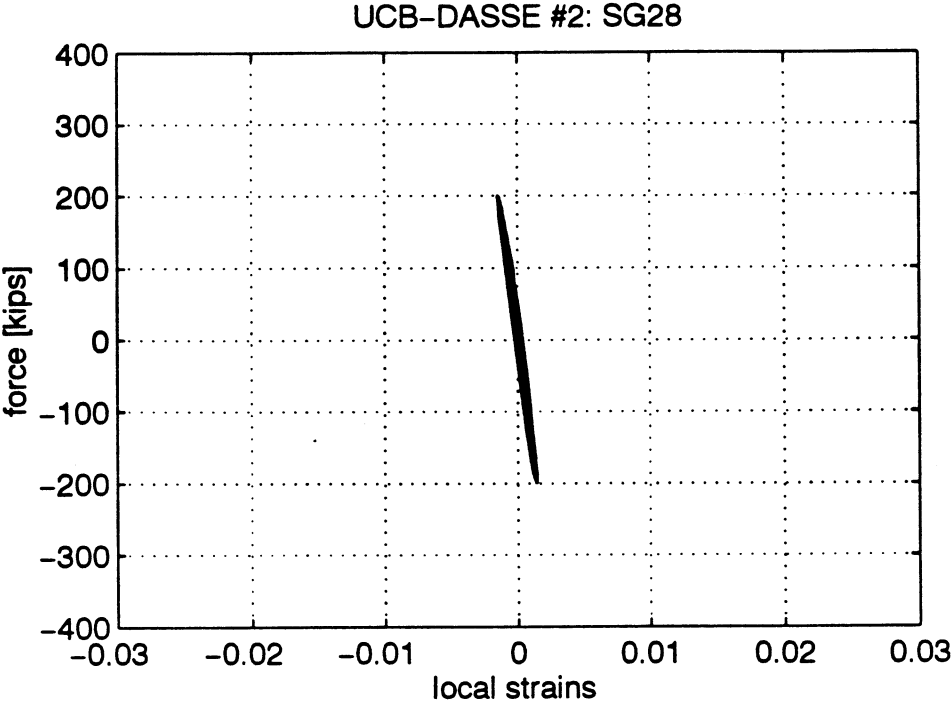


FIGURE 56: LOCAL RESPONSE -- PANEL ZONE (TOP CORNER DIA)

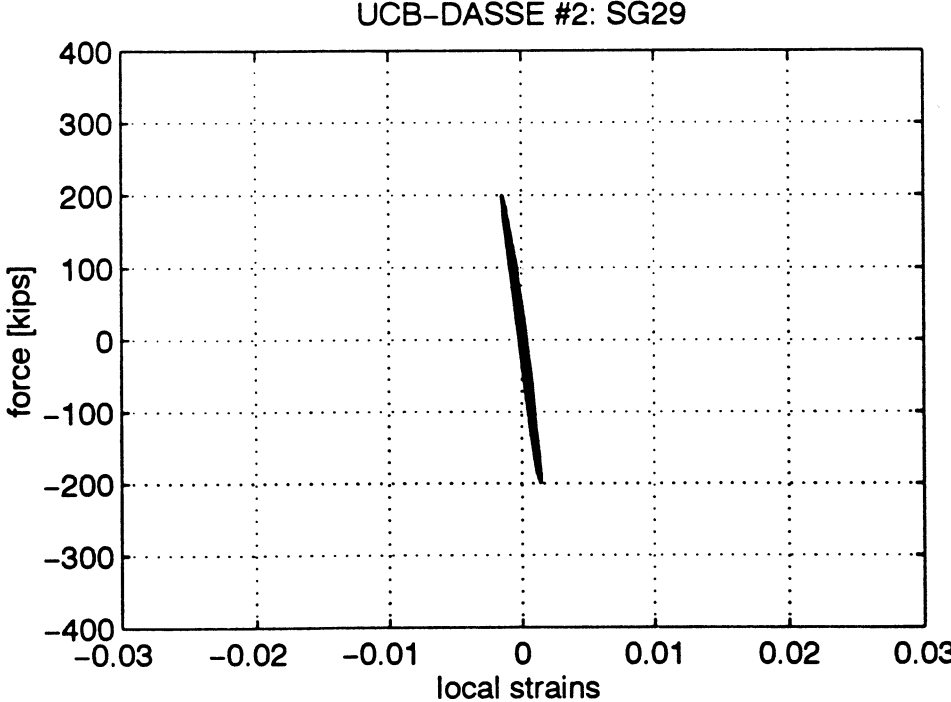


FIGURE 57: LOCAL RESPONSE -- PANEL ZONE (TOP CORNER VER)

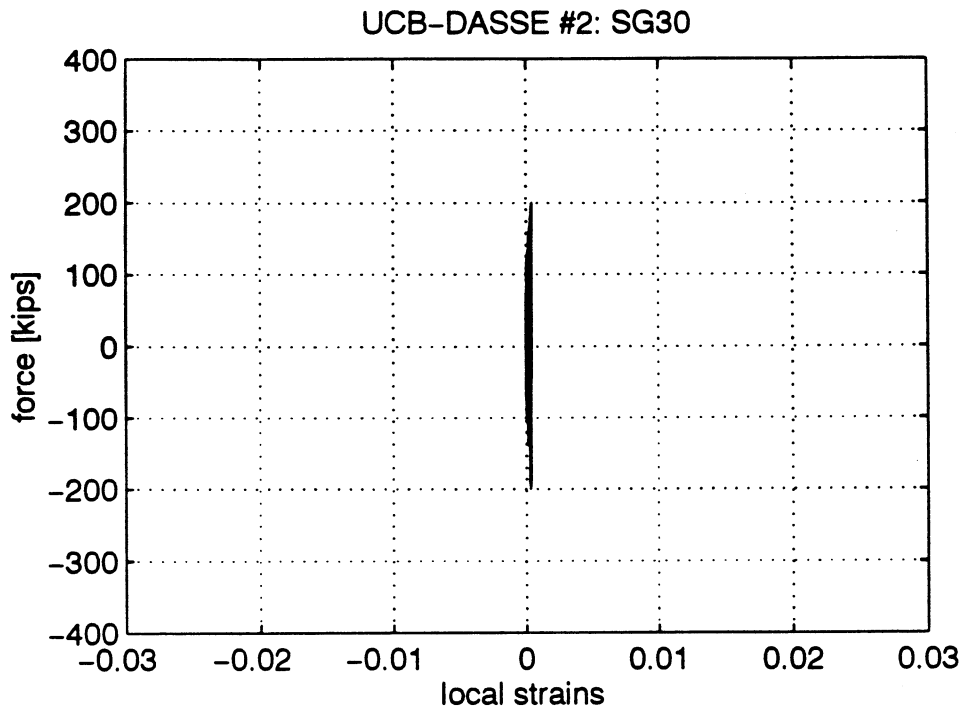


FIGURE 58: LOCAL RESPONSE -- PANEL ZONE (BOTTOM CORNER HOR)

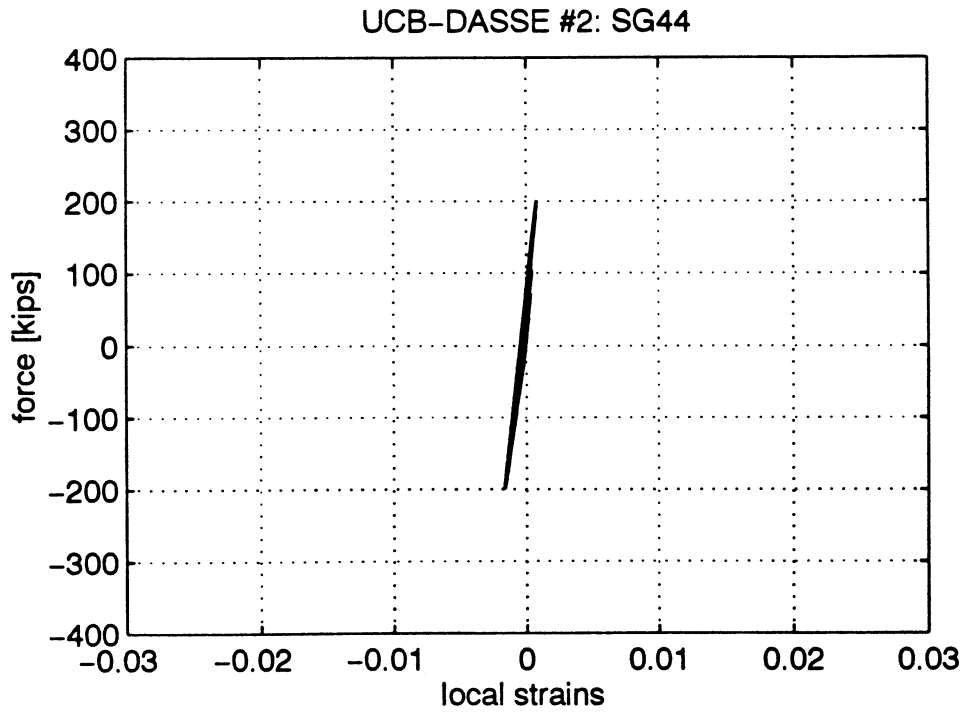


FIGURE 59: LOCAL RESPONSE -- PANEL ZONE (BOTTOM CORNER DIA)

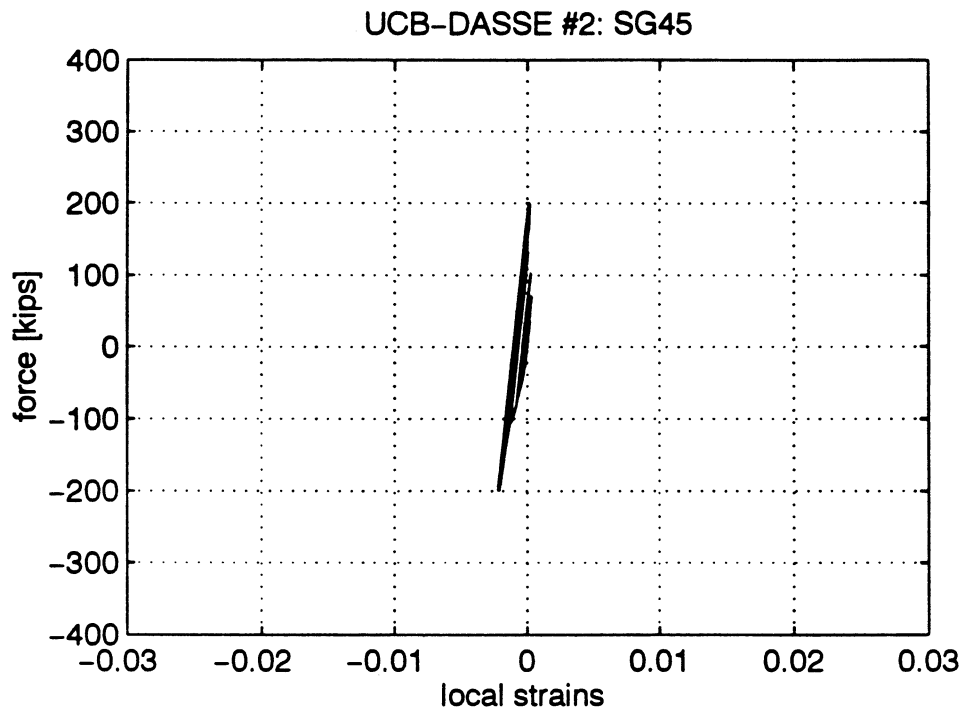


FIGURE 60: LOCAL RESPONSE -- PANEL ZONE (BOTTOM CORNER VER)

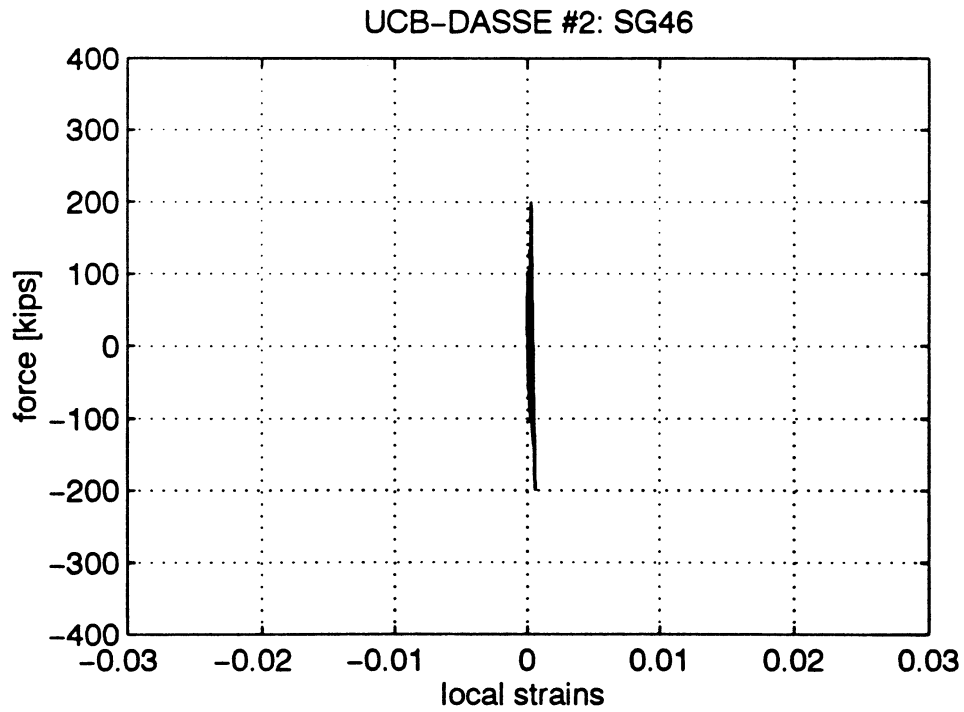


FIGURE 65: SPECIMEN 2 -- FAILURE OF THE BEAM BOTTOM FLANGE

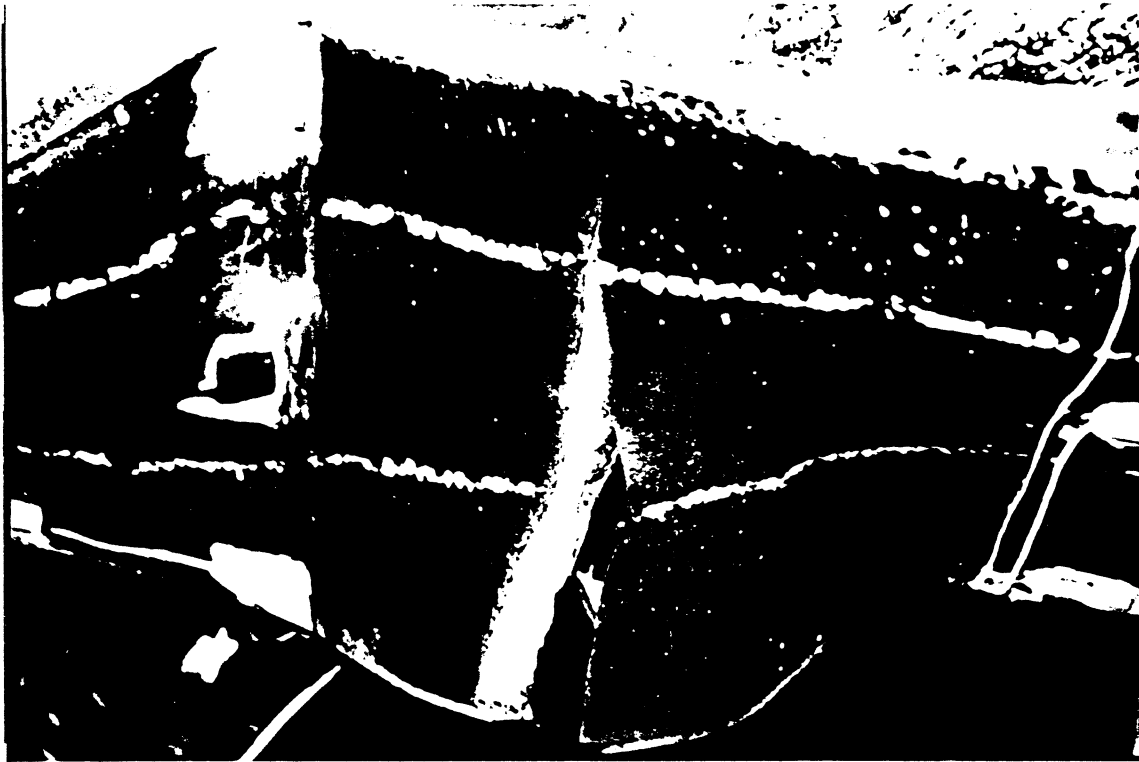


FIGURE 66: SPECIMEN 2 -- CRACK PROPAGATED INTO THE BEAM WEB

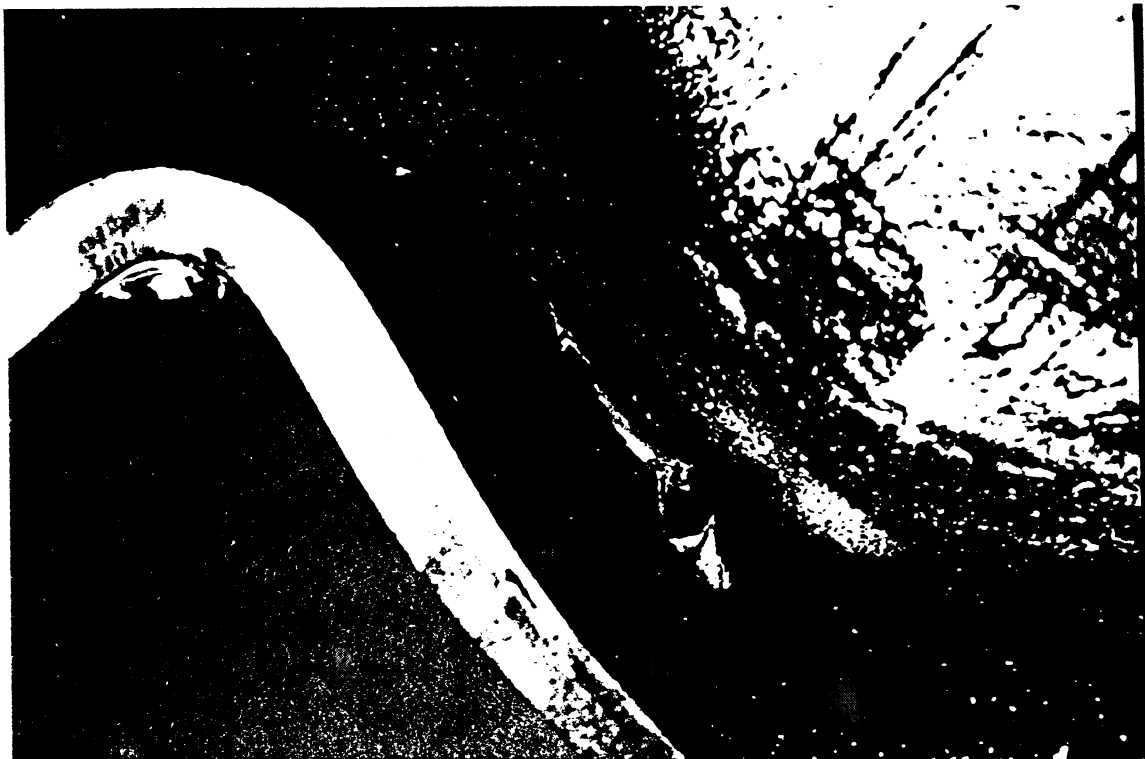


FIGURE 63: SPECIMEN 2 -- BEAM BOTTOM FLANGE
(after 2nd 5.5" cycle)

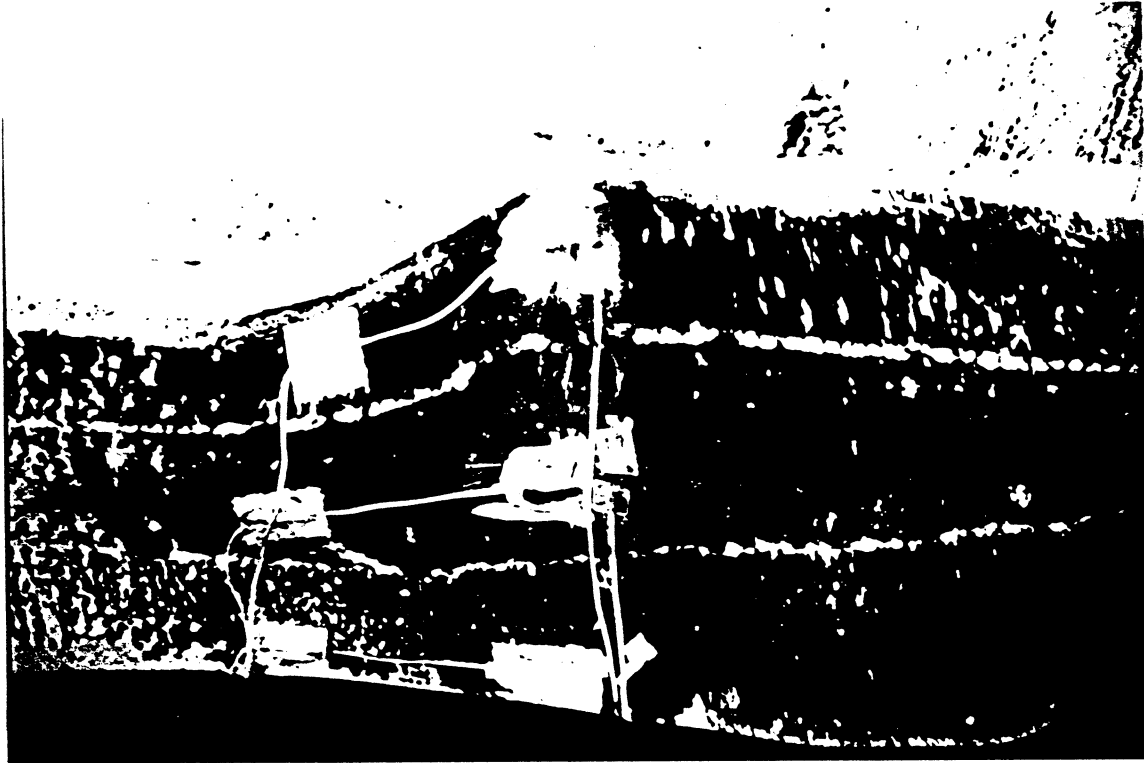


FIGURE 64: SPECIMEN 2 -- CRACK APPEARANCE IN THE BEAM BOTTOM FLANGE
(@ 3rd 5.5" cycle)

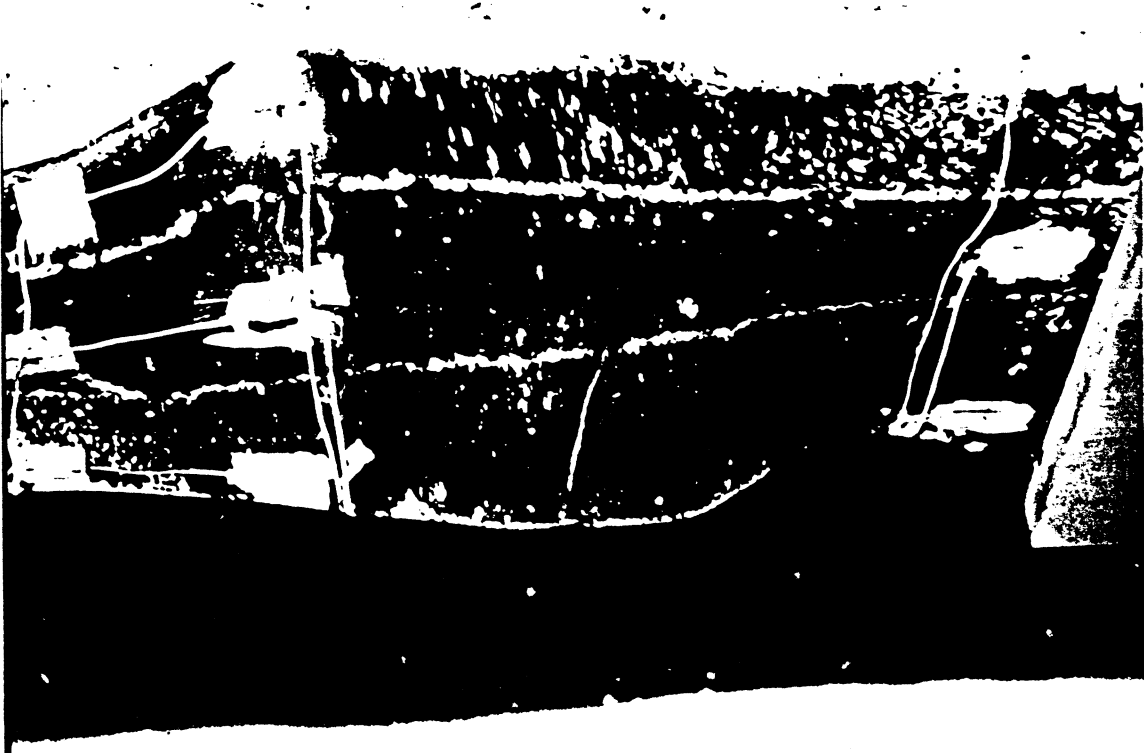


FIGURE 62A: SPECIMEN 2 -- BEAM AFTER 4" CYCLES



FIGURE 62B: SPECIMEN 2 -- BEAM AFTER THE TEST

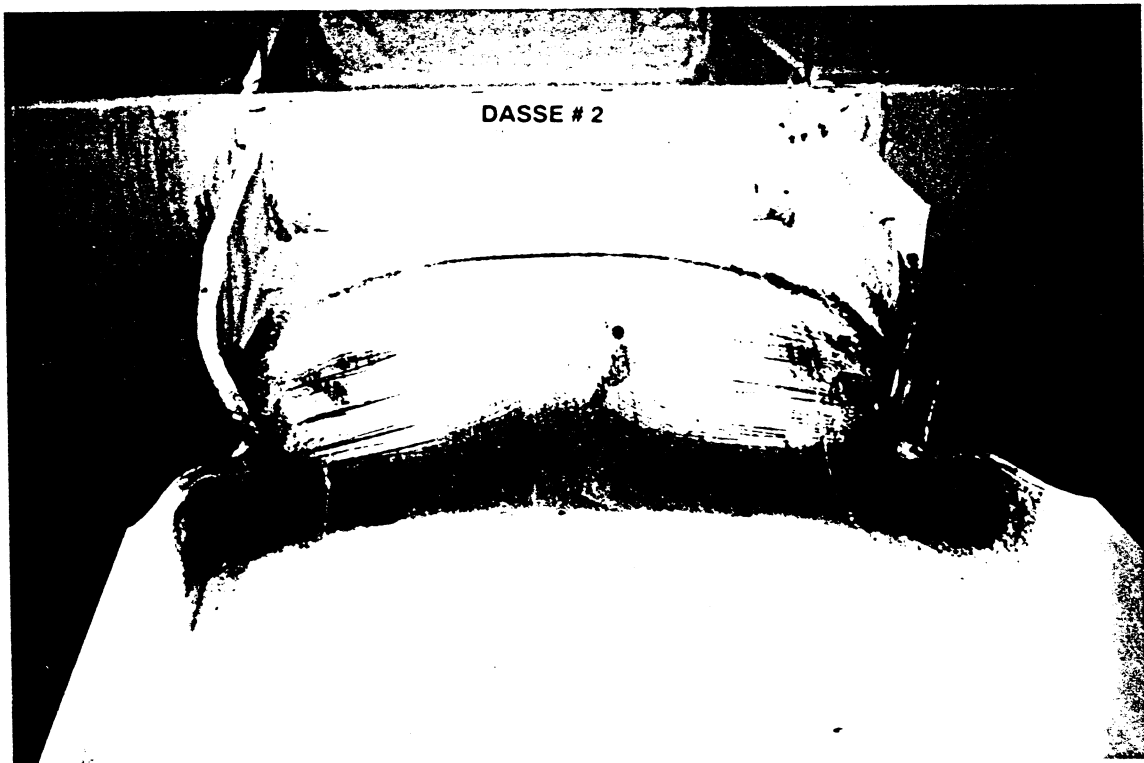


FIGURE 61C: SPECIMEN 2 -- BEAM TOP FLANGE
(after 2" cycles)

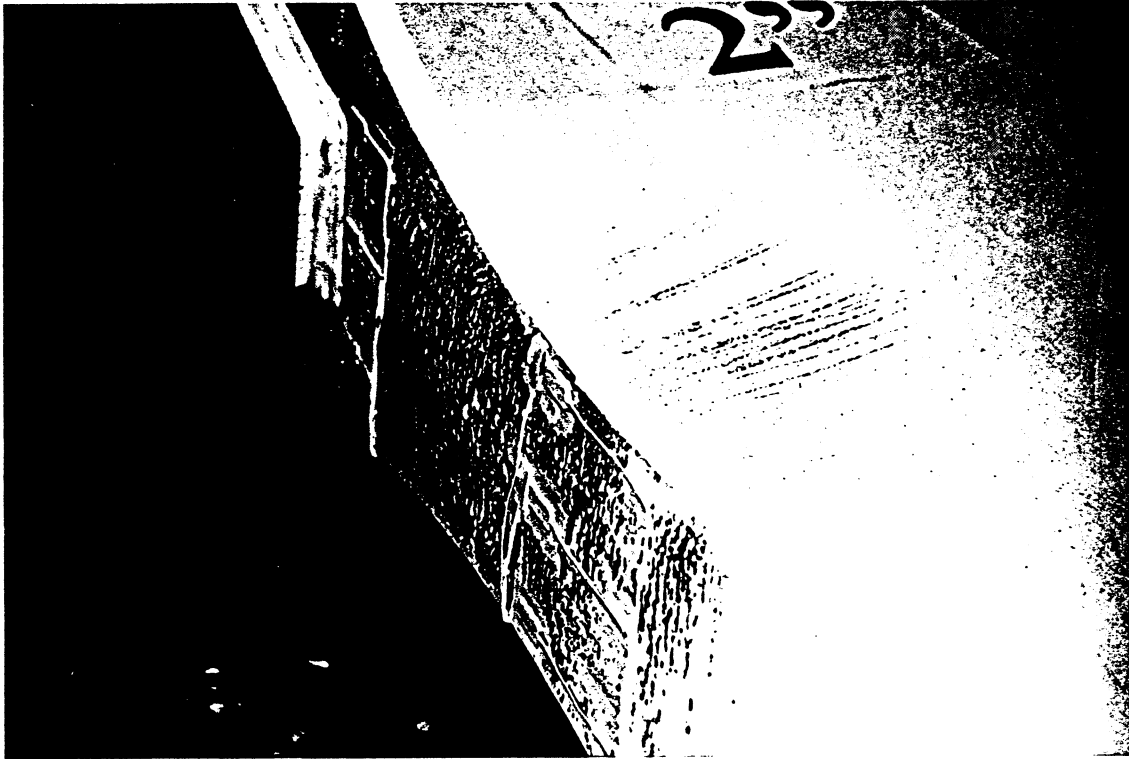


FIGURE 61D: SPECIMEN 2 -- BEAM TOP FLANGE
(after 3" cycles)



FIGURE 61A: SPECIMEN 2 -- WHITE-WASH FLAKES ON BEAM TOP FLANGE
(@ +0.75" actuator displacement)

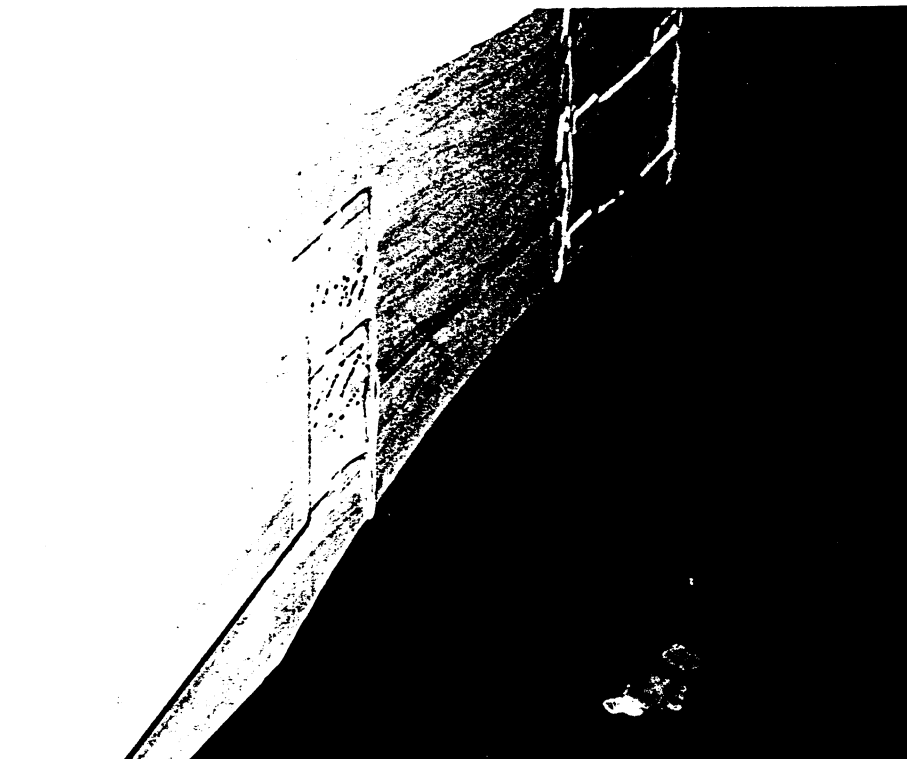


FIGURE 61B: SPECIMEN 2 -- BEAM TOP FLANGE
(@ +1" actuator displacement)

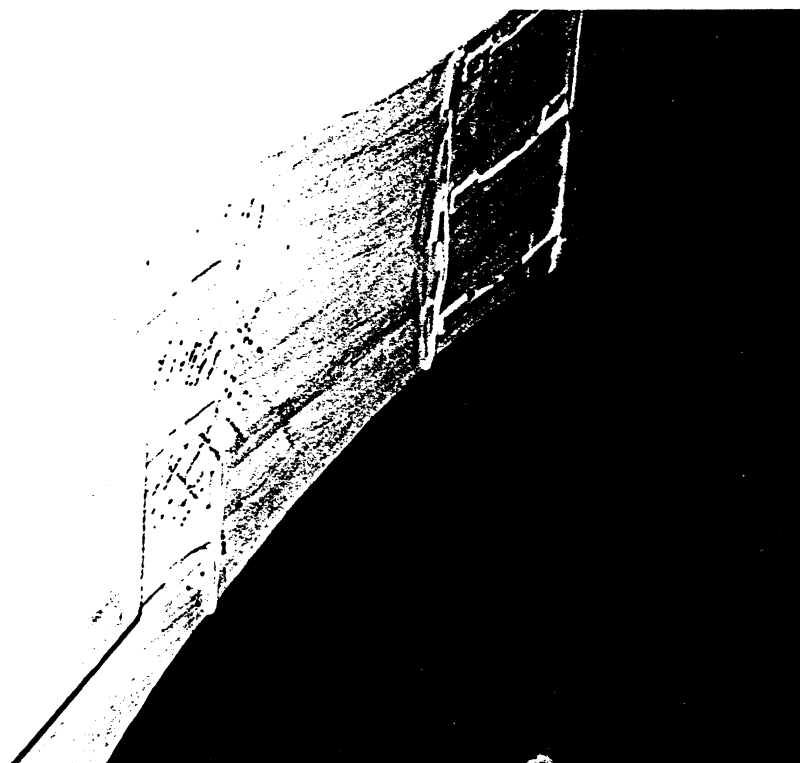


FIGURE 67: IMPOSED LOADING HISTORY -- ACTUATOR DISPLACEMENT
UCB-DASSE #3

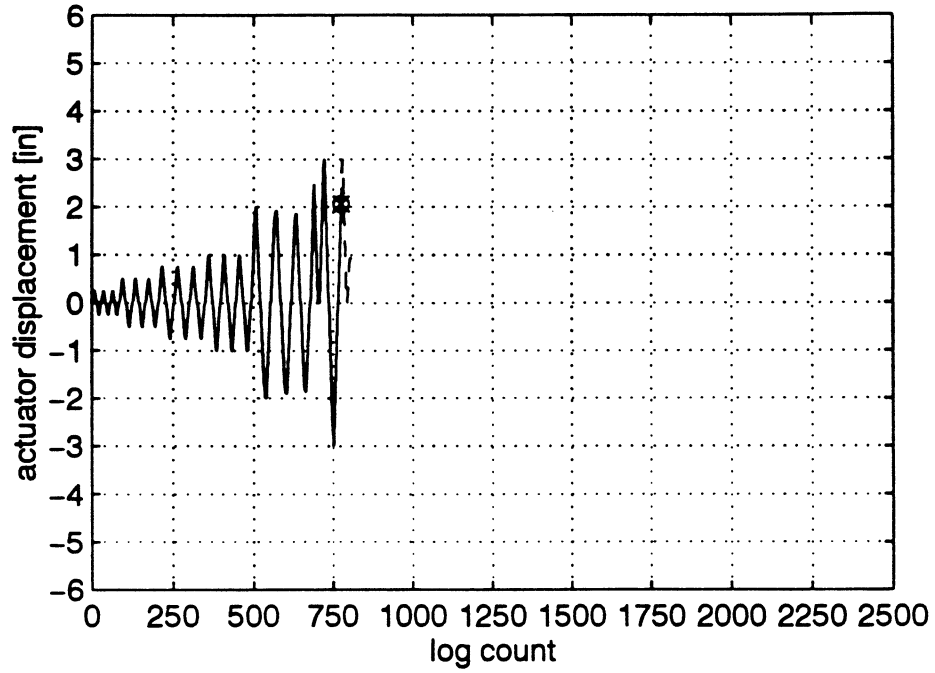


FIGURE 68: APPLIED LOAD / BEAM END DISPLACEMENT RESPONSE
UCB-DASSE #3

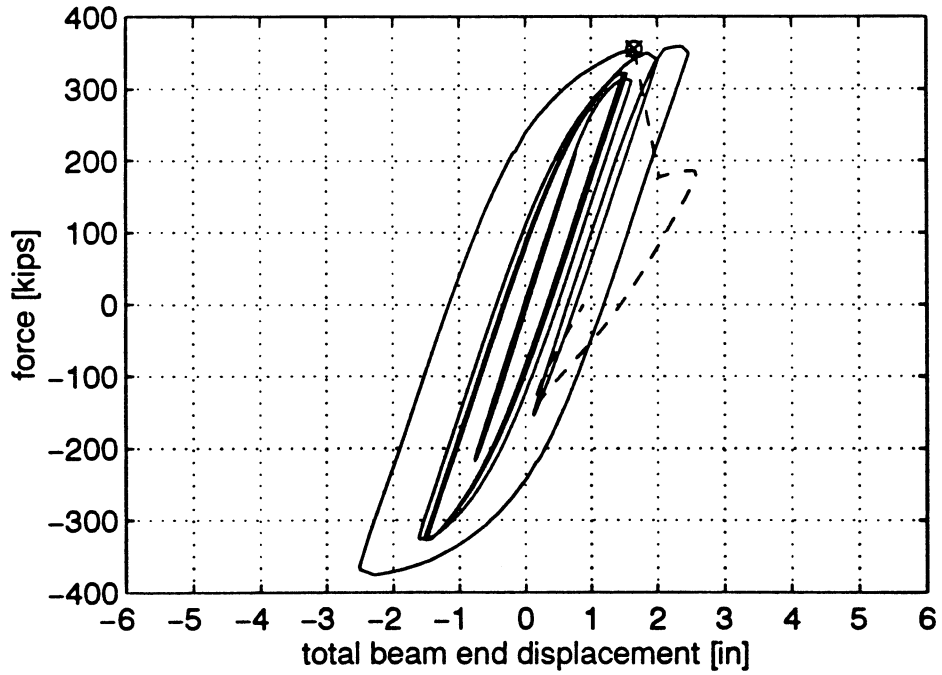


FIGURE 69: PLASTIC ROTATION VERSUS MOMENT @ COVER PLATE EDGE

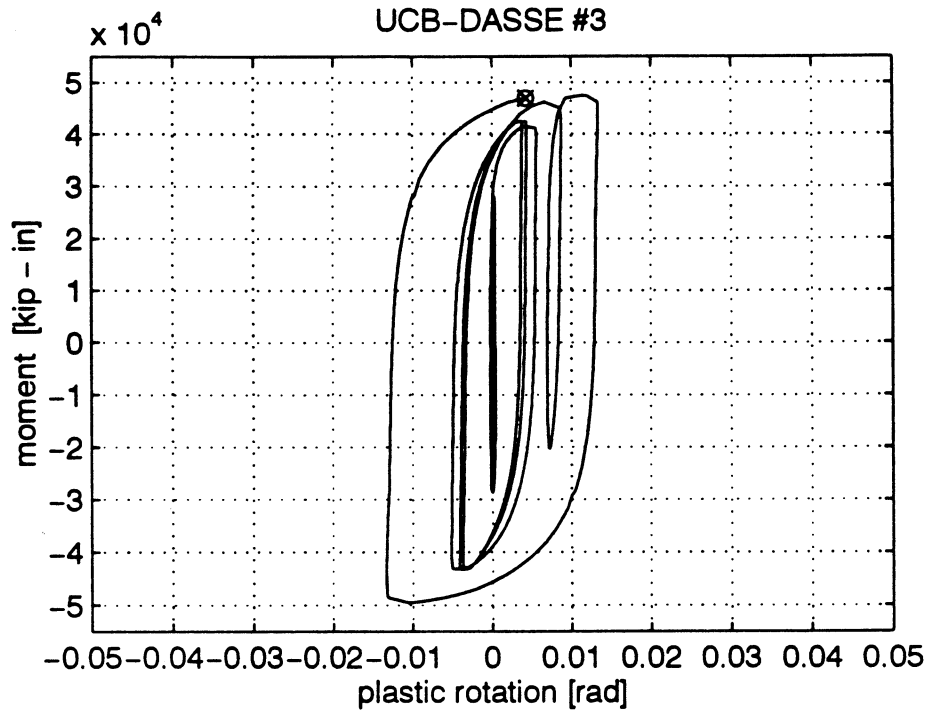


FIGURE 70: DISSIPATED ENERGY

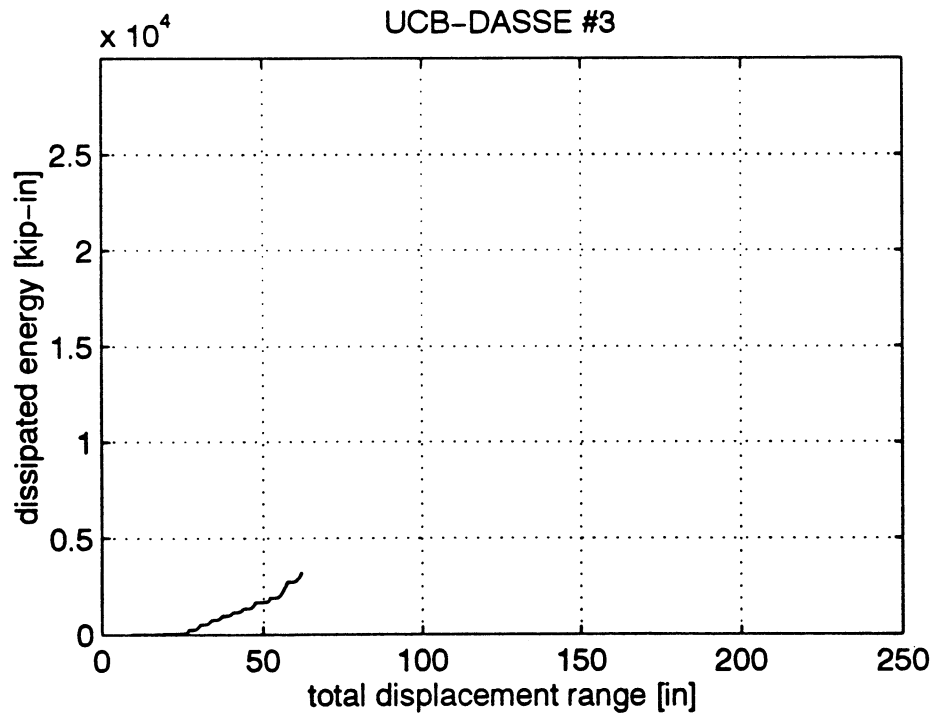


FIGURE 71: PANEL ZONE SHEAR DEFORMATION

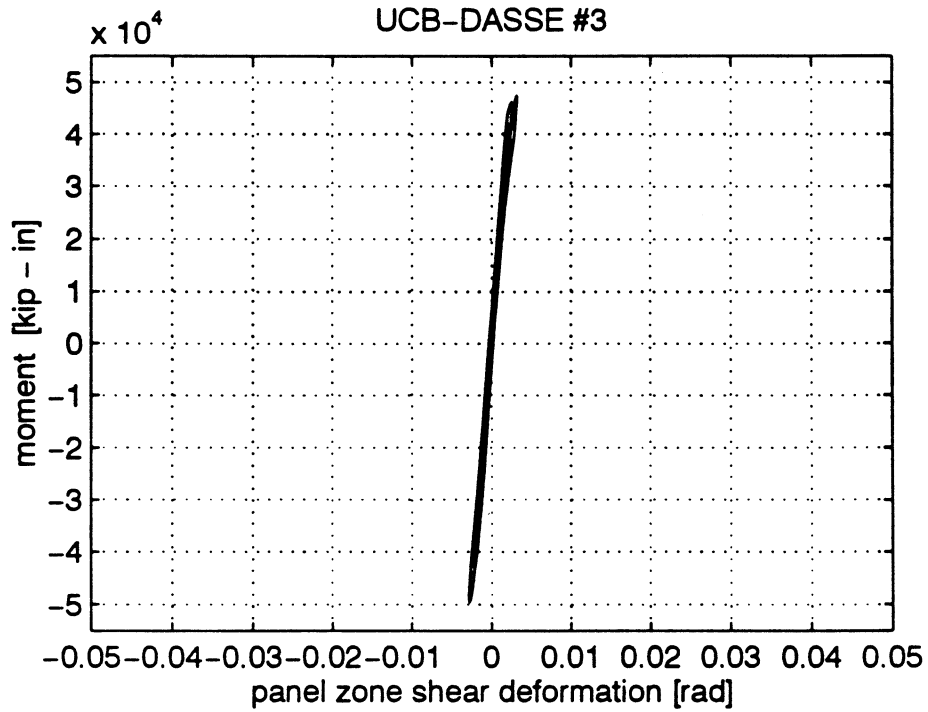


FIGURE 72: BEAM CONTRIBUTION TO TOTAL DISPLACEMENT

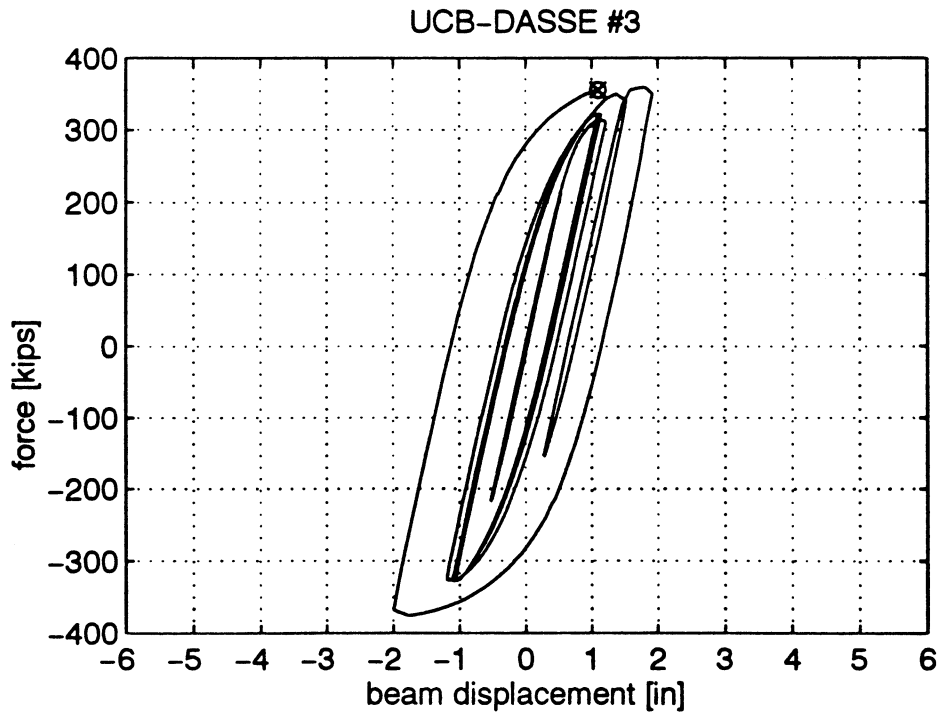


FIGURE 73: LOCAL RESPONSE -- TOP BEAM FLANGE EDGE (@ COVER PLATE)

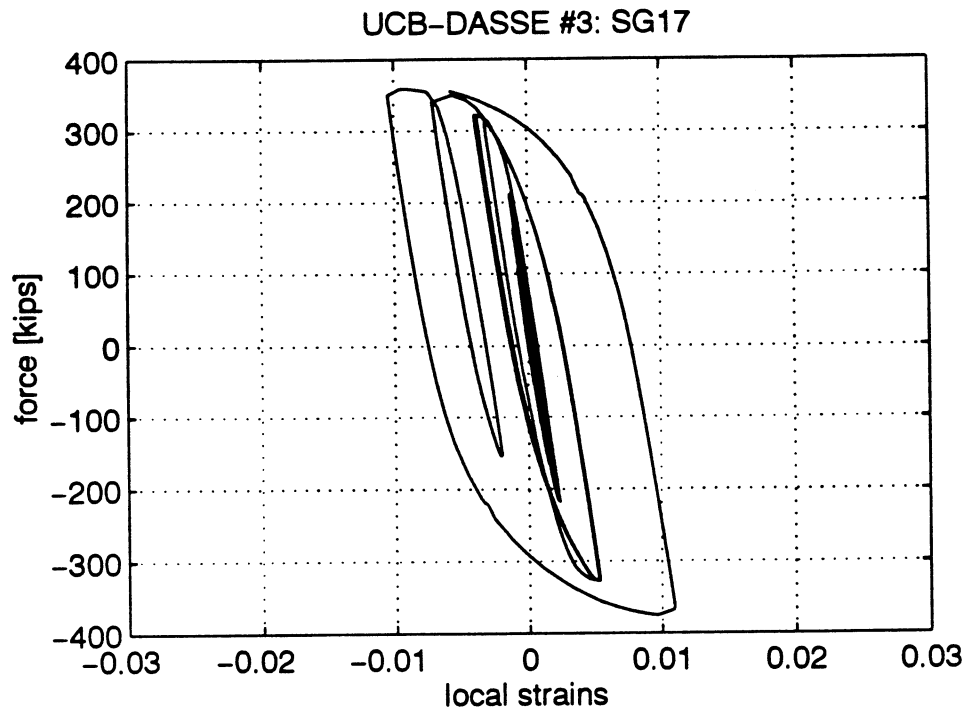


FIGURE 74: LOCAL RESPONSE -- TOP BEAM FLANGE AXIS (@ COVER PLATE)

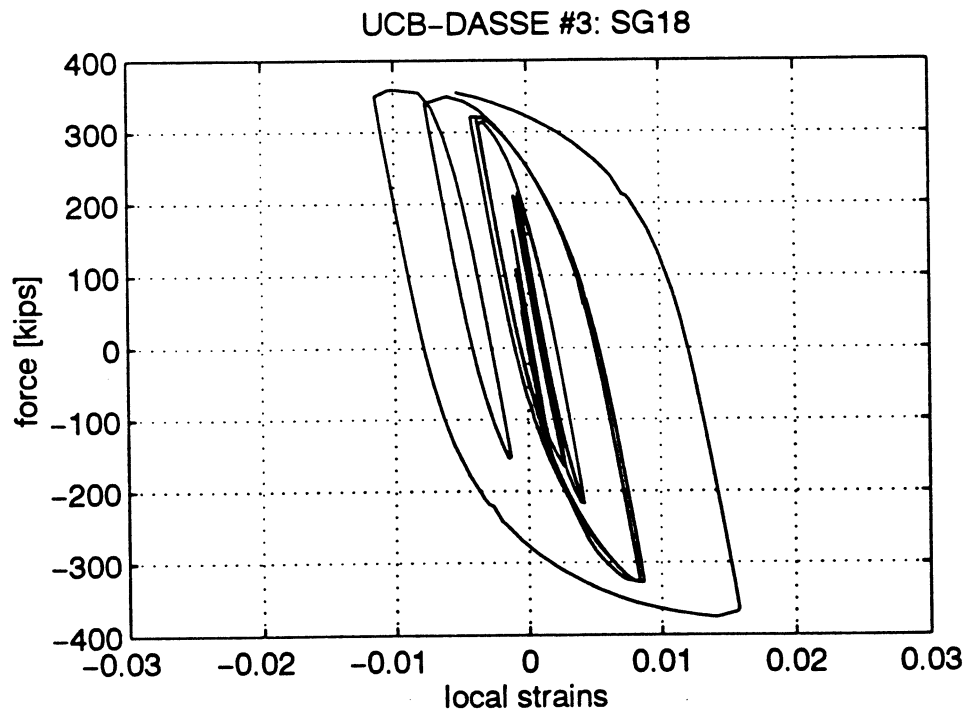


FIGURE 75: LOCAL RESPONSE -- BOTTOM BEAM FLANGE EDGE (@ COVER PLATE)

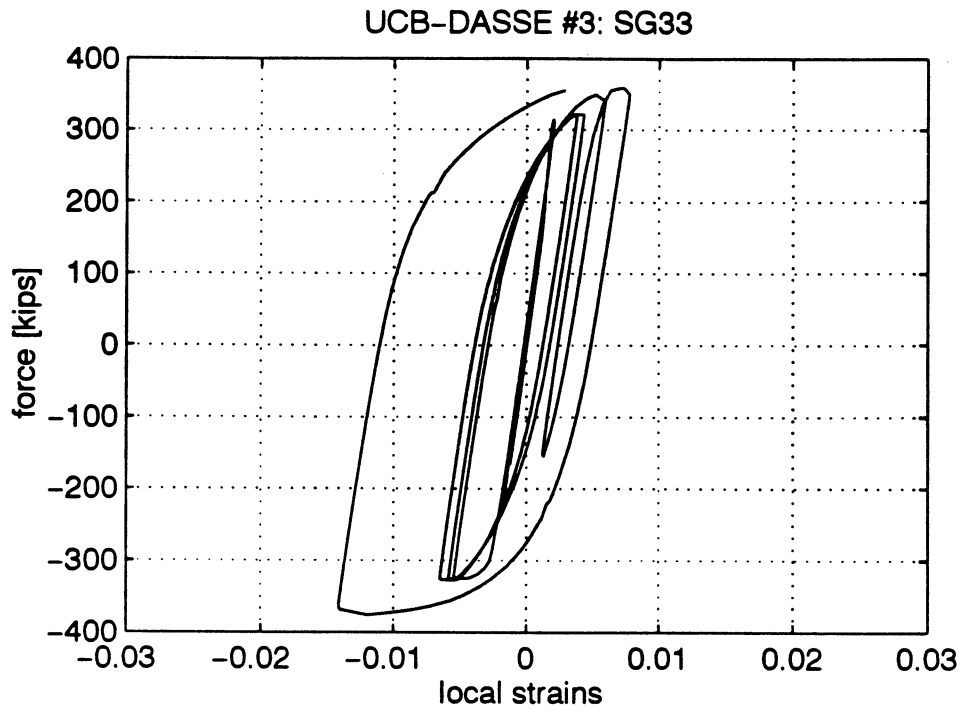


FIGURE 76: LOCAL RESPONSE -- BOTTOM BEAM FLANGE AXIS (@ COVER PLATE)

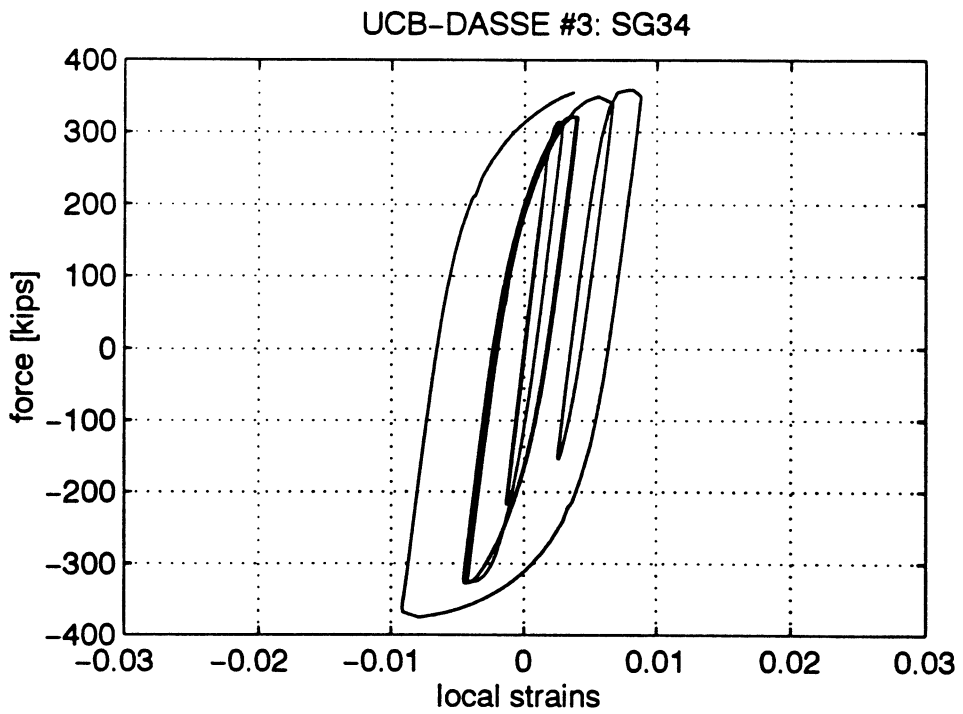


FIGURE 77: LOCAL RESPONSE -- TOP FLANGE EDGE (@ "DOG BONE")

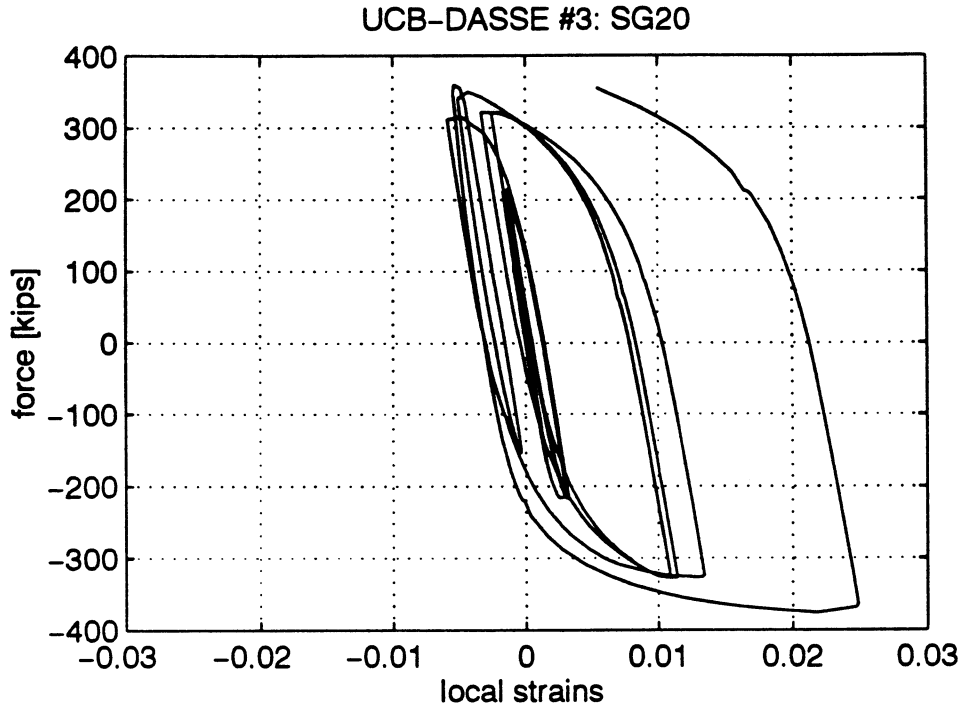


FIGURE 78: LOCAL RESPONSE -- TOP FLANGE AXIS (@ "DOG BONE")

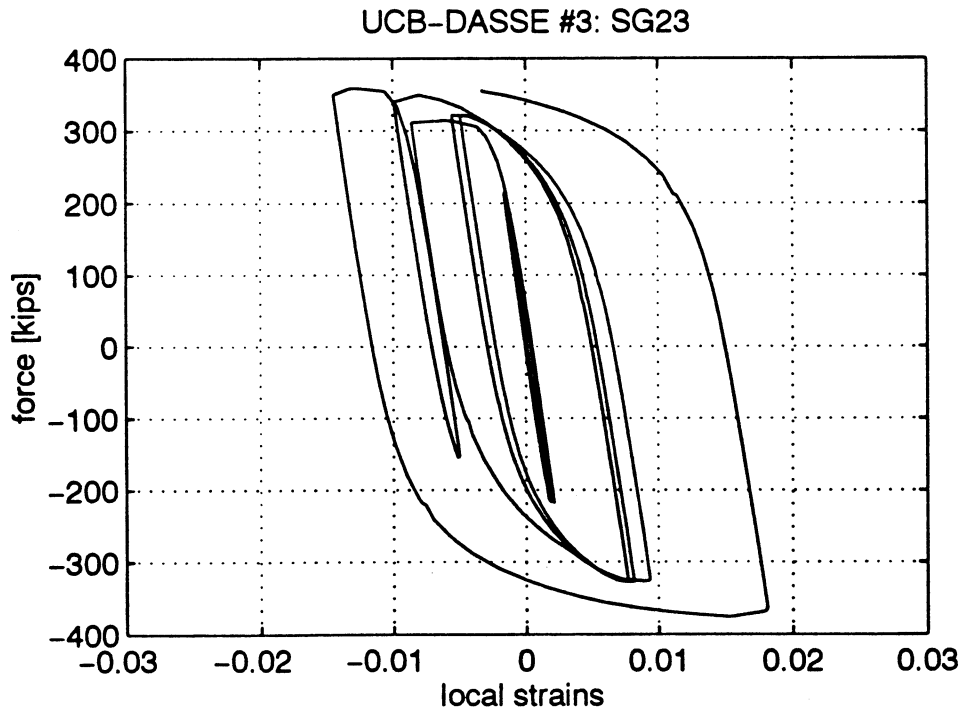


FIGURE 79: LOCAL RESPONSE -- BOTTOM FLANGE EDGE (@ "DOG BONE")

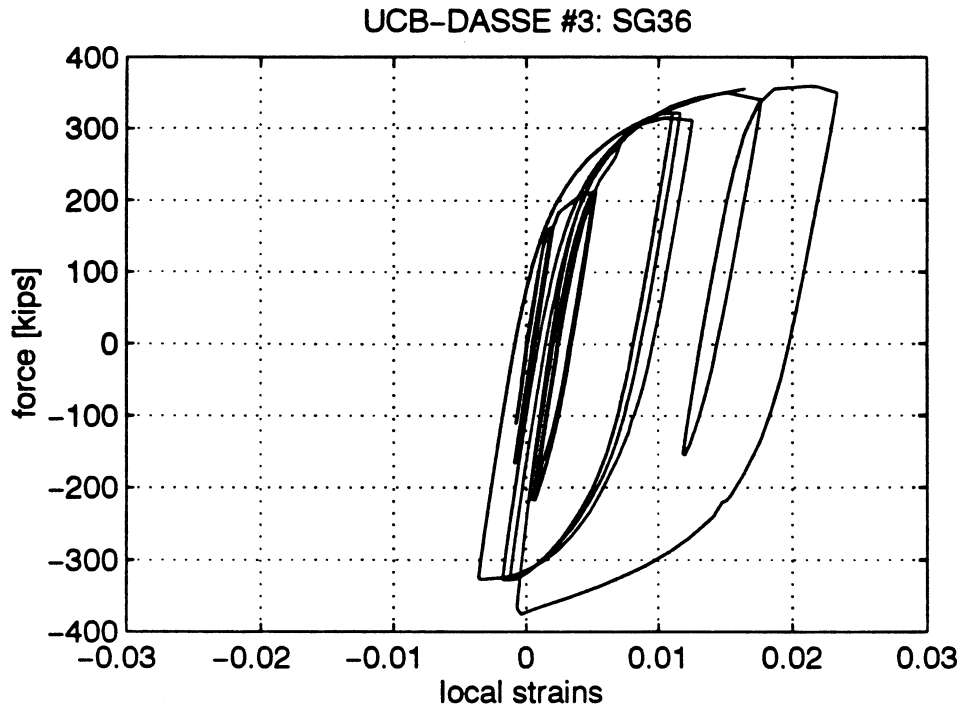


FIGURE 80: LOCAL RESPONSE -- BOTTOM FLANGE AXIS (@ "DOG BONE")

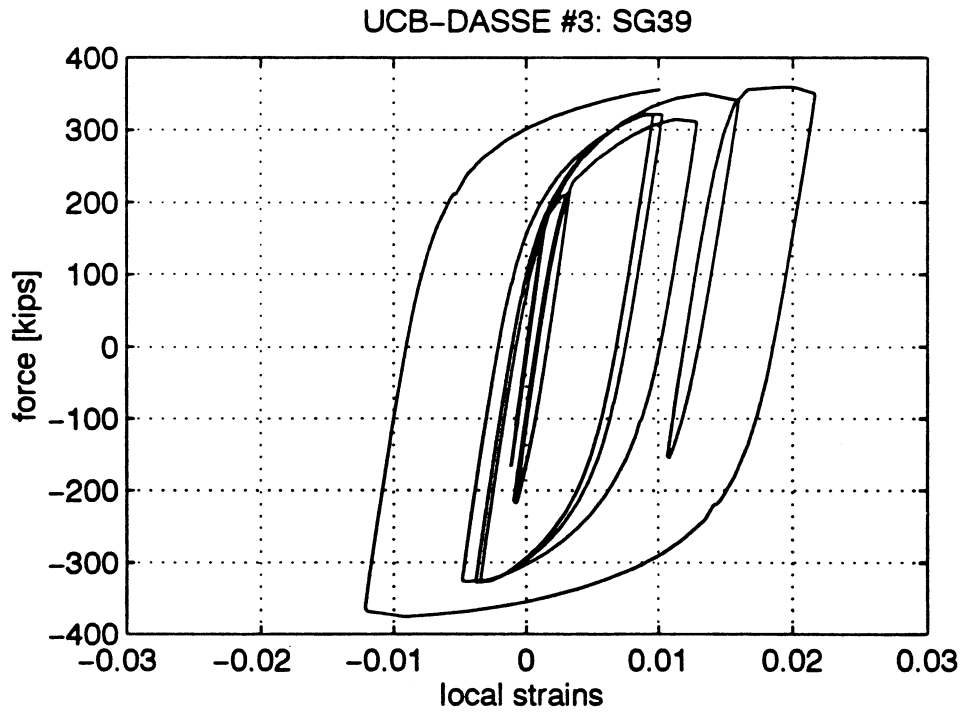


FIGURE 81: SPECIMEN 3 -- FIRST WHITE-WASH FLAKES ON COLUMN WEB
(@ 1" actuator displacement)

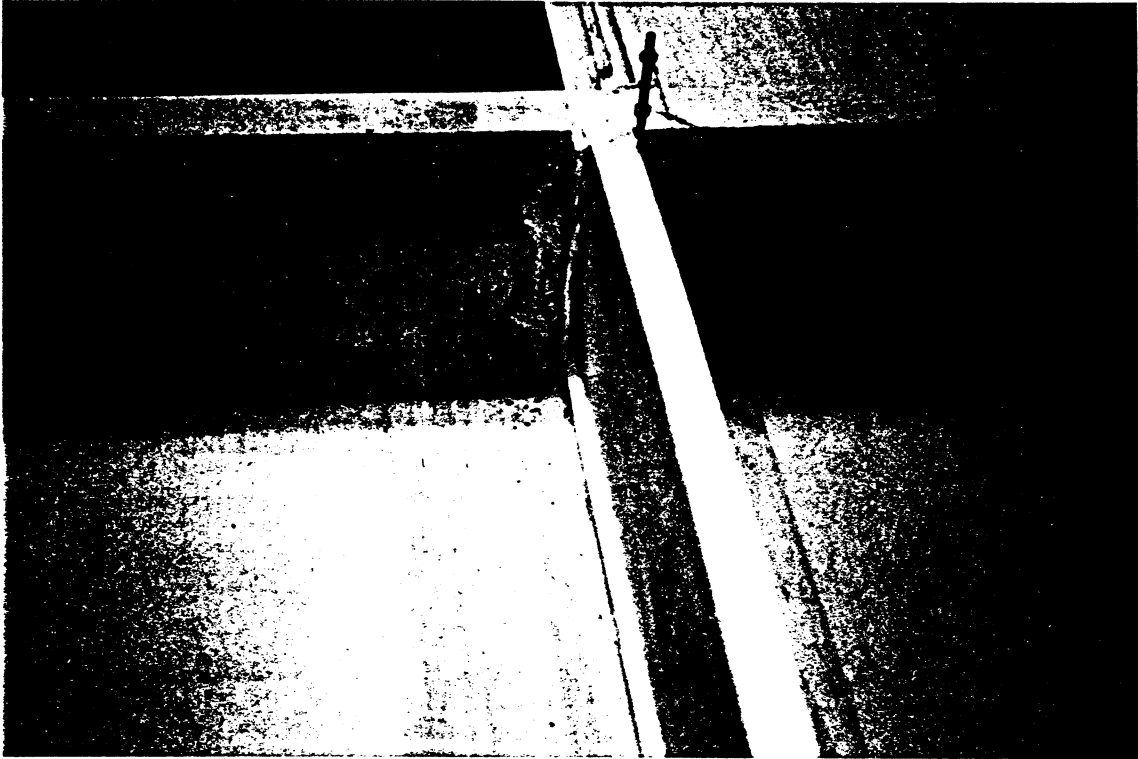


FIGURE 82: SPECIMEN 3 -- PANEL ZONE
(@ 2" actuator displacement)

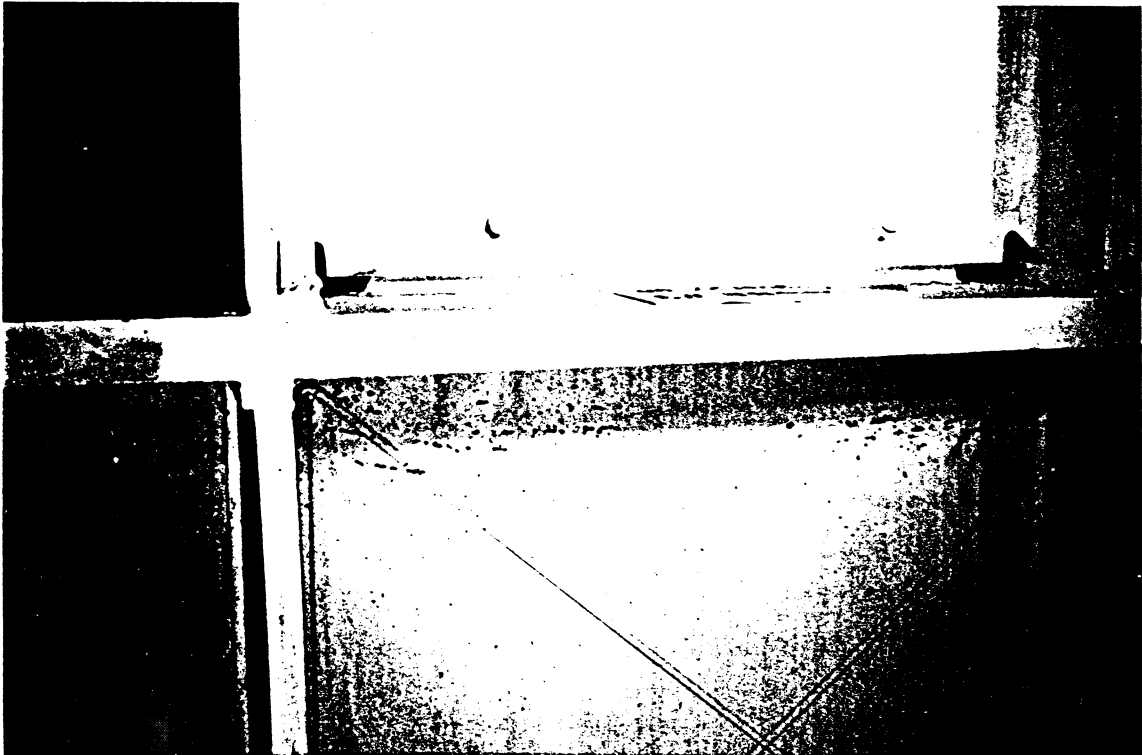


FIGURE 83: SPECIMEN 3 -- BEAM AFTER FIRST 3" CYCLE

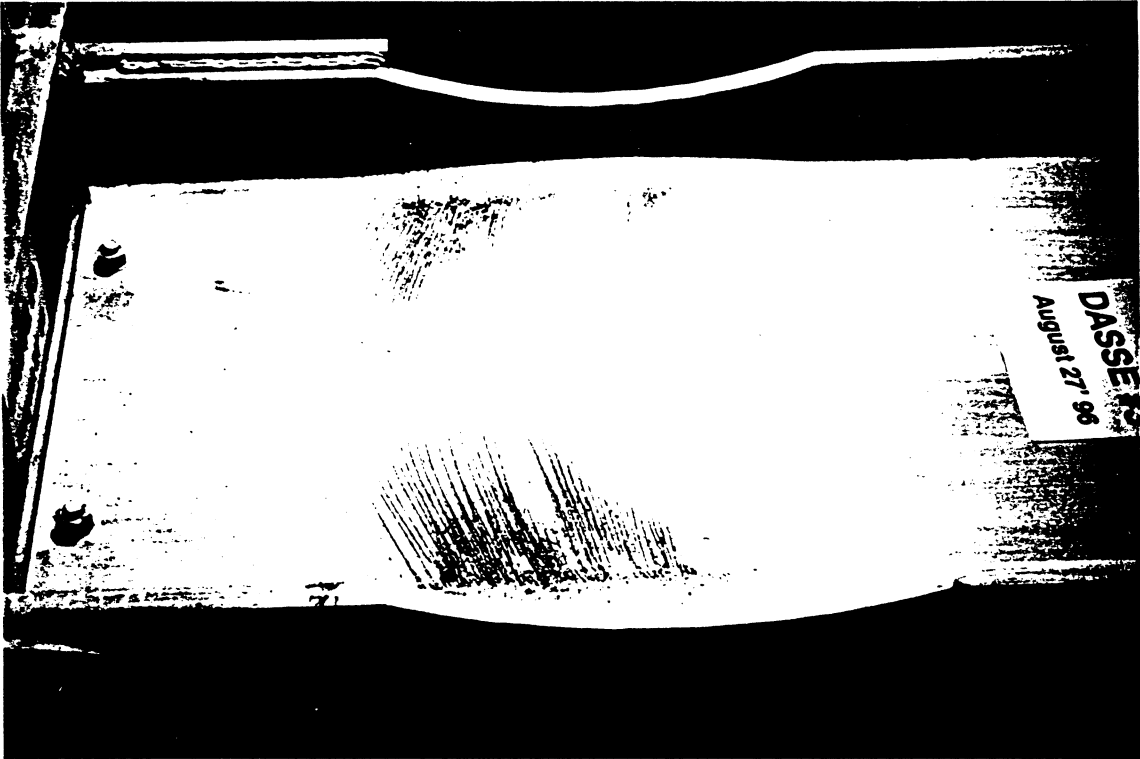


FIGURE 84: SPECIMEN 3 -- FRACTURE PATTERN

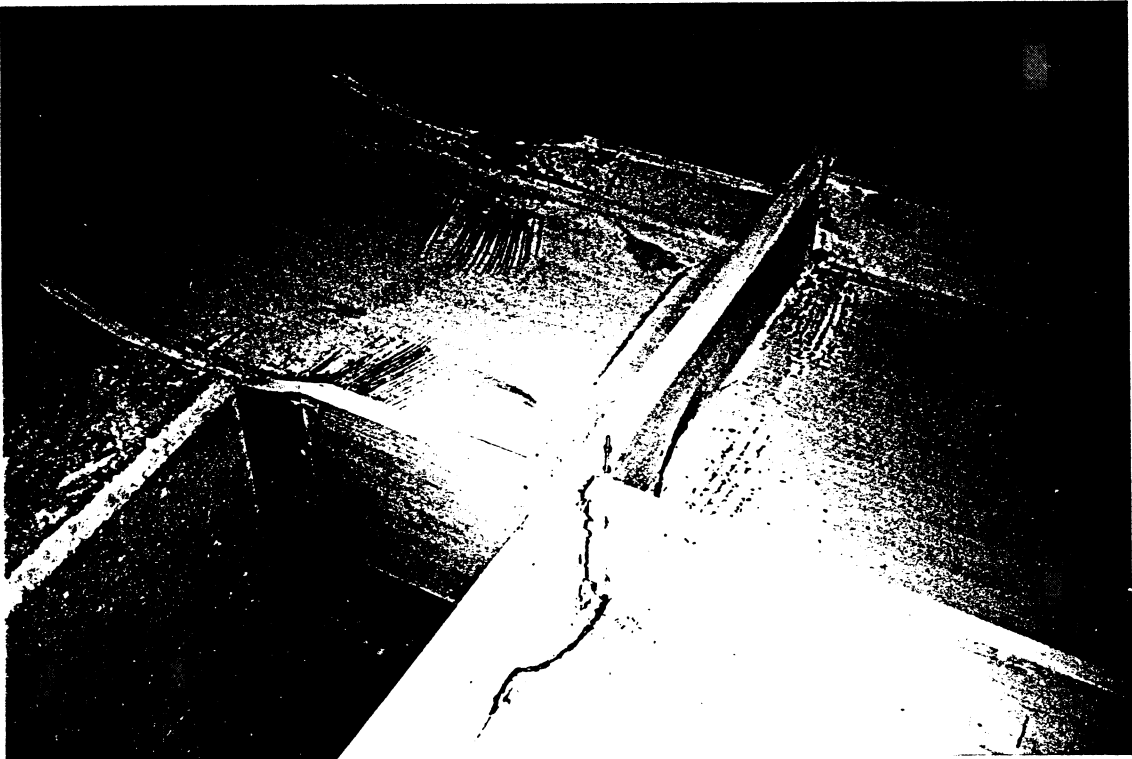
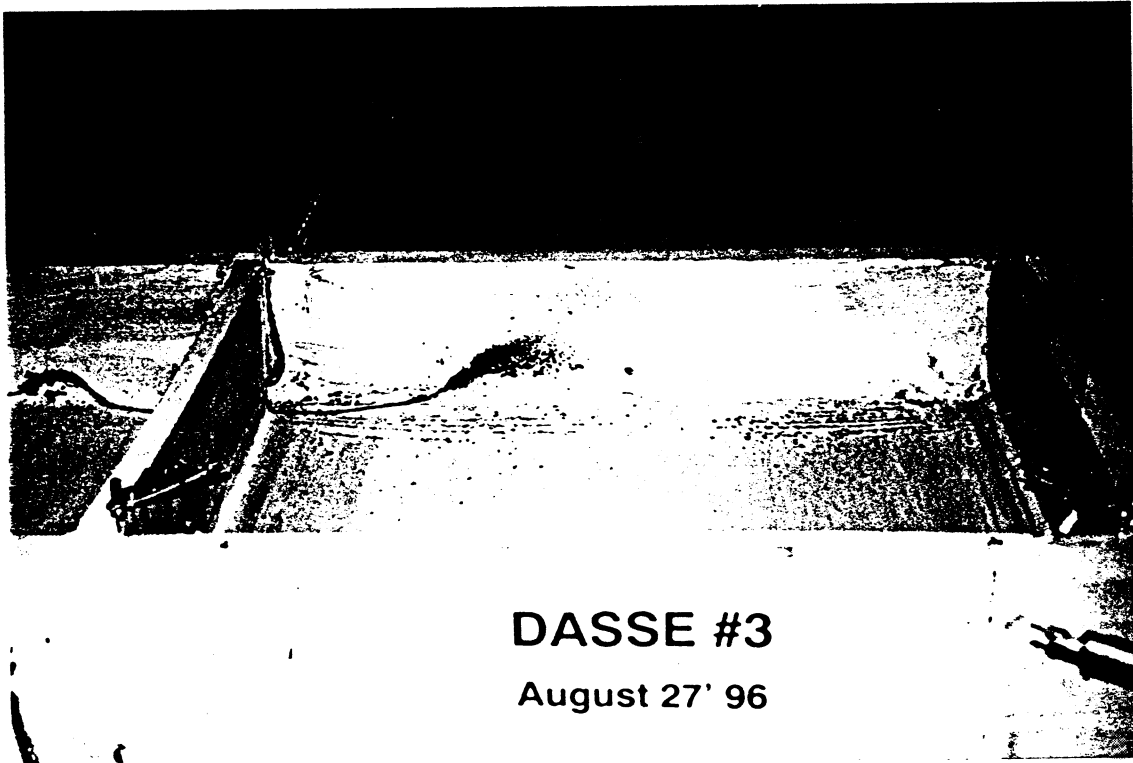


FIGURE 85: SPECIMEN 3 -- FRACTURE



FIGURE 86: SPECIMEN 3 -- FRACTURE



DASSE #3

August 27' 96

FIGURE 87: SPECIMEN 3 -- UNDERSIDE VIEW OF THE CRACK

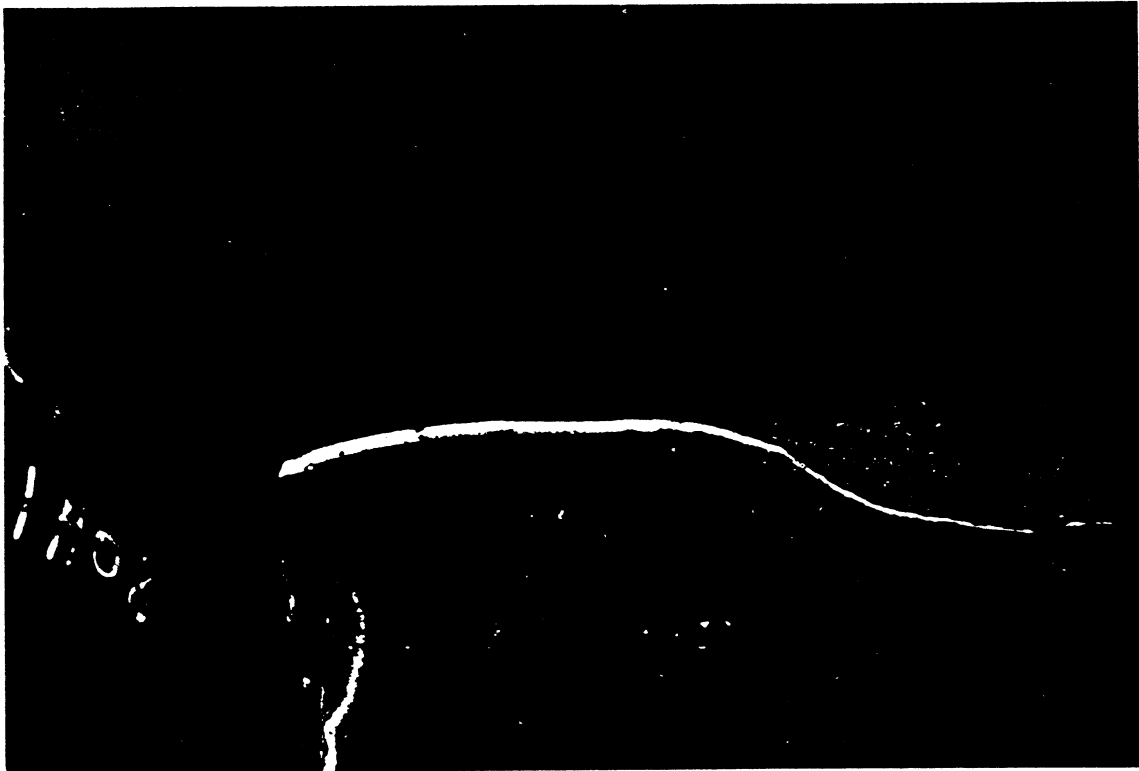


FIGURE 88: SPECIMEN 3 -- CRACK TRACE ON THE OUTER COLUMN SURFACE

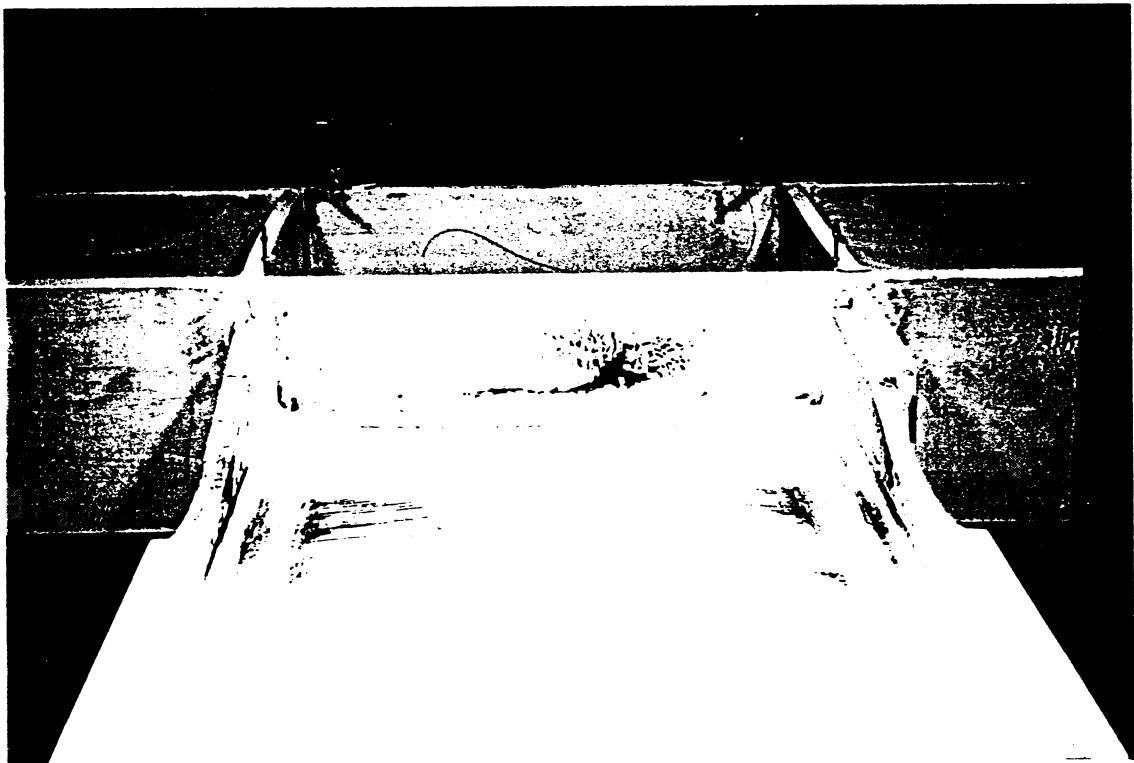


FIGURE 89: IMPOSED LOADING HISTORY -- ACTUATOR DISPLACEMENT
UCB-DASSE #3 (POST-FRACTURE TEST)

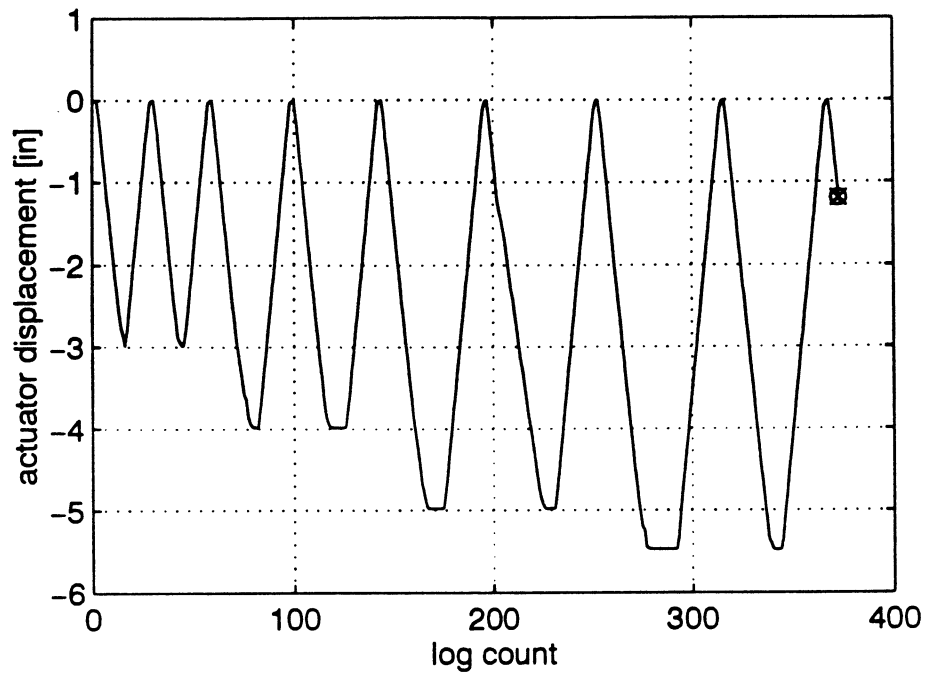


FIGURE 90: LOAD RESPONSE
UCB-DASSE #3 (POST-FRACTURE TEST)

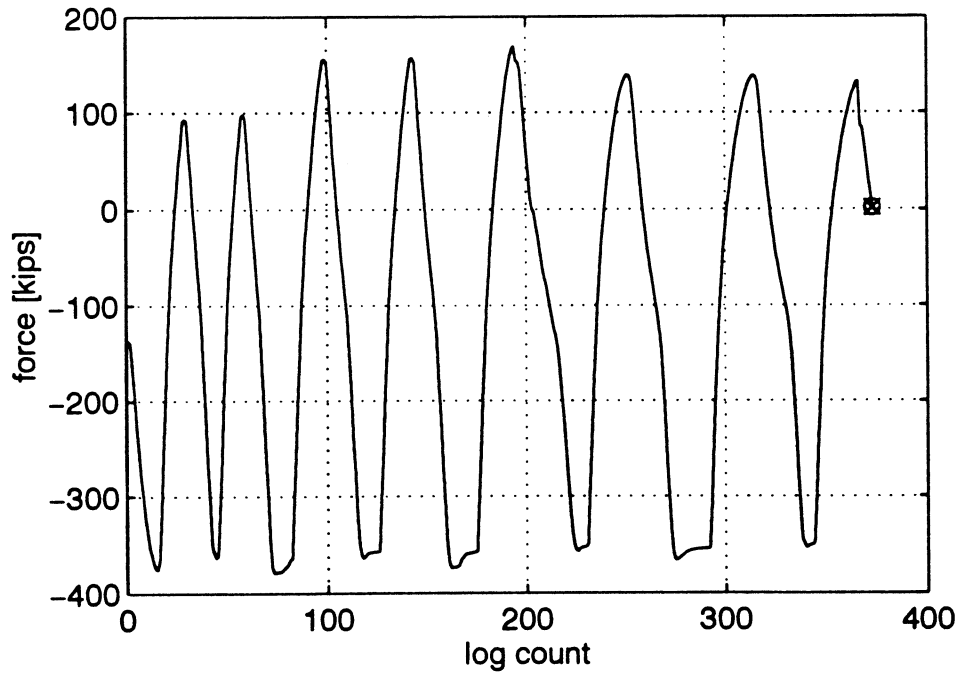


FIGURE 91: IMPOSED LOADING HISTORY -- ACTUATOR DISPLACEMENT
UCB-DASSE #4

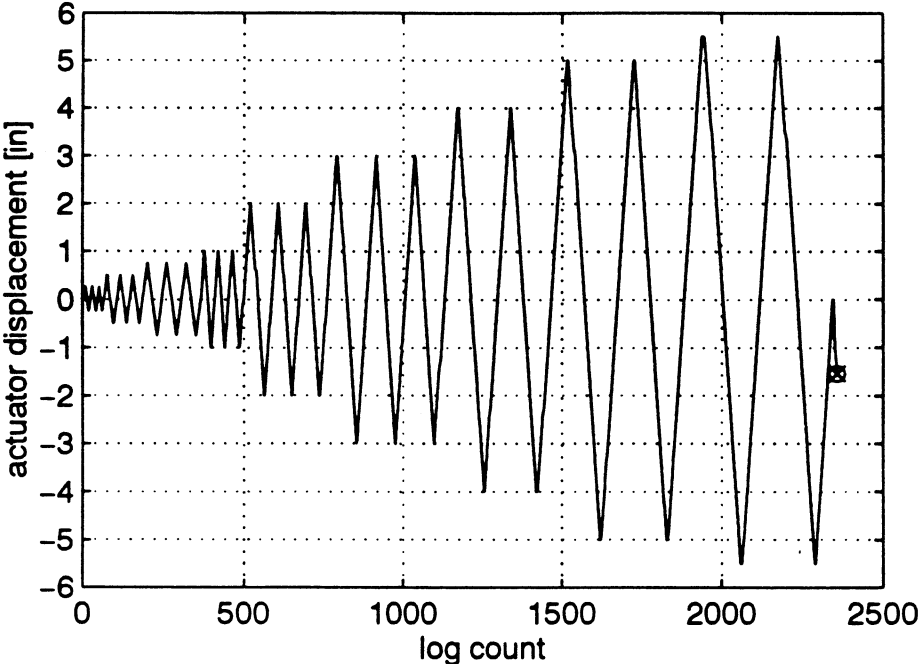


FIGURE 92: APPLIED LOAD / BEAM END DISPLACEMENT RESPONSE
UCB-DASSE #4

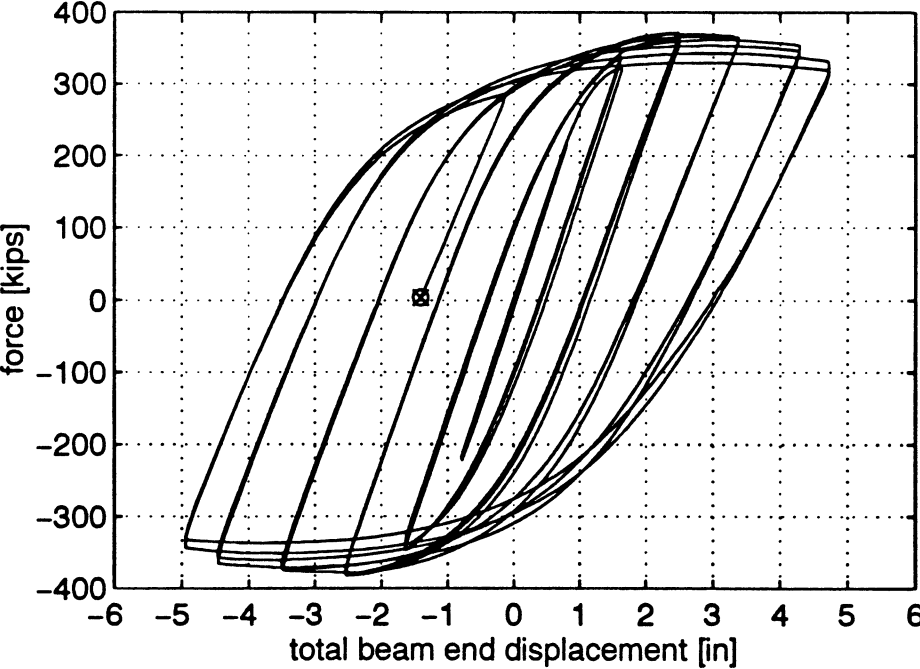


FIGURE 93: PLASTIC ROTATION VERSUS MOMENT @ COVER PLATE EDGE

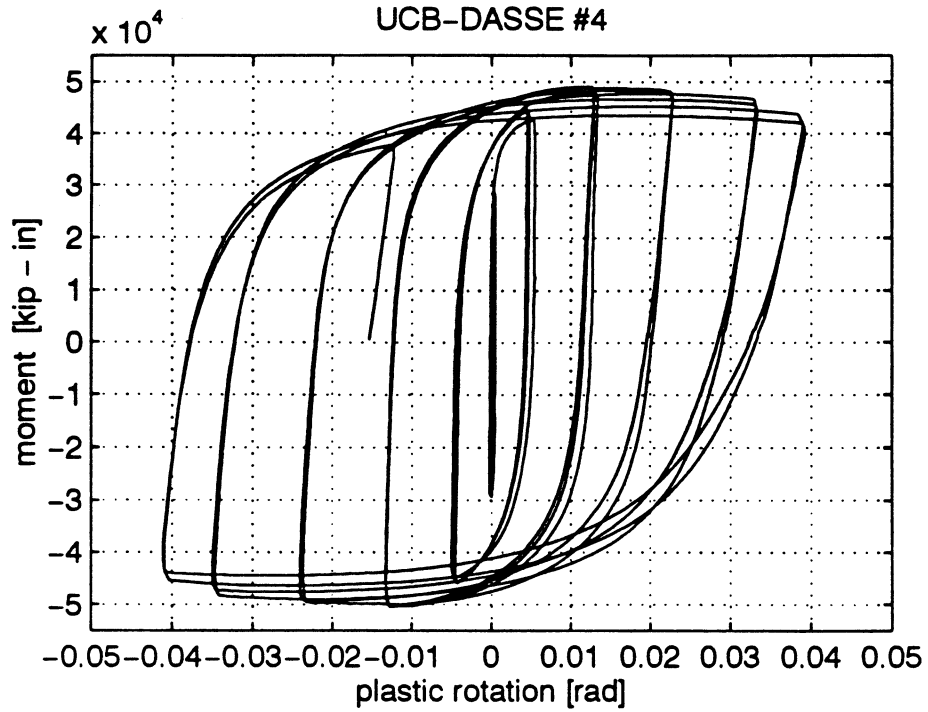


FIGURE 94: DISSIPATED ENERGY

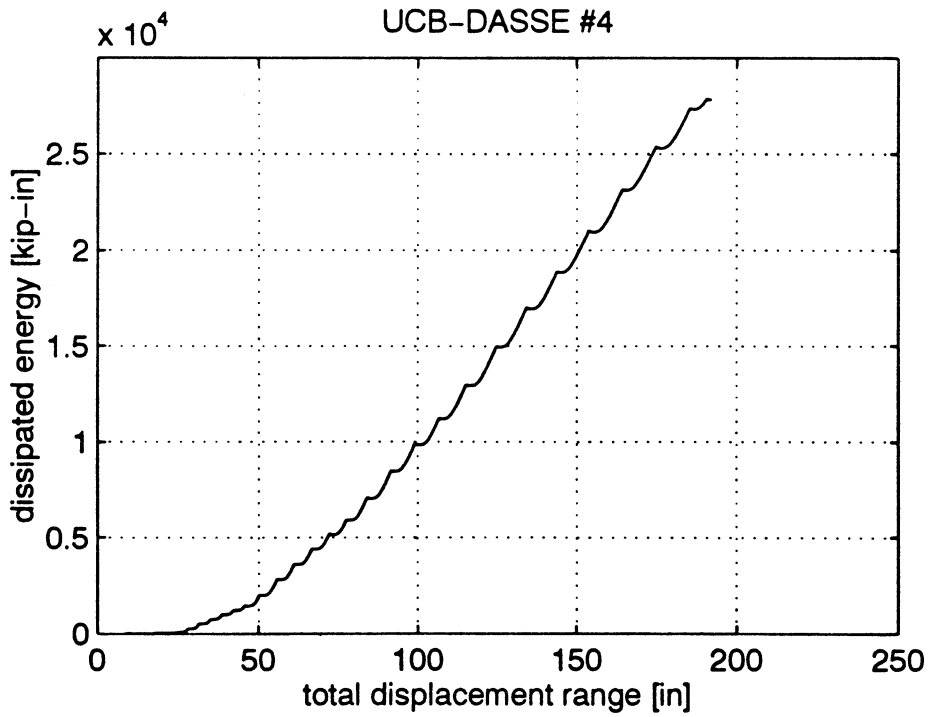


FIGURE 95: PANEL ZONE SHEAR DEFORMATION

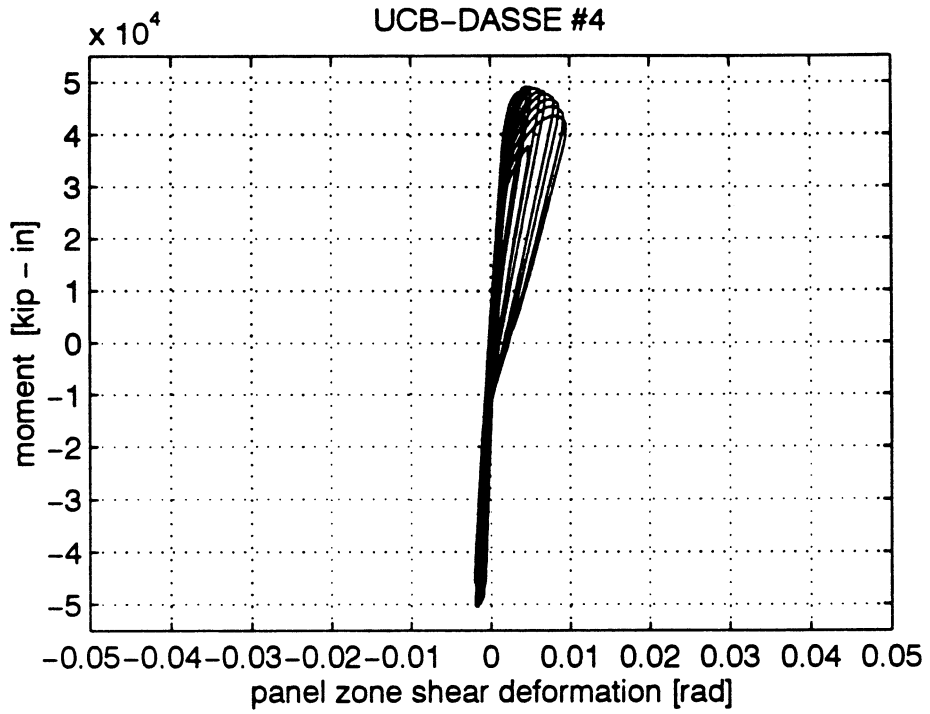


FIGURE 96: BEAM CONTRIBUTION TO TOTAL DISPLACEMENT

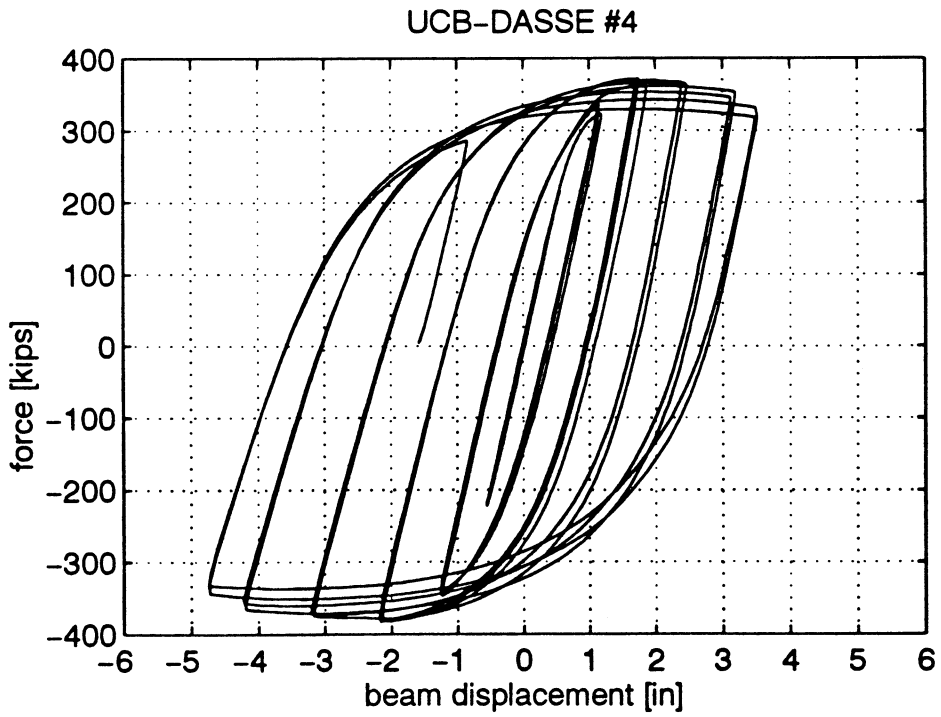


FIGURE 97: LOCAL RESPONSE -- TOP BEAM FLANGE EDGE (@ COVER PLATE)

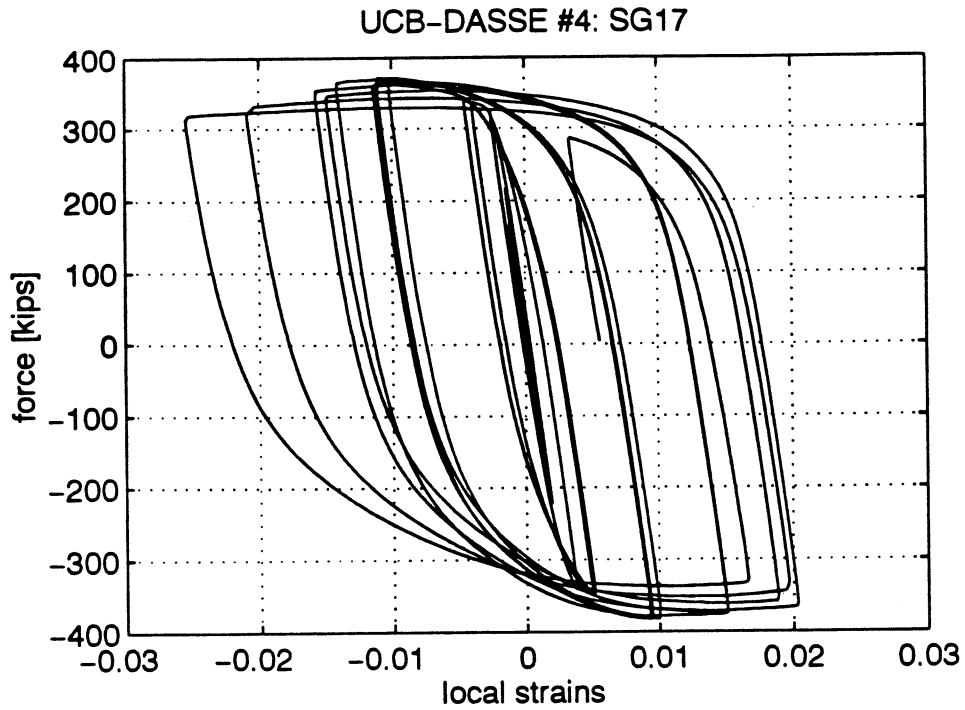


FIGURE 98: LOCAL RESPONSE -- TOP BEAM FLANGE AXIS (@ COVER PLATE)

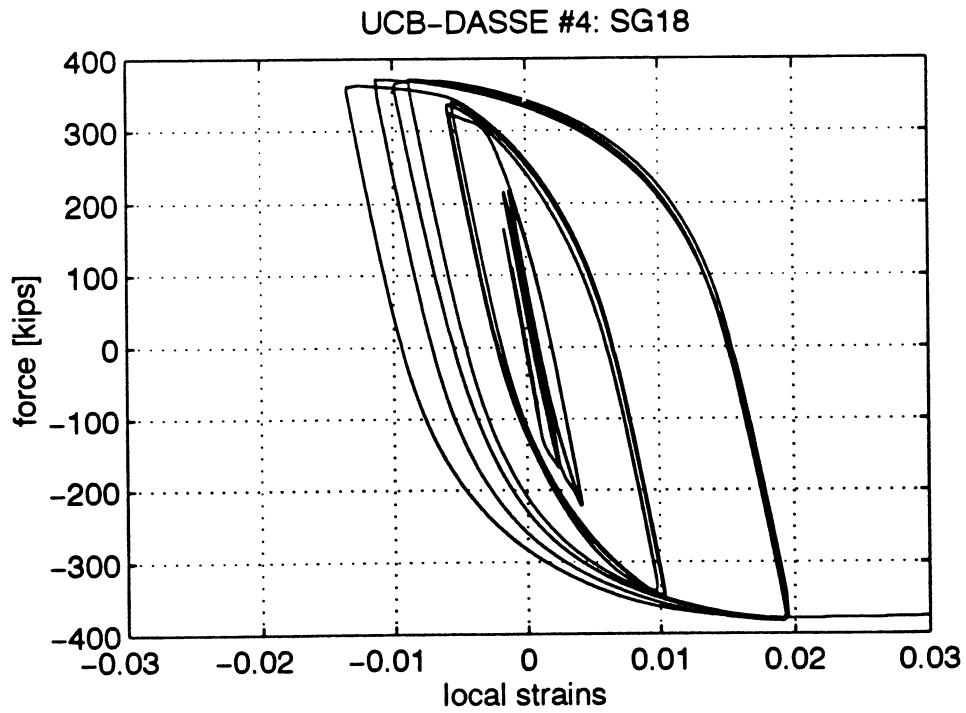


FIGURE 99: LOCAL RESPONSE -- BOTTOM BEAM FLANGE EDGE (@ COVER PLATE)

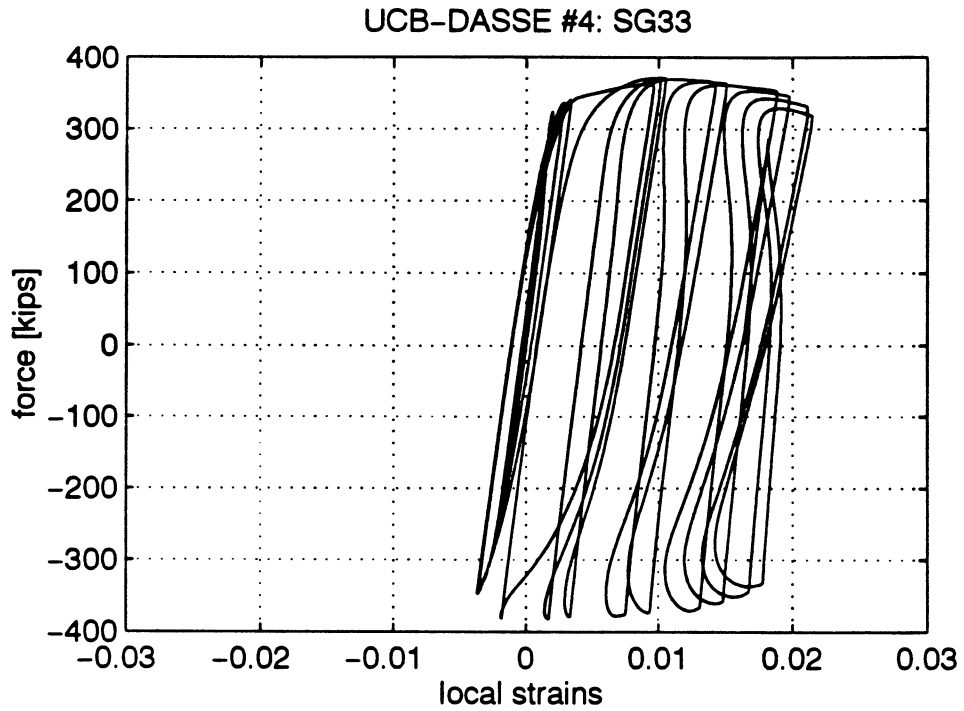


FIGURE 100: LOCAL RESPONSE -- BOTTOM BEAM FLANGE AXIS (@ COVER PLATE)

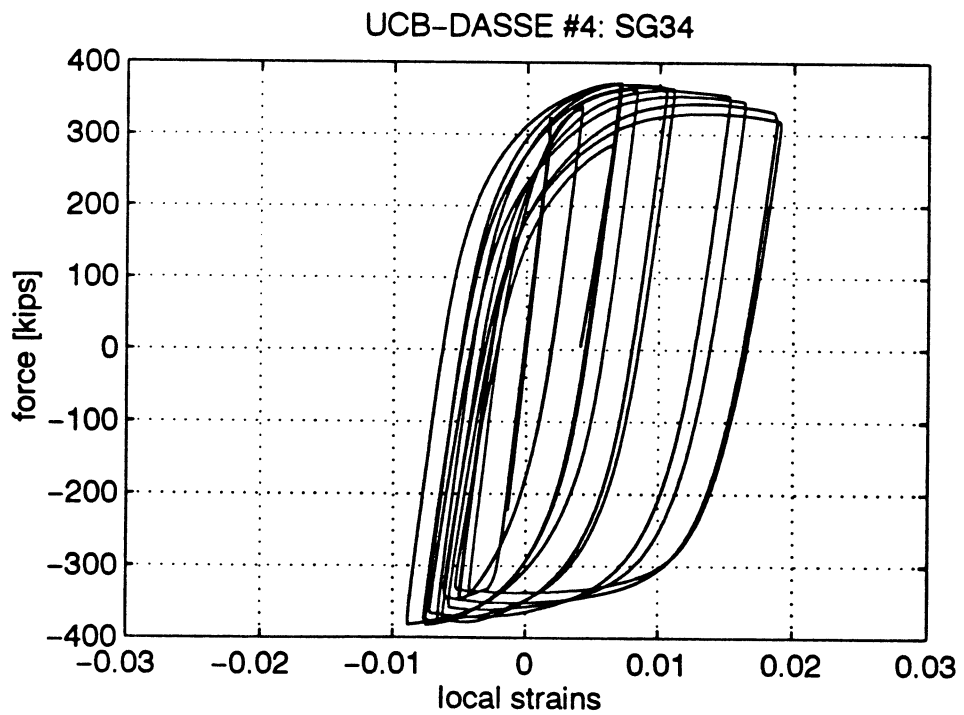


FIGURE 101: LOCAL RESPONSE -- TOP FLANGE EDGE HOR (@ "DOG BONE")

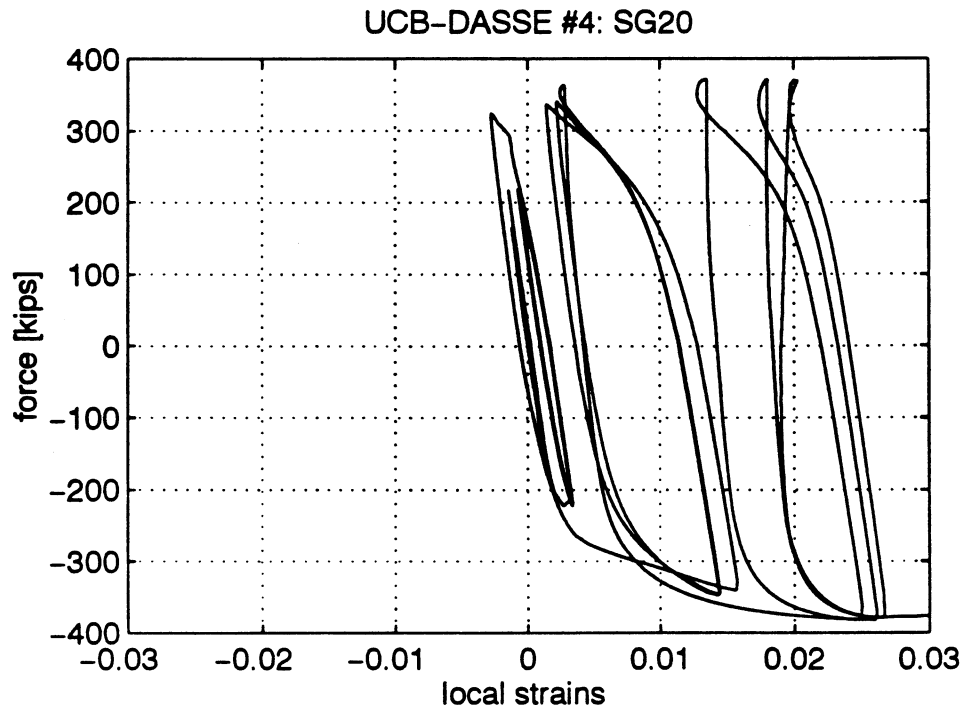


FIGURE 102: LOCAL RESPONSE -- TOP FLANGE AXIS HOR (@ "DOG BONE")

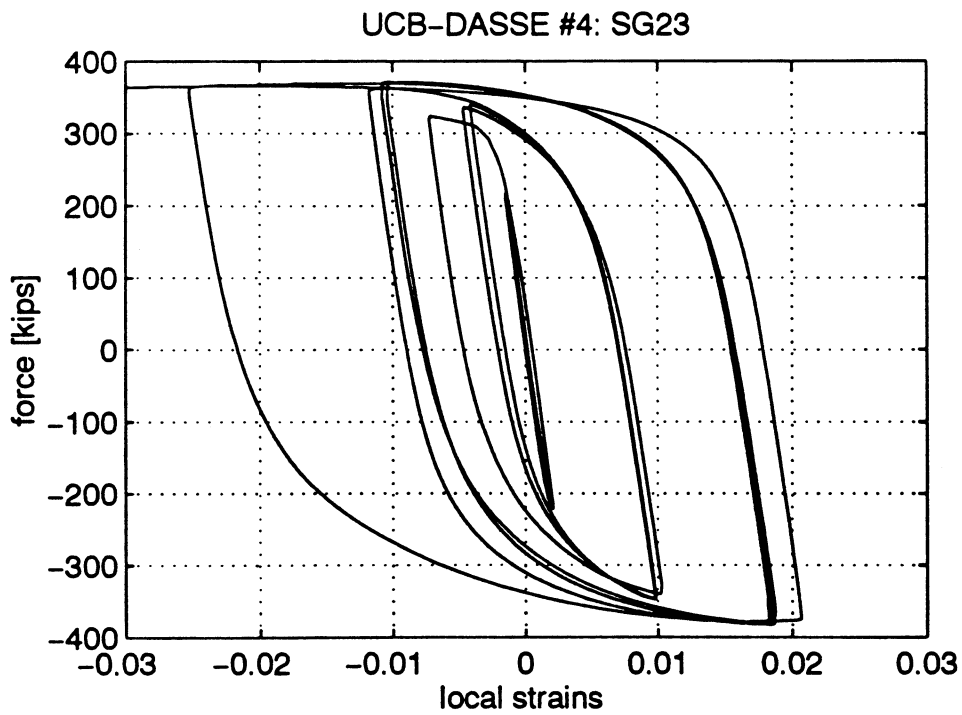


FIGURE 103: LOCAL RESPONSE -- TOP FLANGE EDGE VER (@ "DOG BONE")

UCB-DASSE #4: SG22

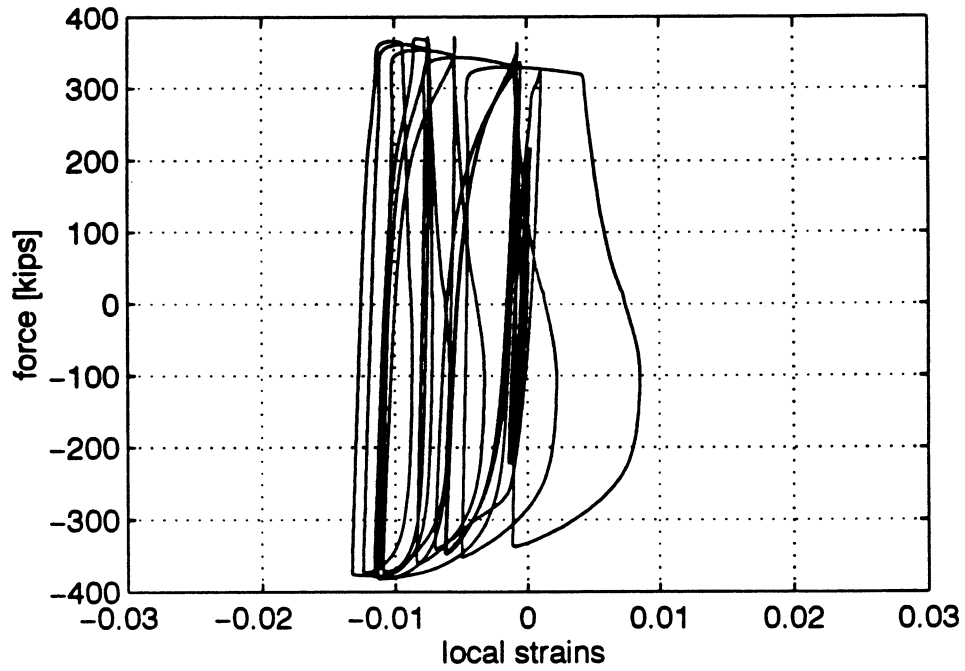


FIGURE 104: LOCAL RESPONSE -- TOP FLANGE AXIS VER (@ "DOG BONE")

UCB-DASSE #4: SG25

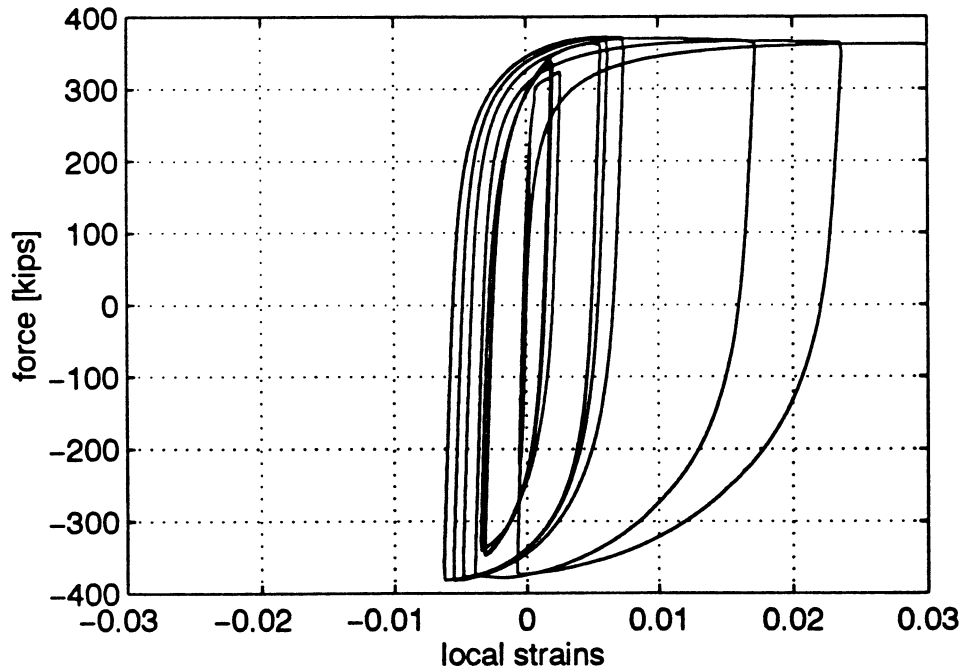


FIGURE 105: LOCAL RESPONSE -- TOP FLANGE EDGE DIA (@ "DOG BONE")
UCB-DASSE #4: SG21

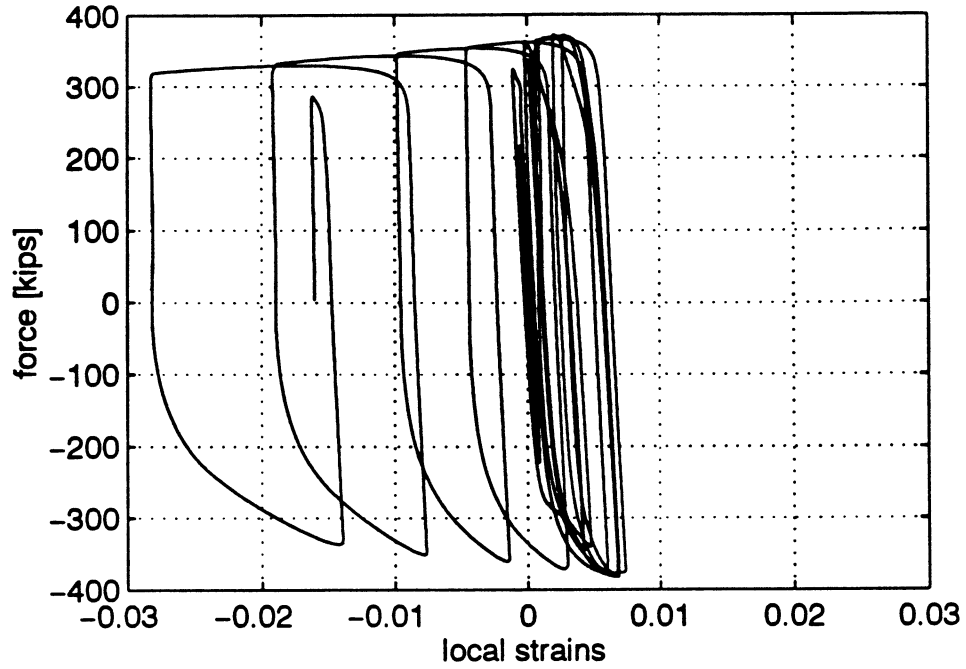


FIGURE 106: LOCAL RESPONSE -- TOP FLANGE AXIS DIA (@ "DOG BONE")
UCB-DASSE #4: SG24

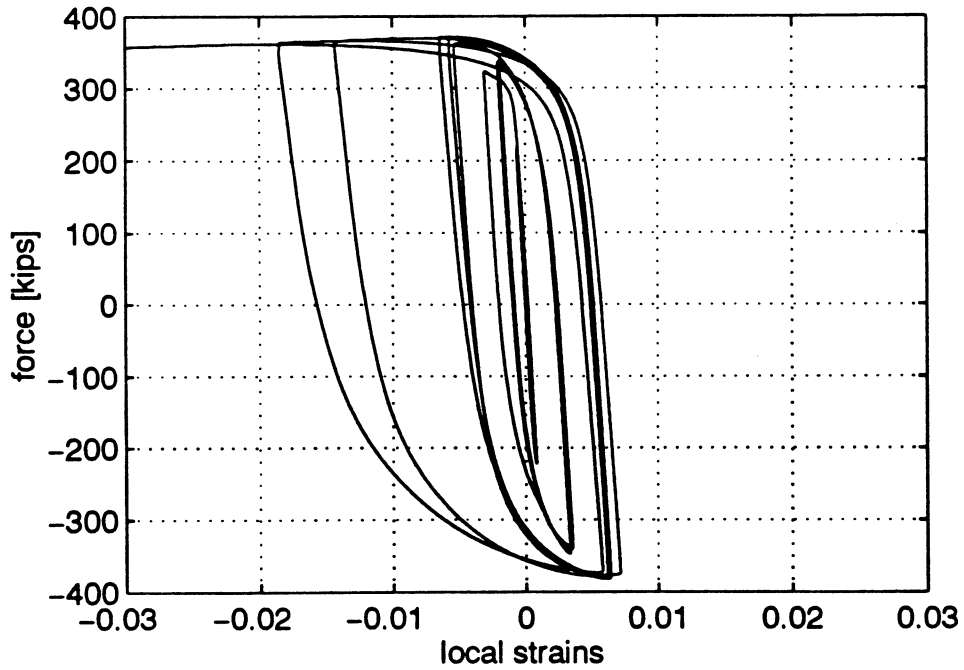


FIGURE 107: LOCAL RESPONSE -- BOTTOM FLANGE EDGE HOR (@ "DOG BONE")

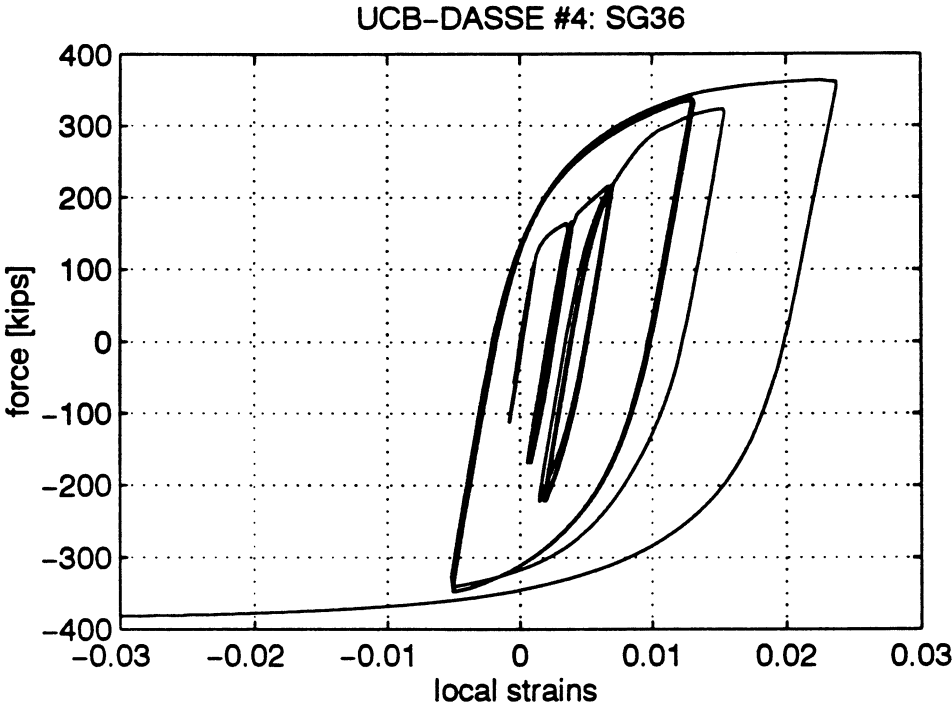


FIGURE 108: LOCAL RESPONSE -- BOTTOM FLANGE AXIS HOR (@ "DOG BONE")

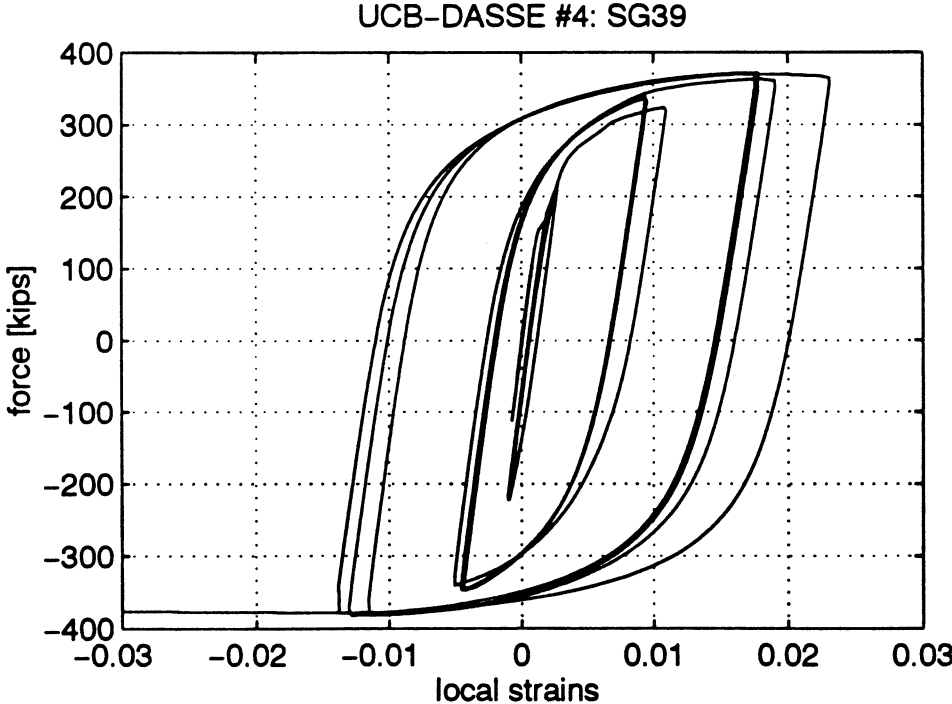


FIGURE 109: LOCAL RESPONSE -- BOTTOM FLANGE EDGE VER (@ "DOG BONE")

UCB-DASSE #4: SG38

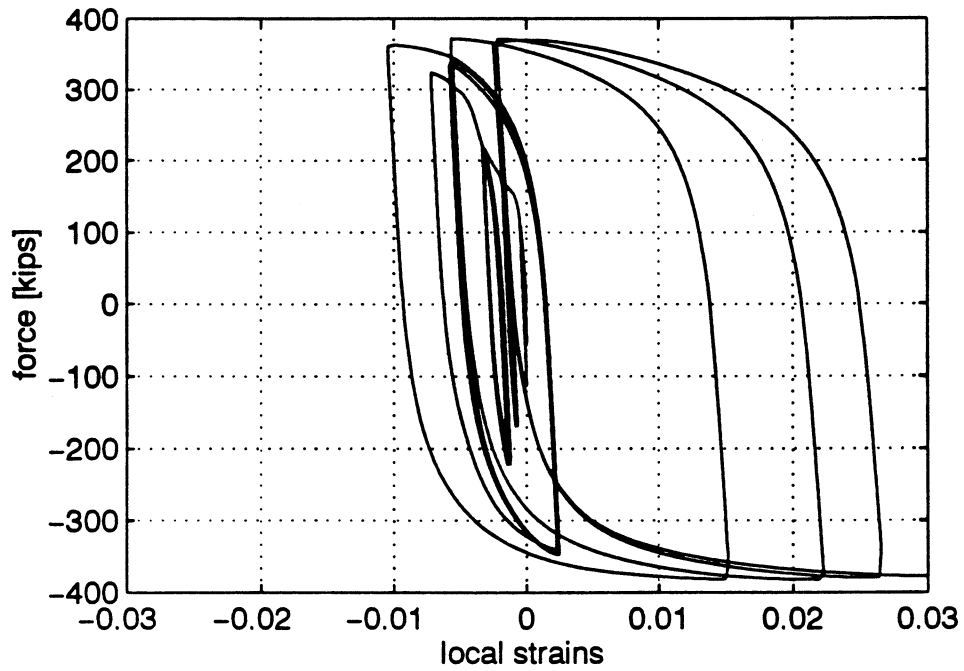


FIGURE 110: LOCAL RESPONSE -- BOTTOM FLANGE AXIS VER (@ "DOG BONE")

UCB-DASSE #4: SG41

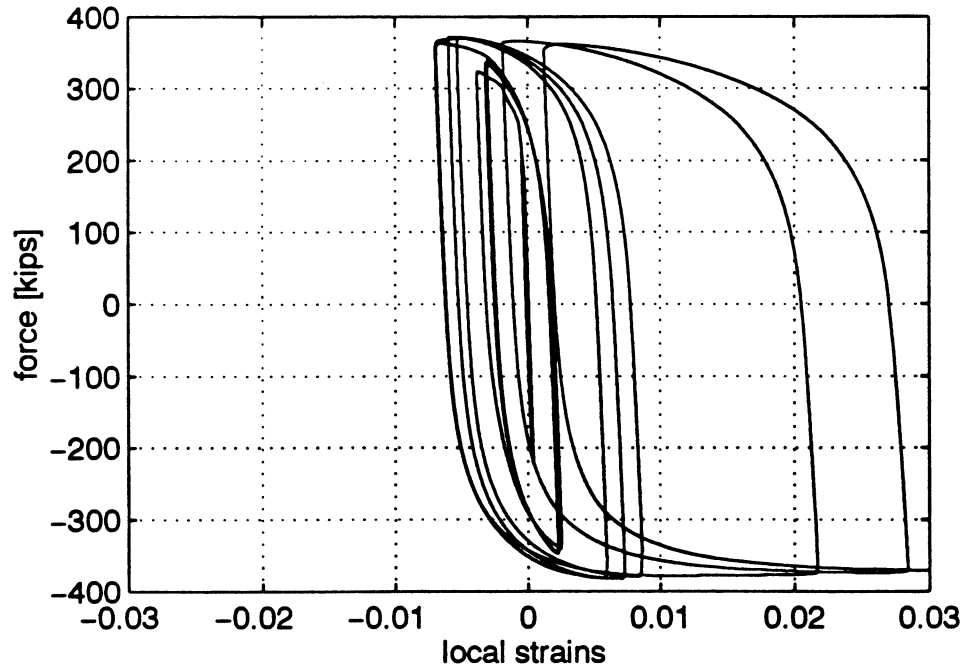


FIGURE 111: LOCAL RESPONSE -- BOTTOM FLANGE EDGE DIA (@ "DOG BONE")
UCB-DASSE #4: SG37

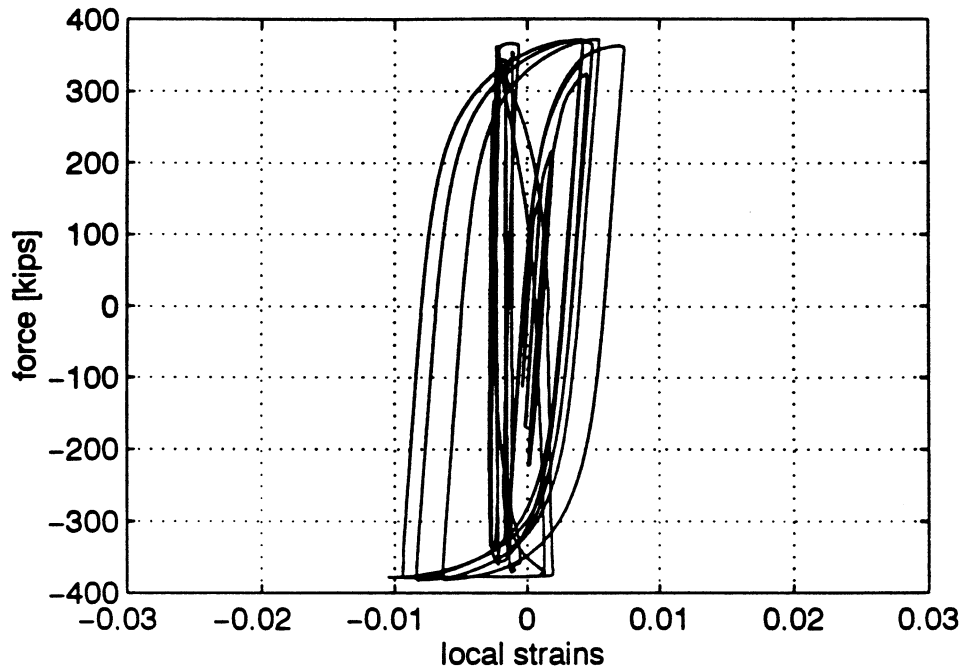


FIGURE 112: LOCAL RESPONSE -- BOTTOM FLANGE AXIS DIA (@ "DOG BONE")
UCB-DASSE #4: SG40

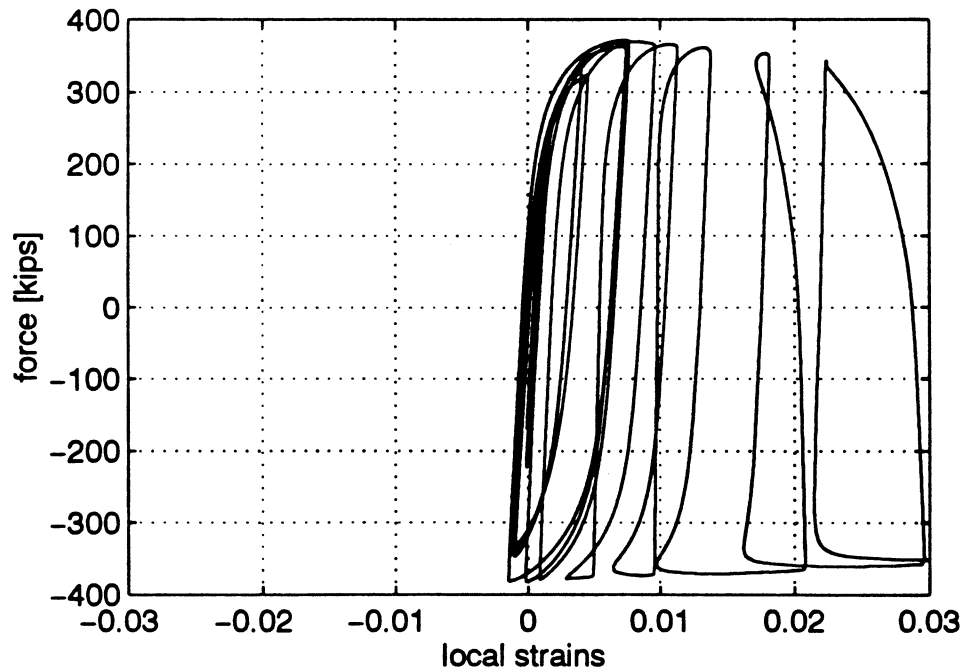


FIGURE 113: LOCAL RESPONSE -- TOP STIFFENER

UCB-DASSE #4: SG27

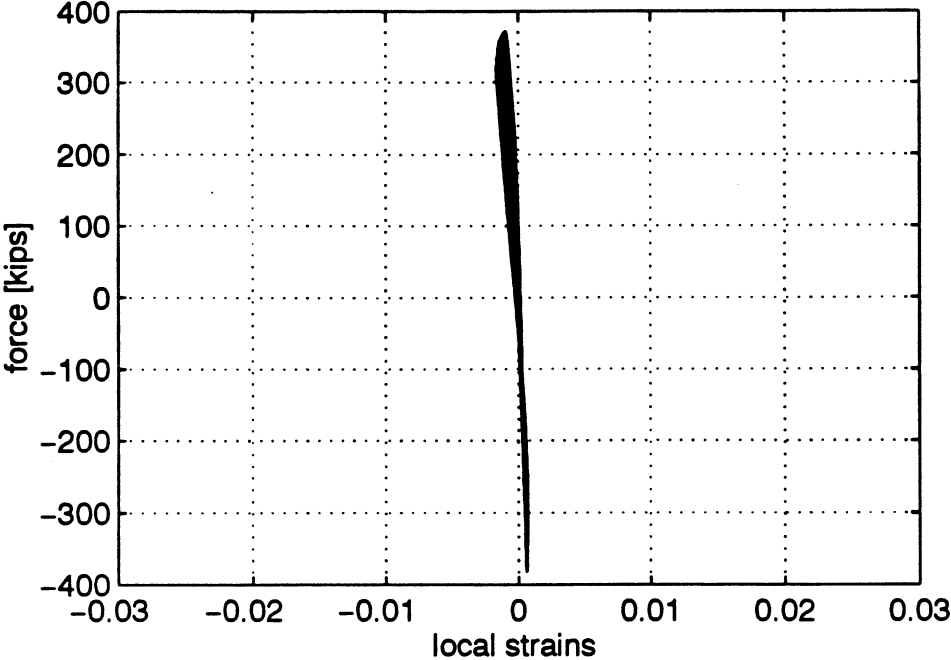


FIGURE 114: LOCAL RESPONSE -- BOTTOM STIFFENER

UCB-DASSE #4: SG43

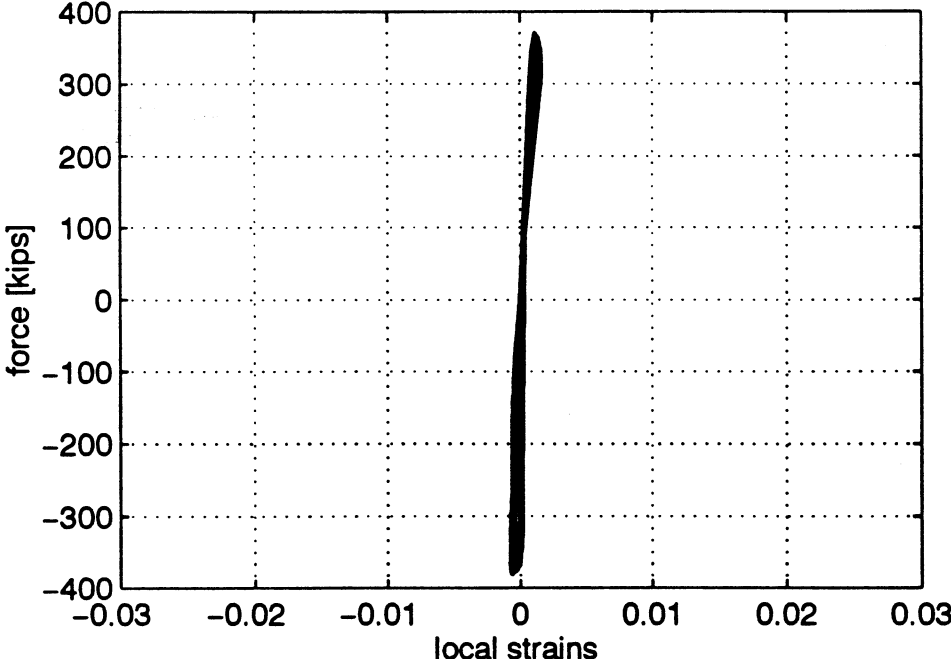


FIGURE 117: LOCAL RESPONSE -- PANEL ZONE (TOP CORNER VER)

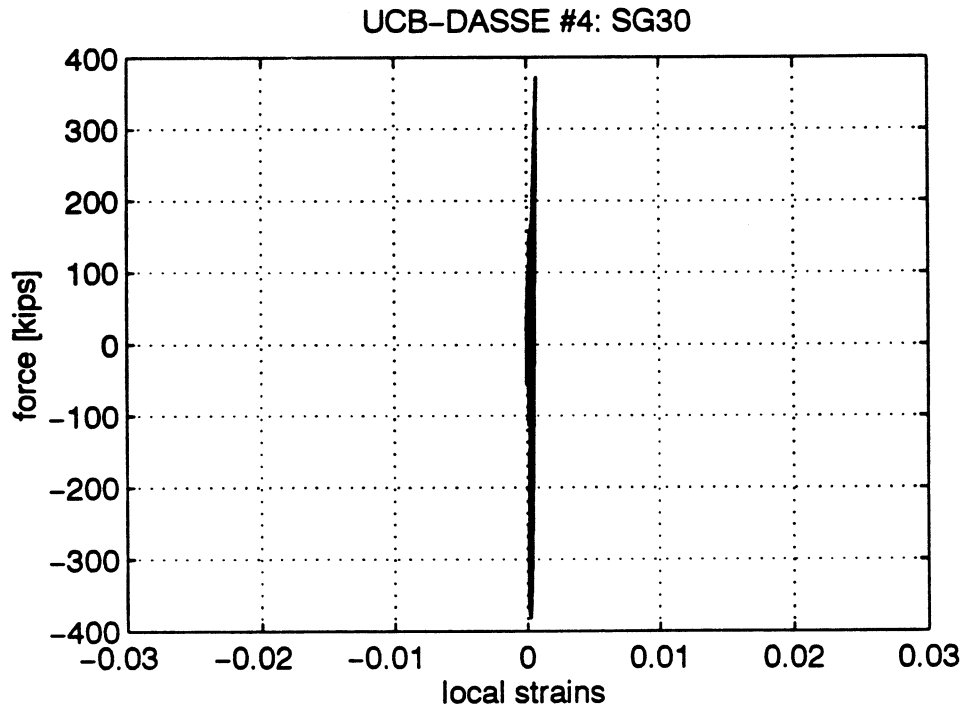


FIGURE 118: LOCAL RESPONSE -- PANEL ZONE (BOTTOM CORNER HOR)

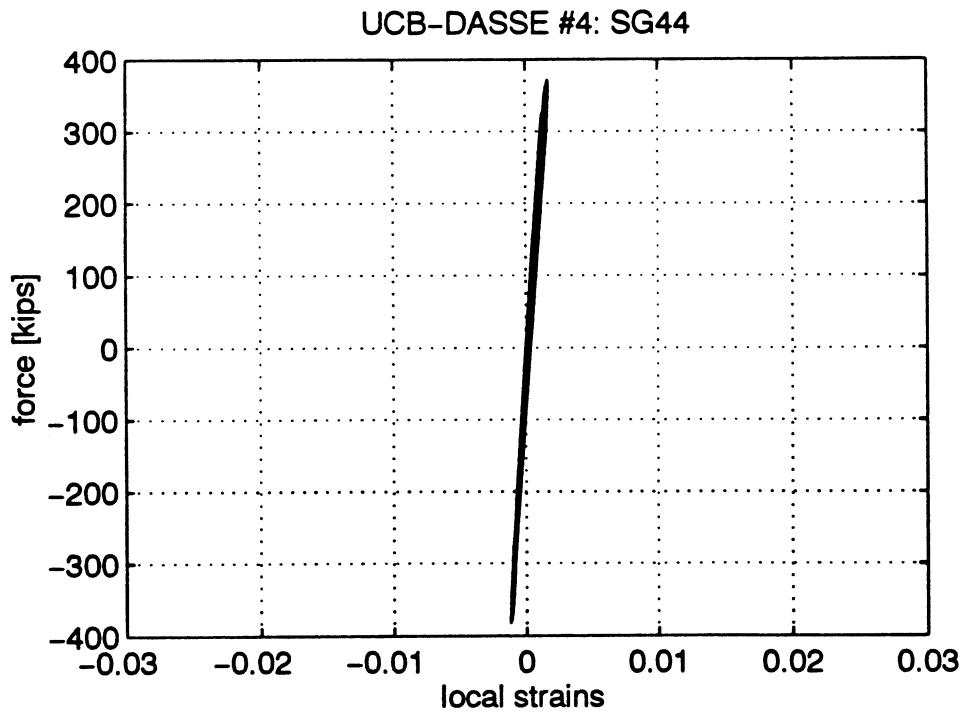


FIGURE 115: LOCAL RESPONSE -- PANEL ZONE (TOP CORNER HOR)

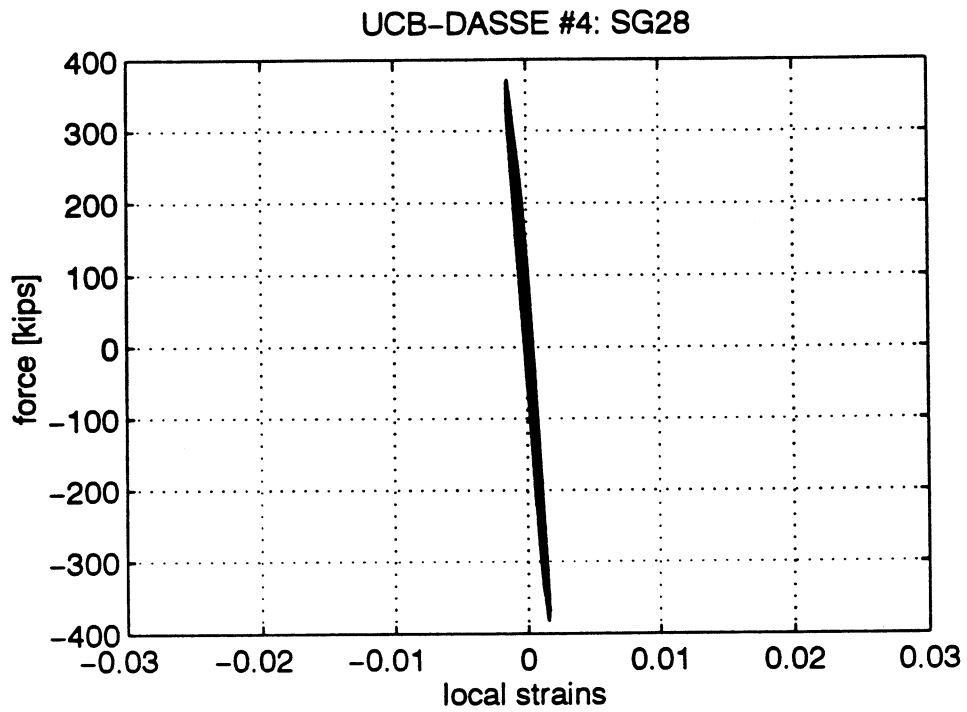


FIGURE 116: LOCAL RESPONSE -- PANEL ZONE (TOP CORNER DIA)

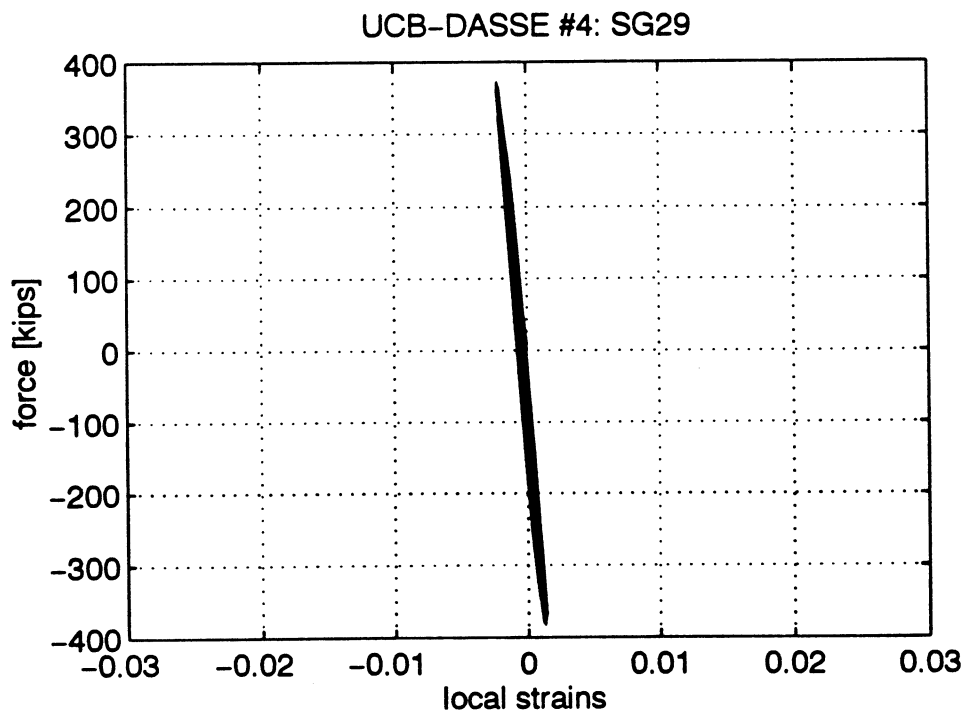


FIGURE 121: SPECIMEN 4 -- BEAM TOP FLANGE
(after 2" cycles)



FIGURE 122: SPECIMEN 4 -- BEAM BOTTOM FLANGE
(after 2" cycles)



FIGURE 123: SPECIMEN 4 -- BEAM TOP FLANGE
(after 3" cycles)

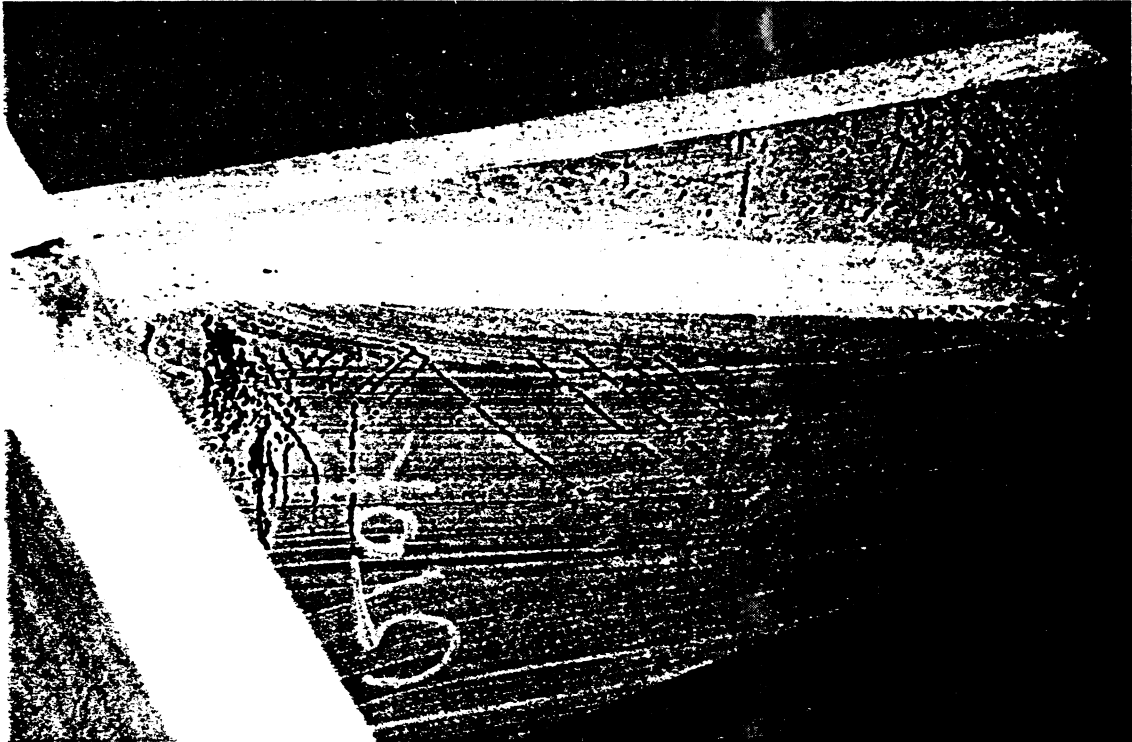


FIGURE 124: SPECIMEN 4 -- BEAM TOP FLANGE
(after 5" cycles)



FIGURE 125: SPECIMEN 4 -- BEAM TOP FLANGE
(@ -5" actuator displacement)



FIGURE 126: SPECIMEN 4 -- BEAM TOP FLANGE
(after the test)

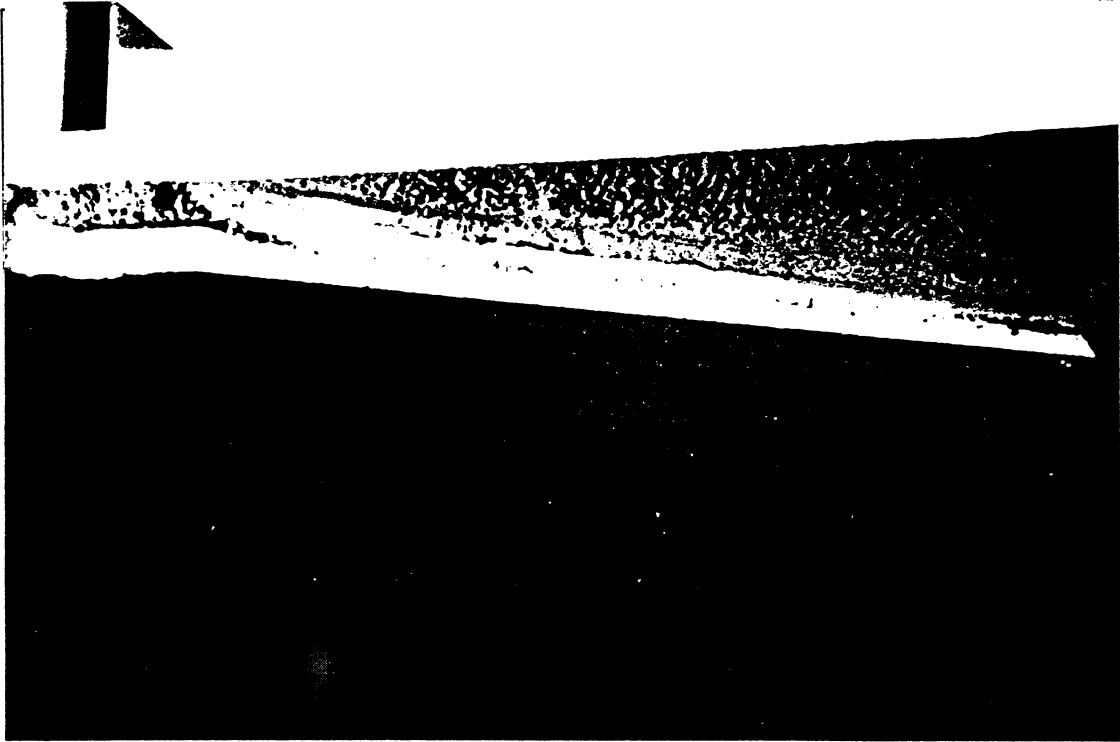


FIGURE 127: SPECIMEN 4 -- PANEL ZONE TOP CORNER
(after the test)



FIGURE 128: SPECIMEN 4 -- BEAM AFTER THE TEST



APPENDIX A

MATERIAL PROPERTIES

NUCOR-YAMATO STEEL CO.

P.O. BOX 1228
BLYTHEVILLE, AR 72319

CERTIFIED MILL REPORT

QUALITY STEEL - MADE IN THE USA

ALL STEEL PRODUCED BY NUCOR-YAMATO STEEL COMPANY WAS MELTED AND MANUFACTURED IN THE UNITED STATES OF AMERICA.

SOLD TO:

CCC STEEL, INC.
2576 E. VICTORIA ST.
PO BOX 5932
COMPTON, CA

SHIP TO:

CCC STEEL, INC.
S.P. TRACK 7242
DOMINGUEZ, CA

90224-5932

00000-0

CUSTOMER RD: LMS420 E

GRADE: ASTM A572GR50-92

DATE	CUSTOMER NO.	INVOICE NO.	BILL OF LADING
1/11/94	1101	113398	129097

ITEM DESCRIPTION	HEAT NUMBER	MECHANICAL PROPERTIES				CHEMICAL PROPERTIES				
		YIELD STRENGTH	TENSILE STRENGTH	ELONGATION	REDUCTION OF AREA	C	Mn	P	S	SI
IX18 -046.0 25'	39783	51700	67900	.29	.08	.73	.002	.03	.13	.36
		51100	68200	30	V=	.03	NB=	.001		
IX18 -046.0 25'	39785	54400	69500	.27	.10	.63	.012	.04	.18	.34
		50000	68000	29	V=	.03	NB=	.000		
IX36 -135.0 23' 5"	39452	58300	74000	.28	.09	.97	.021	.01	.24	.35
		59000	74600	27	V=	.04	NB=	.003		
IX36 -160.0 25'	35173	55100	68000	.27	.05	.80	.011	.02	.24	.37
		55100	67600	27	V=	.01	NB=	.001		
IX36 -194.0 25' 5"	40309	58400	75100	.24	.09	1.00	.015	.01	.18	.30
		58200	75200	25	V=	.04	NB=	.002		
IX36 -194.0 26'	36073	62900	76900	.24	.06	1.24	.017	.02	.23	.33
		64600	79200	26	V=	.05	NB=	.002		
IX36 -194.0 26'	36076	61400	75900	.28	.05	1.29	.022	.02	.24	.35
		59900	75700	26	V=	.05	NB=	.002		
IX40 -183.0 20'	38724	58600	73500	.24	.08	.93	.014	.02	.22	.37
		60300	73500	24	V=	.03	NB=	.002		
IX40 -183.0 25'	38724	58600	73500	.24	.08	.93	.014	.02	.22	.37
		60300	73500	24	V=	.03	NB=	.002		

ELONGATION BASED ON 8.00 INCH GAGE LENGTH.

I HEREBY certify, that the contents of this report are accurate and correct. All test results and operations performed by material manufacturer are in compliance with the requirements of the material specification, and when designated by purchaser, meet the applicable specification.

STATE OF ARKANSAS
COUNTY OF MISSISSIPPI
WORN TO AND SUBSCRIBED BEFORE ME THIS

P.O. 70901
501-4

Day of _____

notary public

GARY OXFORD

PLANT METALLURGIST - QUALITY ASSUR.

NUCOR-YAMATO STEEL CO.
 P.O. BOX 1228 • DAYTONEVILLE, OH 45316

DATE
10/16/95

All beams produced by Nucor-Yamato Steel are cast and rolled to a fully killed and fine grain practice.

CERTIFIED MILL TEST REPORT
 100% MELTED AND MANUFACTURED IN U.S.A.

GRADES: ASTM A372GR50-93
 GRADES: ASTM A709-93A GR50

HERRICK CORPORATION
 C/O STOCKTON STEEL
 3003 E. HANNER LN.
 STOCKTON, CA 95212-0000

INVOICE#
219108

CUSTOMER NO.
1382

Job 7090

HERRICK CORPORATION
 PO BOX 9125
 PLEASANTON, CA 94566-0000

BILL OF LADING
208068

CUSTOMER PO.
67209

ITEM DESCRIPTION	QTY	WEIGHT	MECHANICAL PROPERTIES				CHEMICAL PROPERTIES										
			YIELD STRENGTH MPA	TENSILE STRENGTH MPA	ELONGATION %	CHARPY IMPACT TEMP	C	Mn	P	S	Si	Cu	Ni	Cr	Mo	V	Nb
W20 x 124.0	1	68407	35500	57000	21	.07	.96	.006	.02	.22	.43	.11	.05	.02	.04	.016	.25
W20 x 130.0	1	68376	35500	57000	21	.06	.00	.017	.02	.21	.42	.14	.10	.03	.04	.013	.30
W20 x 130.0	1	67019	35500	57000	21	.08	.02	.006	.02	.20	.39	.13	.08	.03	.03	.013	.31

ELONGATION BASED ON 8.00 INCH GAUGE LENGTH

CARBON EQUIVALENT (CE) = C + Mn/8 + [Cr + Mo + V]5 + [Ni + Cu]15

STATE OF ARKANSAS COUNTY OF MISSISSIPPI
 SHORN TO AND SUBSCRIBED BEFORE ME THIS

Signature

I hereby certify that the contents of this report are accurate and correct. All test results and operations performed by this metallurgical manufacturer are in compliance with the applicable standards.

Day of

RELVE DE CONTROLE - MELL'S TEST CERTIFICATE
 WERKSZEUGNIS

A R O E D
 DIVISION DIFFERDANCE
 GESTION QUALITE

L 4503 DIFFERDANCE
 GRAND-DUCHE DE LUXEMBOURG

4055360

ADVICE NR : 650138

INVOICE NR : 60840 19900801

MELL'S TEST CERTIFICATE - WITH CHEMICAL AND PHYSICAL PROPERTIES
 STEEL AS PER ASTM A 572/b1 GRADE 50 VANADIUM CONTENT TO BE RESTRICTED TO 0.008% MAX.

TRADE ARDED NO : 90 ME 3420 002
 CUSTOMER NR : 488

TRADEARDED NEW YORK
 REL SAN BERNARDINO STEEL
 P.O. BOX 29060
 U.S.A. (WEST C)
 SAN BERNARDINO, CALIF. 92406

ITEM NR INV. ORDER	PRODUCT	SIZE	LENGTH	WEIGHT KG	NUMBER PA LI GUM BAR
01-001	M-BEAMS	WTM 36 X 16 1/2 X 428	26' 1"	10363	2
02-004	M-BEAMS	WTM 36 X 16 1/2 X 328	26' 1"	15518	4
03-007	M-BEAMS	WTM 33 X 15 3/4 X 307	26' 1"	4587	1

NO/NR HEAT	C	MM	P	S	S	SE	HEAT	N	V	NO	(S)	WEIGHT KG	BAR
01-001	01703	0.19	1.23	0.012	0.007	0.31	0.007	0.007	0.038	0.031		10383	2
02-004	00280	0.12	1.17	0.010	0.023	0.16	0.007	0.007	0.038	0.033		15518	4
03-007	03426	0.16	1.34	0.033	0.022	0.27	0.004	0.004				4587	1

NO/NR HEAT	TENSILE TEST		
	PSI YS	PSI UTS	200MM EL. (%)
01-000005	56.686	94.660	24.9
02-000001	52.055	76.540	27.0
03-000001	53.666	75.400	27.5

MTO
2364

LE 28/08/90

PORTEUR DE SIGNATURE SPECIALE

CERTIFICATE OF TEST

British Steel General Steels (A Division of British Steel plc)

Teesside Works

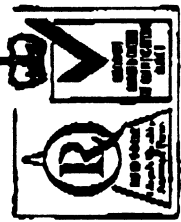
P.O. Box 29, Redcar, Cleveland TS10 5RD
 Telephone: 0642-674731 Telex: 507481

Date 30/10/80

SRIP: SEA MODEL
 CORC No. ES900 12
 ALBERNI DAW

P. 5/6

Customer:
BRITISH STEEL INC
 475 NORTH MAIN STABLE DRIVE
 SUITE 400
 SCHALBURG
 ILLINOIS 60173, U.S.A.
MTO
2364



Inspection

Order No. 2702 BK/196
 Confirmation Order No. 102041
 Specification A572 S1
 ASTM A572 68C GR. 50 (S1-KILLED)
 TEST CERTIFICATE & ANALYSIS
 TEST CERTS TO SHOW BAR NO. &
 CAST NO.
 6 COPIES OF TEST CERTIFICATE

Product Description UNIVERSAL BEAM
 36.0" X 16.1/2" X 260 LBS/FT

WRL NO 10
 (260.2) LBS/FT) COLL. WTS 410

BALANCE

Order No.	Description	Quantity	Dimensions	Yield Stress	Tensile Strength	Elongation	Charpy Impact Values					BASIC OXYGEN STEEL ANALYSIS %						
							Av.	C	SI.	Min.	P.	S.	MR	V				
8-536	28' 1.0" (7.950)	2	7C13656	58780	80000	18	.15	.306	1.06	.018	.019	.030	.003					

GENERAL MARK PAGE No. 1 and 1881
 HEAT NO
 SAN BERNARD W/O/P R 486
 ITEM MARK
 LOS ANGELES
 MADE IN U.K.
 SIZE/SPEC/LENGTH

All Test Certificates issued by British Steel plc will contain the embossed security seal and a copy of a British Steel plc Test Certificate without the seal should obtain from the supplier that it is a true and accurate reproduction of the original.
 These results are certified by British Steel plc and comply with the requirements of the Product Description.

S. Adame



SCHWEIN/CHRISTENSEN
LABORATORIES, INC.

materials consulting
laboratory testing
failure analysis

August 9, 1996

SCL Project No. 96257

Mr. Jim Passaglia
DASSE Design Inc.
33 Montgomery Street, Suite 850
San Francisco, CA 94105

Re: McCandless Tower #2
Santa Clara, California
DASSE Design Project No. 96B168X1

TENSILE TEST RESULTS
McCandless Tower Test Coupons

SAMPLE NO.	SIZE/HEAT #	DIAMETER (in.)	YIELD STRENGTH ⁽¹⁾ (psi)	YIELD STRENGTH ⁽²⁾ (psi)	TENSILE STRENGTH (psi)	ELONGATION IN 2"
1W	W36 X 280 HT. 14454	0.505	63,100	60,500	83,600	29%
1F ⁽³⁾	W36 X 280 HT. 14454	0.505	62,500	61,500	78,500	33%
2W	W36 X 280 HT. 13856	0.508	57,500	53,300	75,100	32%
2F	W36 X 280 HT. 13856	0.502	56,600	53,100	73,400	34%
3W	W33 X 387 HT. 03426	0.492	60,500	57,200	85,300	30%
3F	W33 X 387 HT. 03426	0.501	59,600	54,500	77,700	33%
4W	W33 X 130 HT. 67019	0.505	53,500	52,500	69,900	36%
4F	W33 X 130 HT. 67019	0.505	55,000	51,900	69,600	36%
5W	W36 X 194 HT. 36073	0.507	65,600	61,900	77,800	31%
5F	W36 X 194 HT. 36073	0.506	63,200	59,200	76,200	32%

(1) Yield at proportional limit (i.e., upper yield point)

(2) Yield at 0.2% offset (i.e., lower yield point)

(3) As received at SCL, this sample marked "1W". It was 1 1/4" thick and appeared to be cut from flange. We assumed it was mislabeled, and remarked it "1F".

All specimens meet minimum mechanical property requirements for ASTM A572GR50 steel.

Respectfully submitted

SCHWEIN/CHRISTENSEN LABORATORIES, INC.

Mark S. Kellogg dg

Mark S. Kellogg
Materials Engineer

MSK:dg



SPECIMEN #4

November 25, 1996

Mr. Jim Passaglia
DASSE Design Inc.
33 Montgomery Street, Suite 850
San Francisco, CA 94105

Re: McCandless Tower #2
Santa Clara, California
DASSE Design Project No. 96B168X1

FAX TRANSMITTAL

Pages _____

TO	JIM
CO	
DEPT	
FAX #	243-9165
FROM	SCHWEIN
CO	S/C Labs, Inc.
PHONE #	(510) 284-3311
FAX #	(510) 284-3360

SCHWEIN/CHRISTENSEN
LABORATORIES, INC.

materials consulting
laboratory testing
failure analysis

SCL Project 96403

TENSILE TEST RESULTS McCandless Tower Test Coupons		
LOCATION	FLANGE	WEB
SIZE	W36 x 194	W36 x 194
HEAT NUMBER	36073	36073
DIAMETER (in.)	0.508	0.501
YIELD STRENGTH ⁽¹⁾ (psi)	57,500	64,700
YIELD STRENGTH ⁽²⁾ (psi)	54,500	60,400
TENSILE STRENGTH (psi)	77,000	77,100
ELONGATION IN 2"	32%	33%

(1) Yield at proportional limit (i.e., upper yield point)
(2) Yield at 0.2% offset (i.e., lower yield point)

All specimens meet minimum mechanical property requirements for ASTM A572 GR50 steel.

Respectfully submitted,

SCHWEIN/CHRISTENSEN LABORATORIES, INC.

Conrad P. Christensen, P.E.
Metallurgical Engineer

CPC:at